Developed at the request of:

Department of Energy & Climate Change

Research conducted by:

Met Office Hadley Centre

The University of Nottingham
UNITED KINGDOM · CHINA · MALAYSIA

Walker Institute

Centre for Ecology & Hydrology
Natural Environment Research Council

University of Leeds

Tyndall Centre for Climate Change Research

Climate: Observations, projections and impacts

Egypt

We have reached a critical year in our response to climate change. The decisions that we made in Cancún put the UNFCCC process back on track, saw us agree to limit temperature rise to 2 °C and set us in the right direction for reaching a climate change deal to achieve this. However, we still have considerable work to do and I believe that key economies and major emitters have a leadership role in ensuring a successful outcome in Durban and beyond.

To help us articulate a meaningful response to climate change, I believe that it is important to have a robust scientific assessment of the likely impacts on individual countries across the globe. This report demonstrates that the risks of a changing climate are wide-ranging and that no country will be left untouched by climate change.

I thank the UK's Met Office Hadley Centre for their hard work in putting together such a comprehensive piece of work. I also thank the scientists and officials from the countries included in this project for their interest and valuable advice in putting it together. I hope this report will inform this key debate on one of the greatest threats to humanity.

The Rt Hon. Chris Huhne MP, Secretary of State for Energy and Climate Change

There is already strong scientific evidence that the climate has changed and will continue to change in future in response to human activities. Across the world, this is already being felt as changes to the local weather that people experience every day.

Our ability to provide useful information to help everyone understand how their environment has changed, and plan for future, is improving all the time. But there is still a long way to go. These reports – led by the Met Office Hadley Centre in collaboration with many institutes and scientists around the world – aim to provide useful, up to date and impartial information, based on the best climate science now available. This new scientific material will also contribute to the next assessment from the Intergovernmental Panel on Climate Change.

However, we must also remember that while we can provide a lot of useful information, a great many uncertainties remain. That's why I have put in place a long-term strategy at the Met Office to work ever more closely with scientists across the world. Together, we'll look for ways to combine more and better observations of the real world with improved computer models of the weather and climate; which, over time, will lead to even more detailed and confident advice being issued.

Julia Slingo, Met Office Chief Scientist

Introduction

Understanding the potential impacts of climate change is essential for informing both adaptation strategies and actions to avoid dangerous levels of climate change. A range of valuable national studies have been carried out and published, and the Intergovernmental Panel on Climate Change (IPCC) has collated and reported impacts at the global and regional scales. But assessing the impacts is scientifically challenging and has, until now, been fragmented. To date, only a limited amount of information about past climate change and its future impacts has been available at national level, while approaches to the science itself have varied between countries.

In April 2011, the Met Office Hadley Centre was asked by the United Kingdom's Secretary of State for Energy and Climate Change to compile scientifically robust and impartial information on the physical impacts of climate change for more than 20 countries. This was done using a consistent set of scenarios and as a pilot to a more comprehensive study of climate impacts. A report on the observations, projections and impacts of climate change has been prepared for each country. These provide up to date science on how the climate has already changed and the potential consequences of future changes. These reports complement those published by the IPCC as well as the more detailed climate change and impact studies published nationally.

Each report contains:

- A description of key features of national weather and climate, including an analysis of new data on extreme events.
- An assessment of the extent to which increases in greenhouse gases and aerosols in the atmosphere have altered the probability of particular seasonal temperatures compared to pre-industrial times, using a technique called 'fraction of attributable risk.'
- A prediction of future climate conditions, based on the climate model projections used in the Fourth Assessment Report from the IPCC.
- The potential impacts of climate change, based on results from the UK's Avoiding Dangerous Climate Change programme (AVOID) and supporting literature. For details visit: http://www.avoid.uk.net

The assessment of impacts at the national level, both for the AVOID programme results and the cited supporting literature, were mostly based on global studies. This was to ensure consistency, whilst recognising that this might not always provide enough focus on impacts of most relevance to a particular country. Although time available for the project was short, generally all the material available to the researchers in the project was used, unless there were good scientific reasons for not doing so. For example, some impacts areas were omitted, such as many of those associated with human health. In this case, these impacts are strongly dependant on local factors and do not easily lend themselves to the globally consistent framework used. No attempt was made to include the effect of future adaptation actions in the assessment of potential impacts. Typically, some, but not all, of the impacts are avoided by limiting global average warming to no more than 2 °C.

The Met Office Hadley Centre gratefully acknowledges the input that organisations and individuals from these countries have contributed to this study. Many nations contributed references to the literature analysis component of the project and helped to review earlier versions of these reports.

We welcome feedback and expect these reports to evolve over time. For the latest version of this report, details of how to reference it, and to provide feedback to the project team, please see the website at www.metoffice.gov.uk/climate-change/policy-relevant/obs-projections-impacts

In the longer term, we would welcome the opportunity to explore with other countries and organisations options for taking forward assessments of national level climate change impacts through international cooperation.

Summary

Climate observations

- There have been widespread warming trends over Egypt since 1960 with greater warming in summer than winter.
- Between 1960 and 2003, there has been an increase in the frequency of warm nights and a decrease in the frequency of cool nights.
- There has been a general increase in summer temperatures averaged over the country as a result of human influence on climate, making the occurrence of warm summer temperatures more frequent and cold summer temperatures less frequent.

Climate change projections

- For the A1B emissions scenario the CMIP3 ensemble, projected temperature increases over Egypt are around 3-3.5°C with a consistently good agreement between the models over the Middle East region in general.
- Egypt is projected to experience mainly decreases in precipitation, in common with the wider Mediterranean and majority of the Middle East. Decreases of over 20% are projected in the west of the country, with strong ensemble agreement. Smaller changes are projected towards the southeast.

Climate change impact projections

Crop yields

- Over 90% of crop production in Egypt is fed by irrigation. An important uncertainty in projections of crop yield is therefore the evolution of future water availability with climate change in Egypt.
- Global- and regional-scale studies generally project yield deficits for wheat, rice and maize, three of Egypt's major crops, with climate change. Whether crops are rain-fed or irrigated has an important bearing on the results, and the balance between detrimental ozone effects and CO_2 fertilisation may determine whether losses or gains are realised under climate change.

- National-scale studies agree that crop yields in Egypt could decline with climate change, and that adaptation and management methods could potentially reduce the magnitude of any losses.

Food security

- Egypt is currently a country of extremely low undernourishment. Global-scale studies included here generally project that Egypt could experience increasing pressures on food security as a result of climate change.

- However, recent work by the AVOID programme demonstrates that adaptive measures could be crucial towards maintaining food security in Egypt under climate change.

Water stress and drought

- The majority of national-scale and global-scale studies that have considered the effects of climate change on river discharge suggest that water stress could increase with climate change in Egypt.

- Recent simulations by the AVOID programme demonstrate high uncertainty in estimating the magnitude of increased water stress under climate change for Egypt. However most projections do not show much of the population experiencing a decrease in water stress with climate change.

- National-scale studies indicate that the discharge of the Nile could decline substantially in the future and that the population presents a high vulnerability to water stress with climate change, although precise estimates remain uncertain.

Pluvial flooding and rainfall

- The IPCC AR4 found consistency across GCMs that mean precipitation could decrease with climate change for Egypt, but that wet extremes could increase.

Fluvial flooding

- There the magnitude and sign of future changes in flood season discharge in the Nile River remain uncertain.

- Simulations by the AVOID programme found that a large majority of models show a tendency towards decreasing flood risk with climate change in the early 21st century. Later in the century a majority of the models still agree on a decrease compared to

the present-day average annual flood risk, but, especially in the A1B scenario, a small number of models do show large increases in flood risk by this time.

Coastal regions

- Several studies conclude that Egypt is highly vulnerable to sea level rise (SLR).
- In one study that considered the impact of a 1m SLR for 84 developing countries, Egypt was ranked the 2nd highest with respect to the coastal population affected, 3rd highest for coastal GDP affected and 5th highest for proportion of urban areas affected.
- Around 15% (2.7 million people) of Egypt's coastal population could be affected by a 10% intensification of the current 1-in-100-year storm surge combined with a 1m SLR.

Table of Contents

Chapter 1 – Climate Observations 9
Rationale 10
Climate overview 12
Analysis of long-term features in the mean temperature 12
Temperature extremes 15
Recent extreme temperature events 15
Heat wave July 2007 15
Analysis of long-term features in moderate temperature extremes 15
Attribution of changes in likelihood of occurrence of seasonal mean temperatures 19
Summer 2007 19
Precipitation extremes 21
Recent extreme precipitation events 21
Flooding, January 2010 21
Analysis of long-term features in precipitation 21
Storms 23
Recent storm events 23
Summary 24
Methodology annex 25
Recent, notable extremes 25
Observational record 26
Analysis of seasonal mean temperature 27
Analysis of temperature and precipitation extremes using indices 27
Presentation of extremes of temperature and precipitation 36
Attribution 40
References 43
Acknowledgements 46
Chapter 2 – Climate Change Projections 47
Introduction 48
Climate projections 50
Summary of temperature change in Egypt 51
Summary of precipitation change in Egypt 51
Chapter 3 – Climate Change Impact Projections 53
Introduction 54
Aims and approach 54
Impact sectors considered and methods 54
Supporting literature 55
AVOID programme results 55
Uncertainty in climate change impact assessment 56
Summary of findings for each sector 60

Crop yields ... 60
Food security ... 60
Water stress and drought ... 61
Pluvial flooding and rainfall ... 61
Fluvial flooding ... 61
Tropical cyclones ... 62
Coastal regions ... 62

Crop yields ... 63
Headline ... 63
Supporting literature ... 63
Introduction ... 63
Assessments that include a global or regional perspective ... 65
National-scale or sub-national scale assessments ... 70
AVOID programme results ... 72
Methodology ... 72
Results ... 73

Food security ... 76
Headline ... 76
Introduction ... 76
Assessments that include a global or regional perspective ... 76
National-scale or sub-national scale assessments ... 85
Water stress and drought ... 86
Headline ... 86
Supporting literature ... 86
Introduction ... 86
Assessments that include a global or regional perspective ... 87
National-scale or sub-national scale assessments ... 93
AVOID programme results ... 94
Methodology ... 94
Results ... 95

Pluvial flooding and rainfall ... 97
Headline ... 97
Introduction ... 97
Assessments that include a global or regional perspective ... 97
National-scale or sub-national scale assessments ... 98

Fluvial flooding ... 99
Headline ... 99
Introduction ... 99
Assessments that include a global or regional perspective ... 100
National-scale or sub-national scale assessments ... 100
AVOID programme results ... 101
Methodology ... 101
Results ... 102

Tropical cyclones ... 104

Coastal regions ... 105
Headline ... 105

Assessments that include a global or regional perspective 105
National-scale or sub-national scale assessments 113
References..... 115

Chapter 1 – Climate Observations

Rationale

Figure 1. *Location of boxes for the regional average time series (red dashed box) in Figures 3 and 5 and the attribution region (grey box) in Figure 4.*

Present day weather and climate play a fundamental role in the day to day running of society. Seasonal phenomena may be advantageous and depended upon for sectors such as farming or tourism. Other events, especially extreme ones, can sometimes have serious negative impacts posing risks to life and infrastructure and significant cost to the economy. Understanding the frequency and magnitude of these phenomena, when they pose risks or when they can be advantageous and for which sectors of society, can significantly improve societal resilience. In a changing climate it is highly valuable to understand possible future changes in both potentially hazardous events and those reoccurring seasonal events that are depended upon by sectors such as agriculture and tourism. However, in order to put potential future changes in context, the present day must first be well understood both in terms of common seasonal phenomena and extremes.

The purpose of this chapter is to summarise the weather and climate from 1960 to present day. This begins with a general climate overview including an up to date analysis of changes in surface mean temperature. These changes may be the result of a number of factors including climate change, natural variability and changes in land use. There is then a focus on extremes of temperature, precipitation and storms selected from 2000 onwards, reported in the World Meteorological Organization (WMO) Annual Statement on the Status of the Global Climate and/or the Bulletin of the American Meteorological Society (BAMS) State of the Climate reports. This is followed by a discussion of changes in moderate extremes from 1960 onwards using the HadEX extremes database (Alexander et al. 2006) which categorises extremes of temperature and precipitation. These are core climate variables which have received significant effort from the climate research community in terms of data acquisition and processing and for which it is possible to produce long high quality records for monitoring. No new analysis is included for storms (see the methodology annex for background). For seasonal temperature extremes, an attribution analysis then puts the seasons with highlighted extreme events into context of the recent climate versus a hypothetical climate in the absence of anthropogenic emissions (Christidis et al, 2011). It is important to note that we carry out our attribution analyses on seasonal mean temperatures

over the entire country. Therefore these analyses do not attempt to attribute the changed likelihood of individual extreme events. The relationship between extreme events and the large scale mean temperature is likely to be complex, potentially being influenced by *inter alia* circulation changes, a greater expression of natural internal variability at smaller scales, and local processes and feedbacks. Attribution of individual extreme events is an area of developing science. The work presented here is the foundation of future plans to systematically address the region's present and projected future weather and climate, and the associated impacts.

The methodology annex provides details of the data shown here and of the scientific analyses underlying the discussions of changes in the mean temperature and in temperature and precipitation extremes. It also explains the methods used to attribute the likelihood of occurrence of seasonal mean temperatures.

Climate overview

Primary factors that affect the climate of Egypt are its sub-tropical latitude range of 22-32°N, and its position both close to the circum-global latitudinal belt of generally high atmospheric pressure and sandwiched between the vast continental land masses of Africa and Asia. These factors make Egypt one of the hottest and sunniest countries in the world, with very low humidity. Only along the northern coastal strip do winter cyclonic disturbances moving eastwards along the Mediterranean Sea bring some significant rainfall and, even at Alexandria on the coast, total annual rainfall averages are only 196mm. Some 160km inland at Cairo, average annual rainfall has reduced to 25mm and southwards it reduces still further to only 5mm at Hurghada on the Red Sea coast and less than 2mm at Aswan in the Nile valley. In central and southern Egypt several years may pass without any significant rain. When rain does fall it is usually in the form of a brief and sometimes damaging downpour.

Annual mean temperatures increase from around 20°C on the Mediterranean coastline to around 24°C on the Red Sea coastline, 25°C at Cairo and 26°C further south at Aswan with a seasonal variation of about ±7°C. Typical daytime maxima in mid-summer range from 30°C at Alexandria southwards to 41°C at Aswan; while the corresponding north-south range in mid-winter daytime maxima is 18-23°C. This makes even winter daytimes in the south pleasantly warm and sunny, albeit with cool nights, as further north.

Climate hazards include dust storms, heat waves, localised floods and, very rarely, unaccustomed snowfall in the north. A particularly unpleasant, occasionally dangerous, phenomenon in spring and early summer is a dry and dust laden ‘Khamsin’ wind that, from time to time, carries very hot air northwards into northern Egypt ahead of weak cyclonic disturbances in the Mediterranean.

Analysis of long-term features in the mean temperature

CRUTEM3 data (Brohan et al., 2006) have been used to provide an analysis of mean temperatures from 1960 to 2010 over Egypt using the median of pairwise slopes method to fit the trend (Sen, 1968; Lanzante, 1996). The methods are fully described in the methodology annex. In agreement with increasing global average temperatures (Sánchez-Lugo et al. 2011), there is a spatially consistent warming signal for temperature over Egypt as shown in Figure 2. For both summer (June to August) and winter (December to February) the spatial pattern is similar. However, for summer, more grid boxes show warming signals with higher confidence (in that the 5^{th} to 95^{th} percentiles of the slopes are of the same sign)

than for winter. Regionally averaged trends (over grid boxes included in the red dashed box in Figure 1) show warming but with higher confidence only for summer. There is stronger warming during summer at 0.31 ^{o}C per decade (5th to 95th percentile of slopes: 0.14 to 0.45 ^{o}C per decade) than during winter at 0.07 ^{o}C per decade (5th to 95th percentile of slopes: -0.15 to 0.28 ^{o}C per decade).

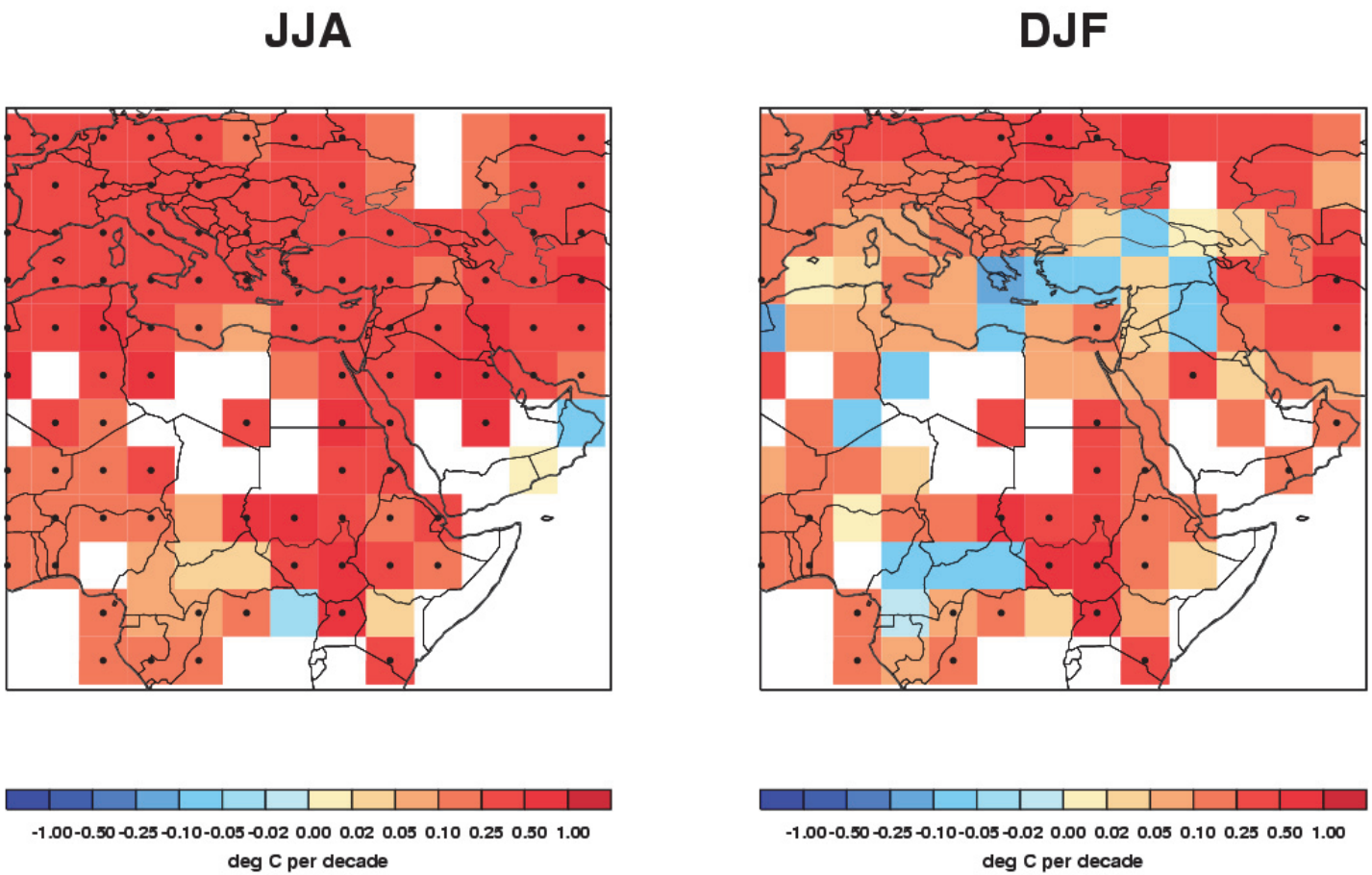

Figure 2. *Decadal trends in seasonally averaged temperatures for Egypt and surrounding areas over the period 1960 to 2010. Monthly mean anomalies from CRUTEM3 (Brohan et al. 2006) are averaged over each 3 month season (June-July-August – JJA and December-January-February – DJF). Trends are fitted using the median of pairwise slopes method (Sen 1968, Lanzante 1996). There is higher confidence in the trends shown if the 5th to 95th percentiles of the pairwise slopes do not encompass zero because here the trend is considered to be significantly different from a zero trend (no change). This is shown by a black dot in the centre of the respective grid box.*

Temperature extremes

Both hot and cold temperature extremes can place many demands on society. While seasonal changes in temperature are normal and indeed important for a number of societal sectors (e.g.,tourism, farming etc.), extreme heat or cold can have serious negative impacts. Importantly, what is 'normal' for one region may be extreme for another region that is less well adapted to such temperatures.Table 1 shows selected extreme events since 2000 that are reported in WMO Statements on Status of the Global Climate and/or BAMS State of the Climate reports. One event, the heat wave in July 2007 is highlighted as an example of a recent extreme temperature event.

Year	Month	Event	Details
2007	Winter	Cold spells	6 cold spells of duration 3-6 days saw temperatures 3-7 °C below normal
2007	July	Heat wave	For Mediterranean area: June and July heat waves prompted record levels of

Table 1. *Selected extreme temperature events reported in WMO Statements on Status of the Global Climate and/or BAMS State of the Climate reports since 2000.*

Recent extreme temperature eventsHeat wave July 2007

The Mediterranean area experienced heat waves in June and July 2007, which prompted record levels of electricity demand and led to around 40 deaths (WMO, 2008). The Egypt news reported temperatures reaching 45˚C in northern Egypt in late July, with record amounts of electricity consumption leading to several power outages (Egypt News, 2007).

Analysis of long-term features in moderate temperature extremes

HadEX extremes indices (Alexander et al. 2006) are used here for Egypt from 1960 to 2003 using daily maximum and minimum temperatures. Here we discuss changes in the frequency of cool days and nights and warm days and nights which are moderate extremes. Cool days/nights are defined as being below the 10^{th} percentile of daily maximum/minimum temperature and warm days/nights are defined as being above the 90^{th} percentile of the daily maximum/minimum temperature. The methods are fully described in the methodology annex.

In agreement with increasing mean temperature, warm nights have become more frequent while cool nights have become less frequent across the region with higher confidence. The signal for warm days and cool days is more mixed. Figure 3 presents annual totals, averaged across all seasons, therefore direct interpretation in terms of summertime heat waves and winter cool snaps is not possible. Also, there are insufficient data to provide estimates beyond 1999. However, previous research suggests increasing numbers of warm and very warm days (EEAA-MSEA 2010).

Night-time temperatures (daily minima) show a widespread positive shift in the distribution with fewer cool nights and more warm nights. Confidence is high throughout (Figure 3 a,b,c,d). Regional averages show high confidence signals of fewer cool nights and more warm nights.

Daytime temperatures (daily maxima) show a mixed signal lacking regional consistency and low in confidence (Figure 3 e,f,g,h). There is low confidence in the regional average signals of small decreases in the frequency of both cool and warm days.

The small numbers of stations present in most grid boxes means that even if there is higher confidence in the signals shown, uncertainty in the signal being representative of the wider grid box is large.

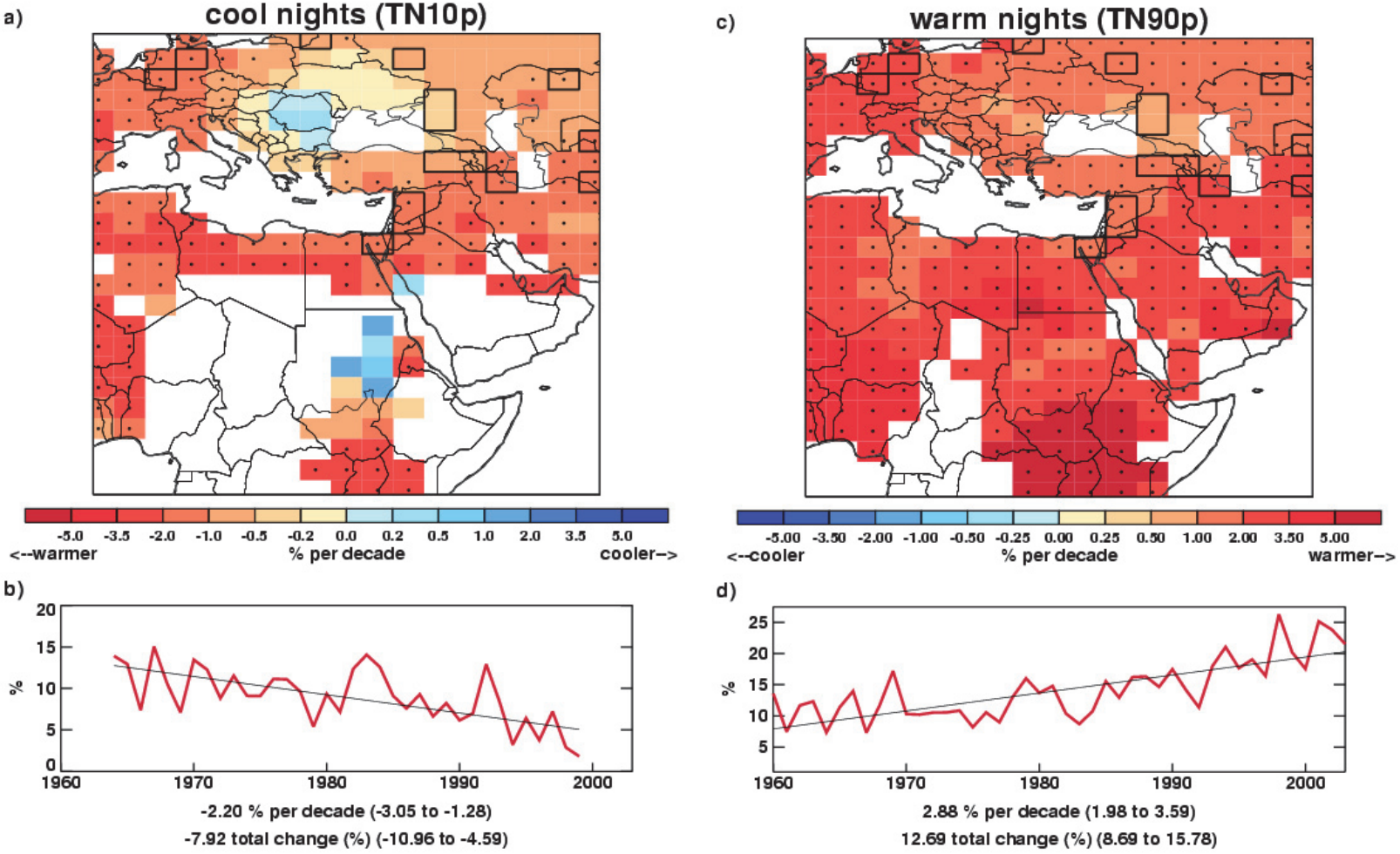
a)
cool nights (TN10p)
-5.0 -3.5 -2.0 -1.0 -0.5 -0.2 0.0 0.2 0.5 1.0 2.0 3.5 5.0
<--warmer
% per decade
cooler-->
b)
%
20
15
10
5
0
1960
1970
1980
1990
2000
-2.20 % per decade (-3.05 to -1.28)
-7.92 total change (%) (-10.96 to -4.59)
c)
warm nights (TN90p)
-5.00 -3.50 -2.00 -1.00 -0.50 -0.25 0.00 0.25 0.50 1.00 2.00 3.50 5.00
<--cooler
% per decade
warmer-->
d)
%
25
20
15
10
5
1960
1970
1980
1990
2000
2.88 % per decade (1.98 to 3.59)
12.69 total change (%) (8.69 to 15.78)

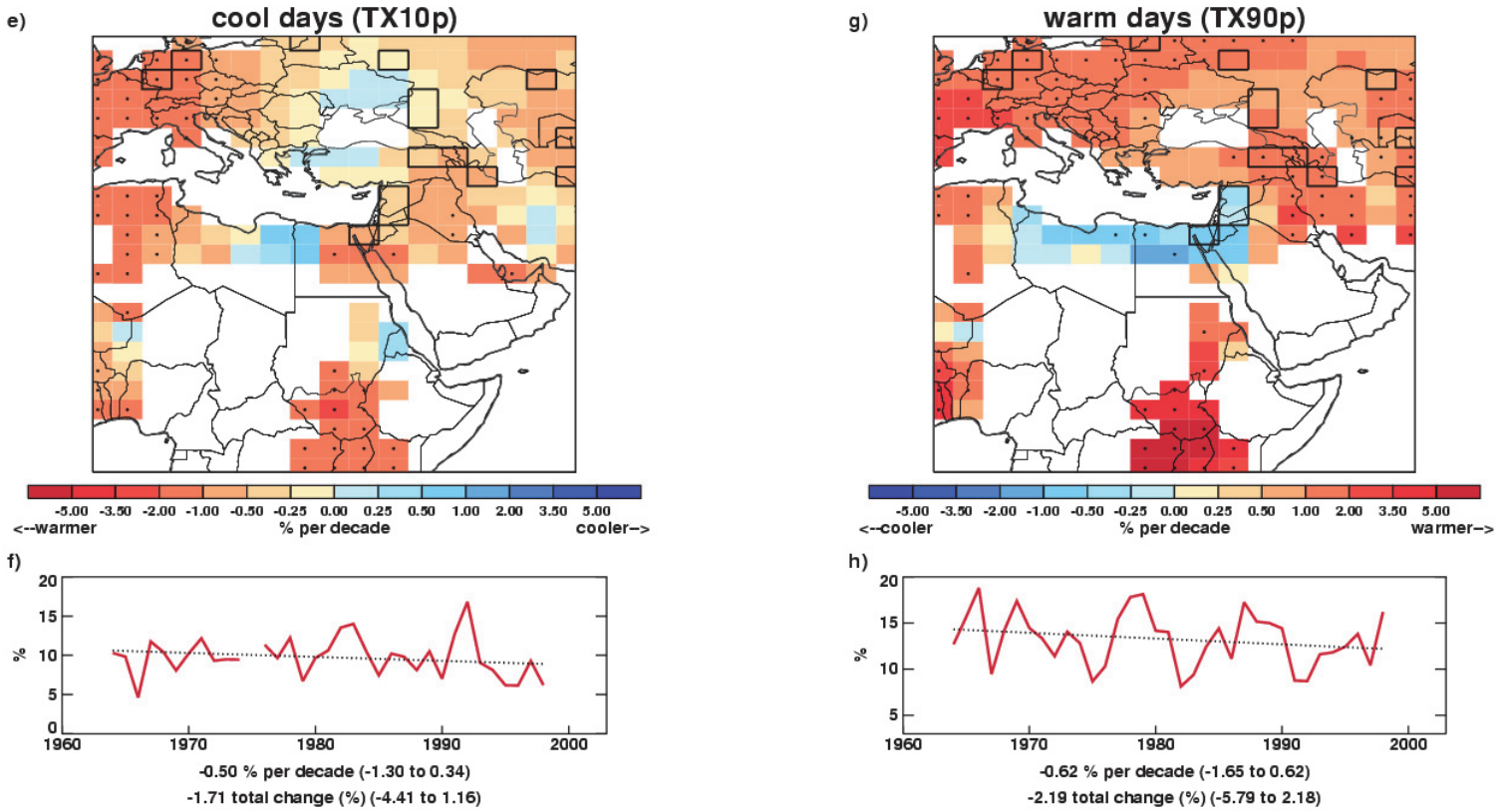

Figure 3. *Change in cool nights (a,b), warm nights (c,d), cool days (e,f) and warm days (g,h) for Egypt over the period 1960 to 2003 relative to 1961-1990 from HadEX (Alexander et al. 2006). a,c,e,g) Grid-box decadal trends. Grid-boxes outlined in solid black contain at least 3 stations and so are likely to be more representative of the wider grid box. Trends are fitted using the median of pairwise slopes method (Sen 1968, Lanzante 1996). Higher confidence in a long-term trend is shown by a black dot if the 5th to 95th percentile slopes are of the same sign. Differences in spatial coverage occur because each index has its own decorrelation length scale (see methodology annex). b,d,f,h) Area averaged annual time series for 24.375 to 35.625 ^{o} E, 21.25 to 31.25 ^{o} N as shown in the red box in Figure 1. Trends are fitted as described above. The decadal trend and its 5th to 95th percentile pairwise slopes are shown as well as the change over the period for which there are data. Higher confidence in the trends, as denoted above, is shown by a solid black line as opposed to a dotted one.*

Attribution of changes in likelihood of occurrence of seasonal mean temperatures

Today's climate covers a range of extremes. Recent research has shown that the temperature distribution of seasonal means would likely be different in the absence of anthropogenic emissions (Christidis et al., 2011). Here we discuss the seasonal means, within which the highlighted extreme temperature events occur, in the context of recent climate and the influence of anthropogenic emissions on that climate. The methods are fully described in the methodology annex.

Summer 2007

The distributions of the summer mean regional temperature in recent years in the presence and absence of anthropogenic forcings are shown in the Figure 4. Analyses with both models suggest that human influences on the climate have shifted the distribution to higher temperatures. Considering the average over the entire region, the summer of 2007 is warm, as it lies near the warm tail of the temperature distributions for the climate influenced by anthropogenic forcings (red distributions), but not as extreme as the summer of 2010, which is the hottest since 1900 in the CRUTEM3 dataset. In the absence of human influences on the climate the season lies further into the warm tail of the temperature distributions (green distributions) and would therefore be a more uncommonly warm season. The attribution results shown here refer to temperature anomalies over the entire region and over an entire season and do not rule out the occurrence of a cold extreme event that has a shorter duration and affects a smaller region.

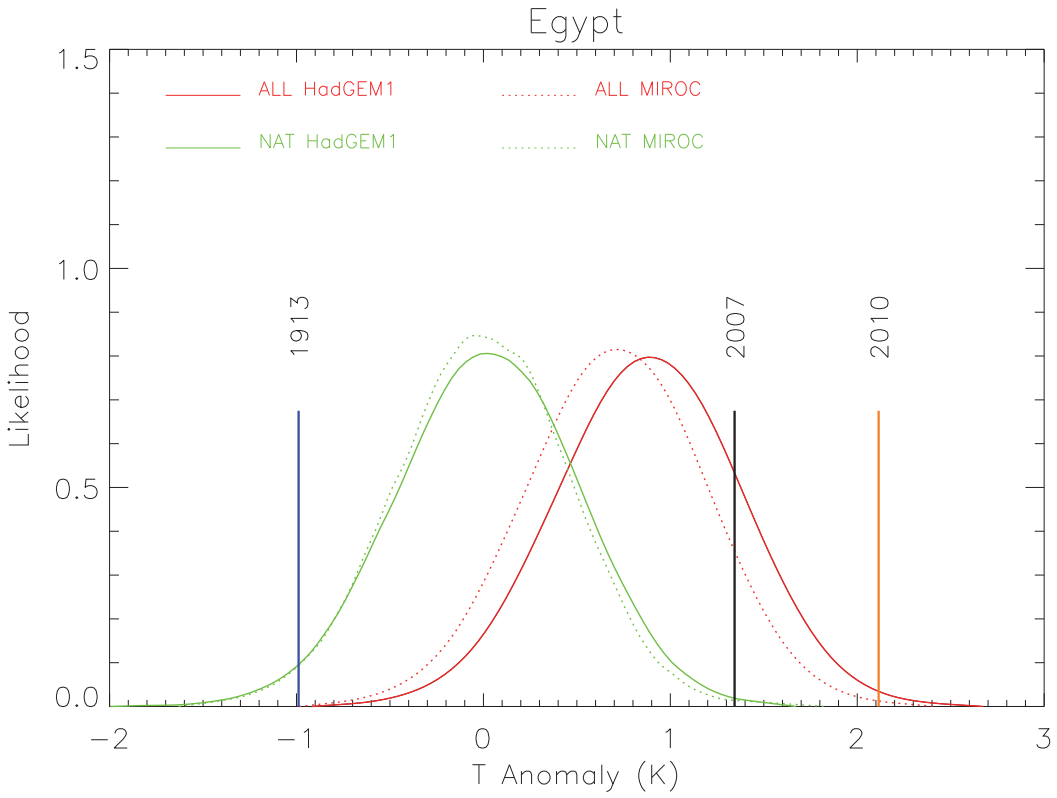

Figure 4. *Distributions of the June-July-August mean temperature anomalies (relative to 1961-1990) averaged over a region centred on Egypt (18-40E, 15-35N – as shown in Figure 1) including (red lines) and excluding (green lines) the influence of anthropogenic forcings. The distributions describe the seasonal mean temperatures expected in recent years (2000-2009) and are based on analyses with the HadGEM1 (solid lines) and MIROC (dotted lines) models. The vertical black line marks the observed anomaly in 2007 and the vertical orange and blue lines correspond to the maximum and minimum anomaly in the CRUTEM3 dataset since 1900 respectively.*

Precipitation extremes

Precipitation extremes, either excess or deficit, can be hazardous to human health, societal infrastructure, and livestock and agriculture. While seasonal fluctuations in precipitation are normal and indeed important for a number of societal sectors (e.g. tourism, farming etc.), flooding or drought can have serious negative impacts. These are complex phenomena and often the result of accumulated excesses or deficits or other compounding factors such as changes in land use. This section deals purely with precipitation amounts.Table 2 shows selected extreme events since 2000 that are reported in WMO Statements on Status of the Global Climate and/or BAMS State of the Climate reports. Flooding during January 2010 is highlighted below as an example of a recent extreme precipitation event affecting Egypt.

Year	Month	Event	Details	Source
2010	January	Flooding	Heavy rain led to worst floods in over a decade	WMO (2011)

Table 2. *Selected extreme precipitation events reported in WMO Statements on Status of the Global Climate and/or BAMS State of the Climate reports since 2000.*

Recent extreme precipitation events

Flooding, January 2010

In January 2010, heavy rain exceeding 80 mm/day, led to the worst flash-floods in Egypt since 1994 (Attaher and Medany, 2011). The floods affected the Sinai Peninsula, the Red Sea coast and the Aswan Governorate in southern Egypt, and led to 15 deaths and hundreds of homes destroyed. Approximately 3500 people were evacuated and material losses were estimated at US$25.3 million (Attaher and Medany, 2011). It was reported that the Israel border crossings with Egypt and Jordan, and five Egyptian ports, were temporarily closed (BBC, 2010).

Analysis of long-term features in precipitation

HadEX extremes indices (Alexander et al. 2006) are used here for Egypt from 1960 to 2003 using daily precipitation totals. Here we discuss changes in the annual total precipitation. The methods are fully described in the methodology annex.

As apparent in Figure 5 there are few data for precipitation over Egypt and so no conclusions can be drawn with any confidence. There is a small region of drying in the north east, where confidence in the signal is high. However, this is likely interpolated from stations over Israel. Previous research shows evidence that the severity and frequency of flash flooding over Egypt has in fact increased in recent years (EEAA-MSEA 2010). Linked to these changes and also trends in atmospheric pressure, increased severity and frequency of sand storms and haze have also been documented (EEAA-MSEA 2010).

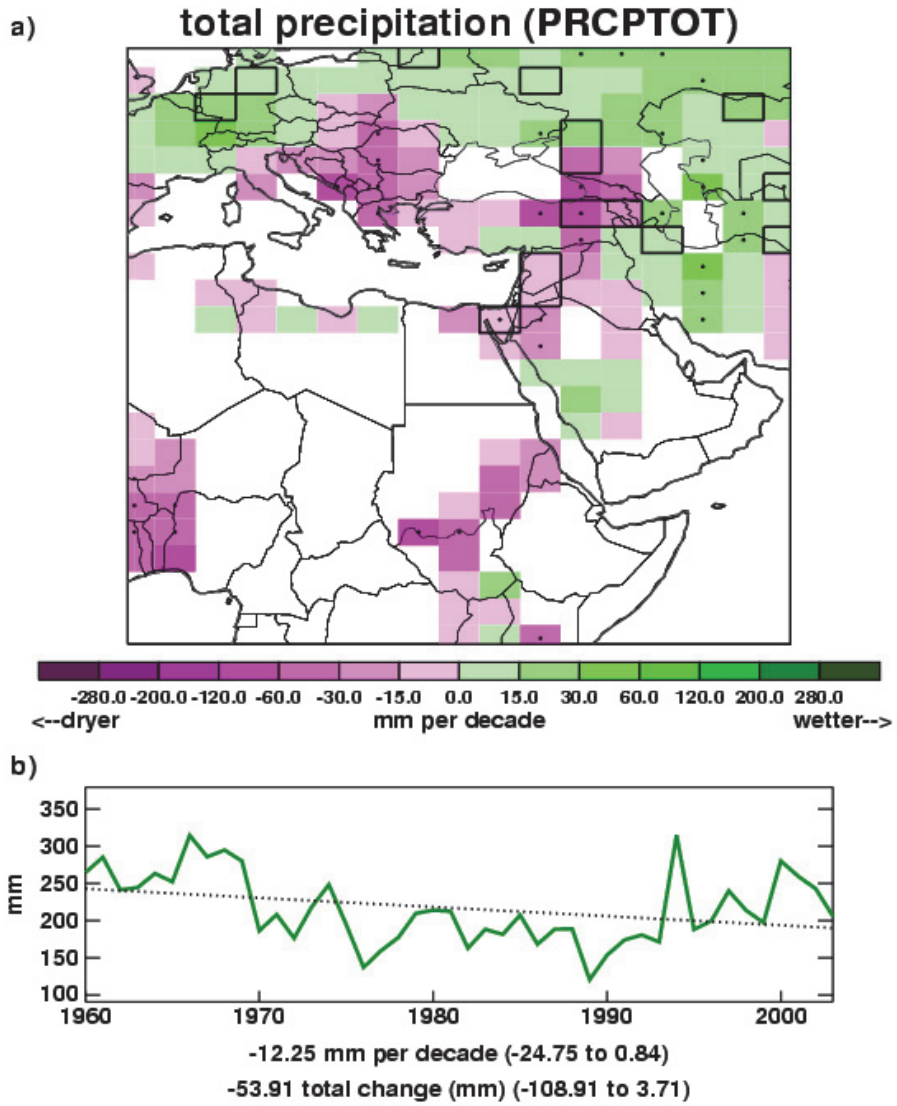

Figure 5. *Total annual precipitation for Egypt over the period 1960 to 2003 relative to 1961-1990 from HadEX (Alexander et al. 2006). a) Decadal trends as described in Figure 3. b) Area average annual time series for 24.375 to 35.625 ^{o} E, 21.25 to 31.25 ^{o} N as described in Figure 3.*

Storms

Storms can be very hazardous to all sectors of society. They can be small with localised impacts or spread across wide areas. There is no systematic observational analysis included for storms because, despite recent progress (Peterson et al., 2011; Cornes & Jones, 2011), wind data are not yet adequate for worldwide robust analysis (see methodology annex). Further progress awaits studies of the more reliable barometric pressure data through the new 20th Century Reanalysis (Compo et al., 2011) and its planned successors.

Table 3 shows selected extreme events since 2000 that are reported in WMO Statements on Status of the Global Climate and/or BAMS State of the Climate reports. In Egypt, strong winds (known as the Khamaseen) and sand storms typically occur in February-April (Attaher and Medany, 2008). A recent strong sand storm, associated with the Khamaseen, is highlighted below.

Year	Month	Event	Details	Source
2007	April	Sand storm	Strongest sand storm in 30 years.	(Attaher and Medany 2008).

***Table 3**. Selected extreme temperature events reported in WMO Statements on Status of the Global Climate and/or BAMS State of the Climate reports since 2000.*

Recent storm events

Sand storm, April 2007On 17 April a sand storm associated with the 'Khamasin' struck Egypt. It was declared the worst such storm in the last 30 years. Wind speeds reached 17 m/s and temperatures reached 36 °C, which was 8 °C above normal. Horizontal visibility fell to 100 metres leading to the shut down of the entire transport system for a day and a half (Attaher and Medany (2008)).

Summary

The main features seen in observed climate over Egypt from this analysis are:

- There have been widespread warming trends over Egypt since 1960 with greater warming in summer than winter.

- Between 1960 and 2003, there has been an increase in the frequency of warm nights and a decrease in the frequency of cool nights.

- There has been a general increase in summer temperatures averaged over the country as a result of human influence on climate, making the occurrence of warm summer temperatures more frequent and cold summer temperatures less frequent.

Methodology annex

Recent, notable extremes

In order to identify that by 'recent' events the authors have used the period since 1994, when WMO Status of the Climate statements were available to the authors. However, where possible, the most notable events during the last 10 years have been chosen as these are most widely reported in the media, remain closest to the forefront of the memory of the country affected, and provide an example likely to be most relevant to today's society. By 'notable' the authors mean any event which has had significant impact either in terms of cost to the economy, loss of life, or displacement and long term impact on the population. In most cases the events of largest impact on the population have been chosen, however this is not always the case.

Tables of recent, notable extreme events have been provided for each country. These have been compiled using data from the World Meteorological Organisation (WMO) Annual Statements on the Status of the Climate. This is a yearly report which includes contributions from all the member countries, and therefore represents a global overview of events that have had importance on a national scale. The report does not claim to capture all events of significance, and consistency across the years of records available is variable. However, this database provides a concise yet broad account of extreme events per country. This data is then supplemented with accounts from the monthly National Oceanic and Atmospheric Administration (NOAA) State of the Climate reports which outline global extreme events of meteorological significance.

We give detailed examples of heat, precipitation and storm extremes for each country where these have had significant impact. Where a country is primarily affected by precipitation or heat extremes this is where our focus has remained. An account of the impact on human life, property and the economy has been given, based largely on media reporting of events, and official reports from aid agencies, governments and meteorological organisations. Some data has also been acquired from the Centre for Research on Epidemiological Disasters (CRED) database on global extreme events. Although media reports are unlikely to be completely accurate, they do give an indication as to the perceived impact of an extreme event, and so are useful in highlighting the events which remain in the national psyche.

Our search for data has not been exhaustive given the number of countries and events included. Although there are a wide variety of sources available, for many events, an official

account is not available. Therefore figures given are illustrative of the magnitude of impact only (references are included for further information on sources). It is also apparent that the reporting of extreme events varies widely by region, and we have, where possible, engaged with local scientists to better understand the impact of such events.

The aim of the narrative for each country is to provide a picture of the social and economic vulnerability to the current climate. Examples given may illustrate the impact that any given extreme event may have and the recovery of a country from such an event. This will be important when considering the current trends in climate extremes, and also when examining projected trends in climate over the next century.

Observational record

In this section we outline the data sources which were incorporated into the analysis, the quality control procedure used, and the choices made in the data presentation. As this report is global in scope, including 24 countries, it is important to maintain consistency of methodological approach across the board. For this reason, although detailed datasets of extreme temperatures, precipitation and storm events exist for various countries, it was not possible to obtain and incorporate such a varied mix of data within the timeframe of this project. Attempts were made to obtain regional daily temperature and precipitation data from known contacts within various countries with which to update existing global extremes databases. No analysis of changes in storminess is included as there is no robust historical analysis of global land surface winds or storminess currently available.

Analysis of seasonal mean temperature

Mean temperatures analysed are obtained from the CRUTEM3 global land-based surface-temperature data-product (Brohan et al. 2006), jointly created by the Met Office Hadley Centre and Climatic Research Unit at the University of East Anglia. CRUTEM3 comprises of more than 4000 weather station records from around the world. These have been averaged together to create 5° by 5° gridded fields with no interpolation over grid boxes that do not contain stations. Seasonal averages were calculated for each grid box for the 1960 to 2010 period and linear trends fitted using the median of pairwise slopes (Sen 1968; Lanzante 1996). This method finds the slopes for all possible pairs of points in the data, and takes their median. This is a robust estimator of the slope which is not sensitive to outlying points. High confidence is assigned to any trend value for which the 5^{th} to 95^{th} percentiles of the pairwise slopes are of the same sign as the trend value and thus inconsistent with a zero trend.

Analysis of temperature and precipitation extremes using indices

In order to study extremes of climate a number of indices have been created to highlight different aspects of severe weather. The set of indices used are those from the World Climate Research Programme (WCRP) Climate Variability and Predictability (CLIVAR) Expert Team on Climate Change Detection and Indices (ETCCDI). These 27 indices use daily rainfall and maximum and minimum temperature data to find the annual (and for a subset of the indices, monthly) values for, e.g., the 'warm' days where daily maximum temperature exceeds the 90^{th} percentile maximum temperature as defined over a 1961 to 1990 base period. For a full list of the indices we refer to the Appendix and the website of the ETCCDI (http://cccma.seos.uvic.ca/ETCCDI/index.shtml).

Index	Description	Shortname	Notes
Cool night frequency	Daily minimum temperatures lower than the 10th percentile daily minimum temperature using the base reference period 1961-1990	TN10p	---
Warm night frequency	Daily minimum temperatures higher than the 90th percentile daily minimum temperature using the base reference period 1961-1990	TN90p	---
Cool day frequency	Daily maximum temperatures lower than the 10th percentile daily maximum temperature using the base reference period 1961-1990	TX10p	---
Warm day frequency	Daily maximum temperatures higher than the 90th percentile daily maximum temperature using the base reference period 1961-1990	TX90p	---
Dry spell duration	Maximum duration of continuous days within a year with rainfall <1mm	CDD	Lower data coverage due to the requirement for a 'dry spell' to be at least 6 days long resulting in intermittent temporal coverage
Wet spell duration	Maximum duration of continuous days with rainfall >1mm for a given year	CWD	Lower data coverage due to the requirement for a 'wet spell' to be at least 6 days long resulting in intermittent temporal coverage
Total annual precipitation	Total rainfall per year	PRCPTOT	---

Table 4. *Description of ETCCDI indices used in this document.*

A previous global study of the change in these indices, containing data from 1951-2003 can be found in Alexander et al. 2006, (HadEX; see http://www.metoffice.gov.uk/hadobs/hadex/). In this work we aimed to update this analysis to the present day where possible, using the most recently available data. A subset of the indices is used here because they are most easily related to extreme climate events (Table 4).

Use of HadEX for analysis of extremes

The HadEX dataset comprises all 27 ETCCDI indices calculated from station data and then smoothed and gridded onto a 2.5° x 3.75° grid, chosen to match the output from the Hadley Centre suite of climate models. To update the dataset to the present day, indices are calculated from the individual station data using the RClimDex/FClimDex software; developed and maintained on behalf of the ETCCDI by the Climate Research Branch of the Meteorological Service of Canada. Given the timeframe of this project it was not possible to obtain sufficient station data to create updated HadEX indices to present day for a number of countries: Brazil; Egypt; Indonesia; Japan (precipitation only); South Africa; Saudi Arabia; Peru; Turkey; and Kenya. Indices from the original HadEX data-product are used here to show changes in extremes of temperature and precipitation from 1960 to 2003. In some cases the data end prior to 2003. Table 2 summarises the data used for each country. Below, we give a short summary of the methods used to create the HadEX dataset (for a full description see Alexander *et al.* 2006), and in Section 2.2.2.3 the quality control, smoothing and gridding procedures used for the updated data are described.

To account for the uneven spatial coverage when creating the HadEX dataset, the indices for each station were gridded, and a land-sea mask from the HadCM3 model applied. The interpolation method used in the gridding process uses a decorrelation length scale (DLS) to determine which stations can influence the value of a given grid box. This DLS is calculated from the e-folding distance of the individual station correlations. The DLS is calculated separately for five latitude bands, and then linearly interpolated between the bands. There is a noticeable difference in spatial coverage between the indices due to these differences in decorrelation length scales. This means that there will be some grid-box data where in fact there are no stations underlying it. Here we apply black borders to grid-boxes where at least 3 stations are present to denote greater confidence in representation of the wider grid-box area there. The land-sea mask enables the dataset to be used directly for model comparison with output from HadCM3. It does mean, however, that some coastal regions and islands over which one may expect to find a grid-box are in fact empty because they have been treated as sea.

Data sources used for updates to the HadEX analysis of extremes

We use a number of different data sources to provide sufficient coverage to update as many countries as possible to present day. These are summarised in Table 5. In building the new datasets we have tried to use exactly the same methodology as was used to create the original HadEX (described in the previous section) to retain consistency with a product that

was created through substantial international effort and widely used, but there are some differences, which are described in the next section.

Wherever new data have been used, the geographical distributions of the trends were compared to those obtained from HadEX, using the same grid size, time span and fitting method. If the pattern of the trends in the temperature or precipitation indices did not match that from HadEX, we used the HadEX data despite its generally shorter time span. Differences in the patterns of the trends in the indices can arise because the individual stations used to create the gridded results are different from those in HadEX, and the quality control procedures used are also very likely to be different. Countries where we decided to use HadEX data despite the existence of more recent data are Egypt and Turkey.

GHCND:

The Global Historical Climate Network Daily data has near-global coverage. However, to ensure consistency with the HadEX database, the GHCND stations were compared to those stations in HadEX. We selected those stations which are within 1500m of the stations used in the HadEX database and have a high correlation with the HadEX stations. We only took the precipitation data if its r>0.9 and the temperature data if one of its r-values >0.9. In addition, we required at least 5 years of data beyond 2000. These daily data were then converted to the indices using the *fclimdex* software.

ECA&D and SACA&D:

The European Climate Assessment and Dataset and the Southeast Asian Climate Assessment and Dataset data are pre-calculated indices comprising the core 27 indices from the ETCCDI as well as some extra ones. We kindly acknowledge the help of Albert Klein Tank, the KNMI[1] and the BMKG[2] for their assistance in obtaining these data.

Mexico:

The station data from Mexico has been kindly supplied by the SMN[3] and Jorge Vazquez. These daily data were then converted to the required indices using the *Fclimdex* software. There are a total of 5298 Mexican stations in the database. In order to select those which have sufficiently long data records and are likely to be the most reliable ones we performed a cross correlation between all stations. We selected those which had at least 20 years of

[1] Koninklijk Nederlands Meteorologisch Instituut – The Royal Netherlands Meteorological Institute

[2] Badan Meteorologi, Klimatologi dan Geofisika – The Indonesian Meteorological, Climatological and Geophysical Agency

[3] Servicio Meteorológico Nacional de México – The Mexican National Meteorological Service

data post 1960 and have a correlation with at least one other station with an *r*-value >0.95. This resulted in 237 stations being selected for further processing and analysis.

Indian Gridded:

The India Meteorological Department provided daily gridded data (precipitation 1951-2007, temperature 1969-2009) on a 1° x 1° grid. These are the only gridded daily data in our analysis. In order to process these in as similar a way as possible the values for each grid were assumed to be analogous to a station located at the centre of the grid. We keep these data separate from the rest of the study, which is particularly important when calculating the decorrelation length scale, which is on the whole larger for these gridded data.

Country	**Region box** (red dashed boxes in Fig. 1 and on each map at beginning of chapter)	**Data source** (T = temperature, P = precipitation)	**Period of data coverage** (T = temperature, P = precipitation)	**Indices included** (see Table 1 for details)	**Temporal resolution available**	**Notes**
Argentina	73.125 to 54.375 ^{o} W, 21.25 to 56.25 ^{o} S	Matilde Rusticucci (T,P)	1960-2010 (T,P)	TN10p, TN90p, TX10p, TX90p, PRCPTOT, CDD, CWD	annual	
Australia	114.375 to 155.625 ^{o} E, 11.25 to 43.75 ^{o} S	GHCND (T,P)	1960-2010 (T,P)	TN10p, TN90p, TX10p, TX90p, PRCPTOT, CDD, CWD	monthly, seasonal and annual	Land-sea mask has been adapted to include Tasmania and the area around Brisbane
Bangladesh	88.125 to 91.875 ^{o} E, 21.25 to 26.25 ^{o} N	Indian Gridded data (T,P)	1960-2007 (P), 1970-2009 (T)	TN10p, TN90p, TX10p, TX90p, PRCPTOT, CDD, CWD	monthly, seasonal and annual	Interpolated from Indian Gridded data
Brazil	73.125 to 31.875 ^{o} W, 6.25 ^{o} N to 33.75 ^{o} S	HadEX (T,P)	1960-2000 (P) 2002 (T)	TN10p, TN90p, TX10p, TX90p, PRCPTOT, CDD, CWD	annual	Spatial coverage is poor
Canada	140.625 to 54.375 ^{o} W, 41.25 to 71.25 ^{o} N	GHCND (T,P)	1960-2010 (T,P)	TN10p, TN90p, TX10p, TX90p, PRCPTOT, CDD, CWD	monthly, seasonal and annual	
China	73.125 to 133.125 ^{o} E, 21.25 to 53.75 ^{o} N	GHCND (T,P)	1960-1997 (P) 1960-2003 (T_{min}) 1960-2010 (T_{max})	TN10p, TN90p, TX10p, TX90p, PRCPTOT, CDD, CWD	monthly, seasonal and annual	Precipitation has very poor coverage beyond 1997 except in 2003-04, and no data at all in 2000-02, 2005-11
Egypt	24.375 to 35.625 ^{o} E, 21.25 to 31.25 ^{o} N	HadEX (T,P)	No data	TN10p, TN90p, TX10p, TX90p, PRCPTOT,	annual	There are no data for Egypt so all grid-box values have been interpolated from stations in Jordan, Israel, Libya and Sudan
France	5.625 ^{o} W to 9.375 ^{o} E, 41.25 to 51.25 ^{o} N	ECA&D (T,P)	1960-2010 (T,P)	TN10p, TN90p, TX10p, TX90p, PRCPTOT, CDD, CWD	monthly, seasonal and annual	

Germany	5.625 to 16.875 ^{o} E, 46.25 to 56.25 ^{o} N	ECA&D (T,P)	1960-2010 (T,P)	TN10p, TN90p, TX10p, TX90p, PRCPTOT, CDD, CWD	monthly, seasonal and annual	
India	69.375 to 99.375 ^{o} E, 6.25 to 36.25 ^{o} N	Indian Gridded data (T,P)	1960-2003 (P), 1970-2009 (T)	TN10p, TN90p, TX10p, TX90p, PRCPTOT, CDD, CWD	monthly, seasonal and annual	
Indonesia	95.625 to 140.625 ^{o} E, 6.25 ^{o} N to 11.25 ^{o} S	HadEX (T,P)	1968-2003 (T,P)	TN10p, TN90p, TX10p, TX90p, PRCPTOT,	annual	Spatial coverage is poor
Italy	5.625 to 16.875 ^{o} E, 36.25 to 46.25 ^{o} N	ECA&D (T,P)	1960-2010 (T,P)	TN10p, TN90p, TX10p, TX90p, PRCPTOT, CDD, CWD	monthly, seasonal and annual	Land-sea mask has been adapted to improve coverage of Italy
Japan	129.375 to 144.375 ^{o} E, 31.25 to 46.25 ^{o} N	HadEX (P) GHCND (T)	1960-2003 (P) 1960-2000 (T_{min}) 1960-2010 (T_{max})	TN10p, TN90p, TX10p, TX90p, PRCPTOT,	monthly, seasonal and annual (T), annual (P)	
Kenya	31.875 to 43.125 ^{o} E, 6.25 ^{o} N to 6.25 ^{o} S	HadEX (T,P)	1960-1999 (P)	TN10p, TN90p, TX10p, TX90p, PRCPTOT	annual	There are no temperature data for Kenya and so grid-box values have been interpolated from neighbouring Uganda and the United Republic of Tanzania. Regional averages include grid-boxes from outside Kenya that enable continuation to 2003
Mexico	118.125 to 88.125 ^{o} W, 13.75 to 33.75 ^{o} N	Raw station data from the Servicio Meteorológico Nacional (SMN) (T,P)	1960-2009 (T,P)	TN10p, TN90p, TX10p, TX90p, PRCPTOT, CDD, CWD	monthly, seasonal and annual	237/5298 stations selected. Non uniform spatial coverage. Drop in T and P coverage in 2009.
Peru	84.735 to 65.625 ^{o} W, 1.25 ^{o} N to 18.75 ^{o} S	HadEX (T,P)	1960-2002 (T,P)	TN10p, TN90p, TX10p, TX90p, PRCPTOT, CDD, CWD	annual	Intermittent coverage in TX90p, CDD and CWD

Russia	West Russia 28.125 to 106.875 ° E, 43.75 to 78.75 ° N, East Russia 103.125 to 189.375 ° E, 43.75 to 78.75 ° N	ECA&D (T,P)	1960-2010 (T,P)	TN10p, TN90p, TX10p, TX90p, PRCPTOT, CDD, CWD	monthly, seasonal and annual	Country split for presentation purposes only.
Saudi Arabia	31.875 to 54.375 ° E, 16.25 to 33.75 ° N	HadEX (T,P)	1960-2000 (T,P)	TN10p, TN90p, TX10p, TX90p, PRCPTOT	annual	Spatial coverage is poor
South Africa	13.125 to 35.625 ° W, 21.25 to 36.25 ° S	HadEX (T,P)	1960-2000 (T,P)	TN10p, TN90p, TX10p, TX90p, PRCPTOT, CDD, CWD	annual	---
South Korea	125.625 to 129.375 ° E, 33.75 to 38.75 ° N	HadEX (T,P)	1960-2003 (T,P)	TN10p, TN90p, TX10p, TX90p, PRCPTOT, CDD	annual	There are too few data points for CWD to calculate trends or regional timeseries
Spain	9.375 ° W to 1.875 ° E, 36.25 to 43.75 ° N	ECA&D (T,P)	1960-2010 (T,P)	TN10p, TN90p, TX10p, TX90p, PRCPTOT, CDD, CWD	monthly, seasonal and annual	
Turkey	24.375 to 46.875 ° E, 36.25 to 43.75 ° N	HadEX (T,P)	1960-2003 (T,P)	TN10p, TN90p, TX10p, TX90p, PRCPTOT, CDD, CWD	annual	Intermittent coverage in CWD and CDD with no regional average beyond 2000
United Kingdom	9.375 ° W to 1.875 ° E, 51.25 to 58.75 ° N	ECA&D (T,P)	1960-2010 (T,P)	TN10p, TN90p, TX10p, TX90p, PRCPTOT, CDD, CWD	monthly, seasonal and annual	
United States of America	125.625 to 65.625 ° W, 23.75 to 48.75 ° N	GHCND (T,P)	1960-2010 (T,P)	TN10p, TN90p, TX10p, TX90p, PRCPTOT, CDD, CWD	monthly, seasonal and annual	

Table 5. *Summary of data used for each country*

Quality control and gridding procedure used for updates to the HadEX analysis of extremes

In order to perform some basic quality control checks on the index data, we used a two-step process on the indices. Firstly, internal checks were carried out, to remove cases where the 5 day rainfall value is less than the 1 day rainfall value, the minimum T_min is greater than the minimum T_max and the maximum T_min is greater than the maximum T_max. Although these are physically impossible, they could arise from transcription errors when creating the daily dataset, for example, a misplaced minus sign, an extra digit appearing in the record or a column transposition during digitisation. During these tests we also require that there are at least 20 years of data in the period of record for the index for that station, and that some data is found in each decade between 1961 and 1990, to allow a reasonable estimation of the climatology over that period.

Weather conditions are often similar over many tens of kilometers and the indices calculated in this work are even more coherent. The correlation coefficient between each station-pair combination in all the data obtained is calculated for each index (and month where appropriate), and plotted as a function of the separation. An exponential decay curve is fitted to the data, and the distance at which this curve has fallen by a factor 1/*e* is taken as the decorrelation length scale (DLS). A DLS is calculated for each dataset separately. For the GHCND, a separate DLS is calculated for each hemisphere. We do not force the fitted decay curve to show perfect correlation at zero distance, which is different to the method employed when creating HadEX. For some of the indices in some countries, no clear decay pattern was observed in some data sets or the decay was so slow that no value for the DLS could be determined. In these cases a default value of 200km was used.

We then perform external checks on the index data by comparing the value for each station with that of its neighbours. As the station values are correlated, it is therefore likely that if one station measures a high value for an index for a given month, its neighbours will also be measuring high. We exploit this coherence to find further bad values or stations as follows. Although raw precipitation data shows a high degree of localisation, using indices which have monthly or annual resolution improves the coherence across wider areas and so this neighbour checking technique is a valid method of finding anomalous stations.

We calculate a climatology for each station (and month if appropriate) using the mean value for each index over the period 1961-1990. The values for each station are then anomalised using this climatology by subtracting this mean value from the true values, so that it is clear if the station values are higher or lower than normal. This means that we do not need to take

differences in elevation or topography into account when comparing neighbours, as we are not comparing actual values, but rather deviations from the mean value.

All stations which are within the DLS distance are investigated and their anomalised values noted. We then calculate the weighted median value from these stations to take into account the decay in the correlation with increasing distance. We use the median to reduce the sensitivity to outliers.

If the station value is greater than 7.5 median-absolute-deviations away from the weighted median value (this corresponds to about 5 standard deviations if the distribution is Gaussian, but is a robust measure of the spread of the distribution), then there is low confidence in the veracity of this value and so it is removed from the data.

To present the data, the individual stations are gridded on a 3.75^{o} x 2.5^{o} grid, matching the output from HadCM3. To determine the value of each grid box, the DLS is used to calculate which stations can reasonably contribute to the value. The value of each station is then weighted using the DLS to obtain a final grid box value. At least three stations need to have valid data and be near enough (within 1 DLS of the gridbox centre) to contribute in order for a value to be calculated for the grid point. As for the original HadEX, the HadCM3 land-sea mask is used. However, in three cases the mask has been adjusted as there are data over Tasmania, eastern Australia and Italy that would not be included otherwise (Figure 6).

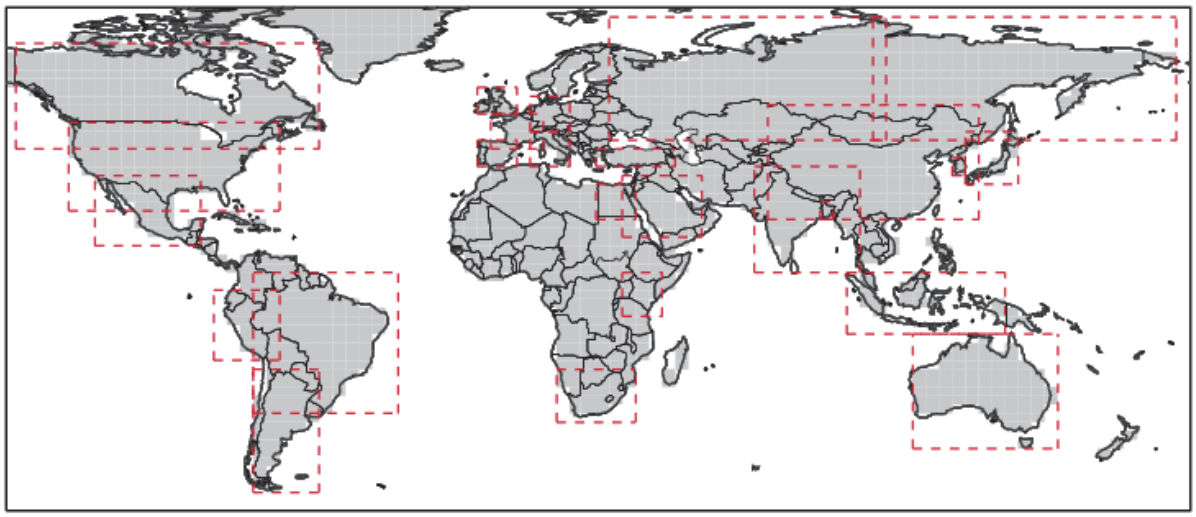

Figure 6. *Land Sea mask used for gridding the station data and regional areas allocated to each country as described in Table 5.*

Presentation of extremes of temperature and precipitation

Indices are displayed as regional gridded maps of decadal trends and regional average time-series with decadal trends where appropriate. Trends are fitted using the median of pairwise

slopes method (Sen 1968, Lanzante 1996). Trends are considered to be significantly different from a zero trend if the 5th to 95th percentiles of the pairwise slopes do not encompass zero. This is shown by a black dot in the centre of the grid-box or by a solid line on time-series plots. This infers that there is high confidence in the sign (positive or negative) of the sign. Confidence in the trend magnitude can be inferred by the spread of the 5th to 95th percentiles of the pairwise slopes which is given for the regional average decadal trends. Trends are only calculated when there are data present for at least 50% of years in the period of record and for the updated data (not HadEX) there must be at least one year in each decade.

Due to the practice of data-interpolation during the gridding stage (using the DLS) there are values for some grid boxes when no actually station lies within the grid box. There is more confidence in grid boxes for which there are underlying data. For this reason, we identify those grid boxes which contain at least 3 stations by a black contour line on the maps. The DLS differs with region, season and index which leads to large differences in the spatial coverage. The indices, by their nature of being largely threshold driven, can be intermittent over time which also effects spatial and temporal coverage (see Table 4).

Each index (and each month for the indices for which there is monthly data) has a different DLS, and so the coverage between different indices and datasets can be different. The restrictions on having at least 20 years of data present for each input station, at least 50% of years in the period of record and at least one year in each decade for the trending calculation, combined with the DLS, can restrict the coverage to only those regions with a dense station network reporting reliably.

Each country has a rectangular region assigned as shown by the red dashed box on the map in Figure 6 and listed in Table 5, which is used for the creation of the regional average. This is sometimes identical to the attribution region shown in grey on the map in Figure 6. This region is again shown on the maps accompanying the time series of the regional averages as a reminder of the region and grid boxes used in the calculation. Regional averages are created by weighting grid box values by the cosine of their grid box centre latitude. To ensure consistency over time a regional average is only calculated when there are a sufficient number of grid boxes present. The full-period median number of grid-boxes present is calculated. For regions with a median of more than six grid-boxes there must be at least 80% of the median number of grid boxes present for any one year to calculate a regional average. For regions with six or fewer median grid boxes this is relaxed to 50%. These limitations ensure that a single station or grid box which has a longer period of record than its neighbours cannot skew the timeseries trend. So sometimes there may be grid-boxes

present but no regional average time series. The trends for the regional averages are calculated in the same way as for the individual grid boxes, using the median of pairwise slopes method (Sen 1968, Lanzante 1996). Confidence in the trend is also determined if the 5^{th} to 95^{th} percentiles of the pairwise slopes are of the same sign and thus inconsistent with a zero trend. As well as the trend in quantity per decade, we also show the full change in the quantity from 1960 to 2010 that this fitted linear trend implies.

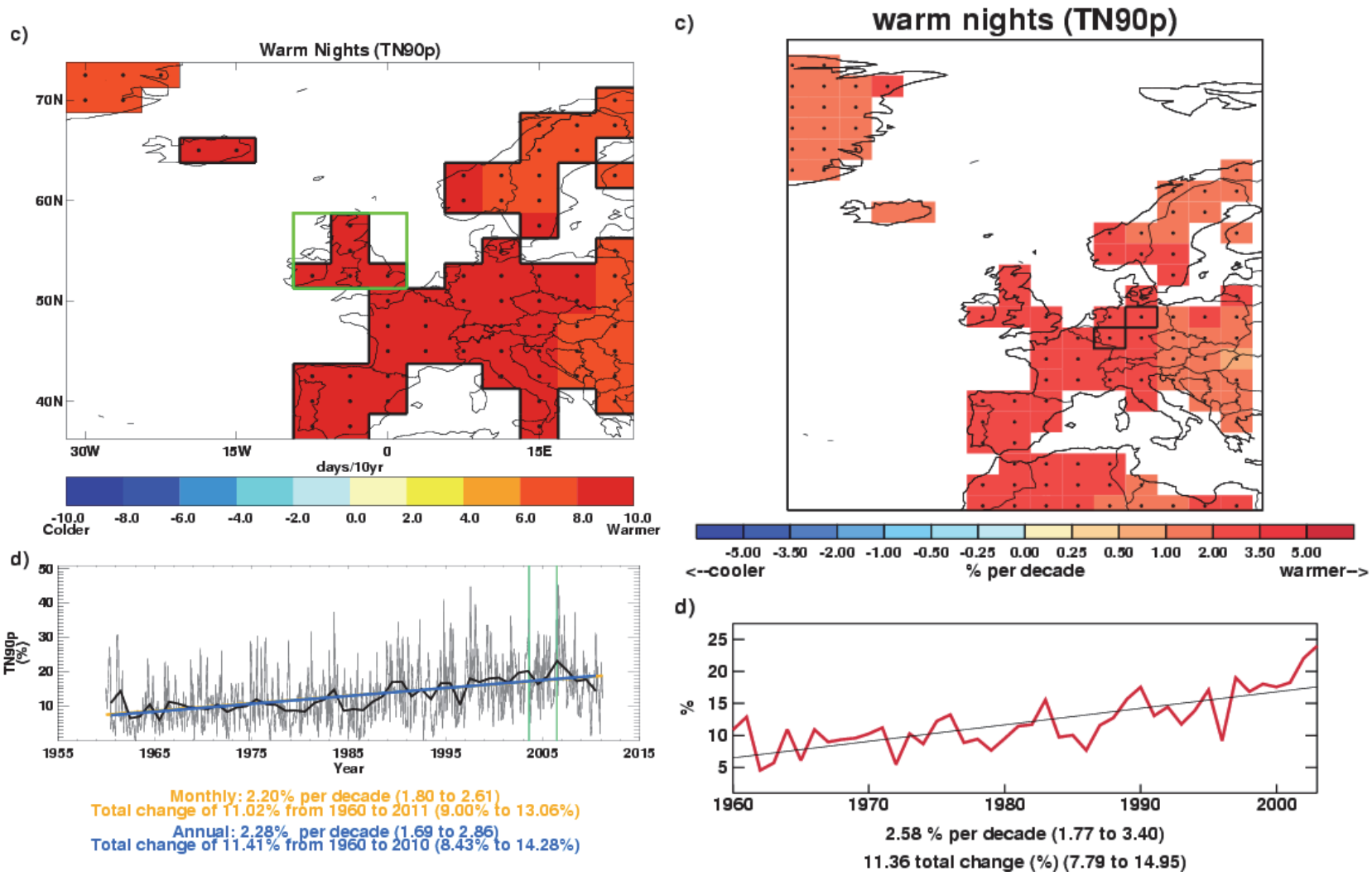

Figure 7. *Examples of the plots shown in the data section. Left: From ECA&D data between 1960-2010 for the number of warm nights, and Right: from HadEX data (1960-2003) for the total precipitation. A full explanation of the plots is given in the text below.*

The results are presented in the form of a map and a time series for each country and index. The map shows the grid box decadal trend in the index over the period for which there are data. High confidence, as determined above, is shown by a black dot in the grid box centre. To show the variation over time, the values for each year (and month if available) are shown in a time series for a regional average. The values of the indices have been normalised to a base period of 1961-1990 (except the Indian gridded data which use a 1971 to 1990 period), both in HadEX and in the new data acquired for this project. Therefore, for example, the percentage of nights exceeding the 90th percentile in T_min is 10% for that period.

There are two influences on whether a grid box contains a value or not – the land-sea mask, and the decorrelation length scale. The land-sea mask is shown in Figure 6. There are grid boxes which contain some land but are mostly sea and so are not considered. The decorrelation length scale sets the maximum distance a grid box can be from stations before no value is assigned to it. Grid boxes containing three or more stations are highlighted by a thick border. This indicates regions where the value shown is likely to be more representative of the grid box area mean as opposed to a single station location.

On the maps for the new data there is a box indicating which grid boxes have been extracted to calculate the area average for the time series. This box is the same as shown in Figure 6 at the beginning of each country's document. These selected grid boxes are combined using area (cosine) weighting to calculate the regional average (both annual [thick lines] and monthly [thin lines] where available). Monthly (orange) and annual (blue) trends are fitted to these time series using the method described above. The decadal trend and total change over the period where there are data are shown with 5th to 95th percentile confidence intervals in parentheses. High confidence, as determined above, is shown by a solid line as opposed to a dotted one. The green vertical lines on the time series show the dates of some of the notable events outlined in each section.

Attribution

Regional distributions of seasonal mean temperatures in the 2000s are computed with and without the effect of anthropogenic influences on the climate. The analysis considers temperatures averaged over the regions shown in Figure 8. These are also identified as grey boxes on the maps in Figure 6. The coordinates of the regions are given in Table 6. The methodology combines information from observations and model simulations using the approach originally introduced in Christidis et al., 2010 and later extended in Christidis et al., 2011, where more details can be found. The analysis requires spatial scales greater than about 2,500 km and for that reason the selected regions (Figure 8 and Table 6) are often

larger than individual countries, or include several smaller countries in a single region (for example UK, Germany and France are grouped in one region).

Observations of land temperature come from the CRUTEM3 gridded dataset (Brohan et al., 2006) and model simulations from two coupled GCMs, namely the Hadley Centre HadGEM1 model (Martin et al., 2006) and version 3.2 of the MIROC model (K-1 Developers, 2004). The use of two GCMs helps investigate the sensitivity of the results to the model used in the analysis. Ensembles of model simulations from two types of experiments are used to partition the temperature response to external forcings between its anthropogenic and natural components. The first experiment (ALL) simulates the combined effect of natural and anthropogenic forcings on the climate system and the second (ANTHRO) includes anthropogenic forcings only. The difference of the two gives an estimate of the effect of the natural forcings (NAT). Estimates of the effect of internal climate variability are derived from long control simulations of the unforced climate. Distributions of the regional summer mean temperature are computed as follows:

a) A global optimal fingerprinting analysis (Allen and Tett, 1999; Allen and Stott, 2003) is first carried out that scales the global simulated patterns (fingerprints) of climate change attributed to different combinations of external forcings to best match them to the observations. The uncertainty in the scaling that originates from internal variability leads to samples of the scaled fingerprints, i.e. several realisations that are plausibly consistent with the observations. The 2000-2009 decade is then extracted from the scaled patterns and two samples of the decadal mean temperature averaged over the reference region are then computed with and without human influences, which provide the Probability Density Functions (PDFs) of the decadal mean temperature attributable to ALL and NAT forcings.

b) Model-derived estimates of noise are added to the distributions to take into account the uncertainty in the simulated fingerprints.

c) In the same way, additional noise from control model simulations is introduced to the distributions to represent the effect of internal variability in the annual values of the seasonal mean temperatures. The result is a pair of estimated distributions of the annual values of the seasonal mean temperature in the region with and without the effect of human activity on the climate. The temperatures throughout the analysis are expressed as anomalies relative to period 1961-1990.

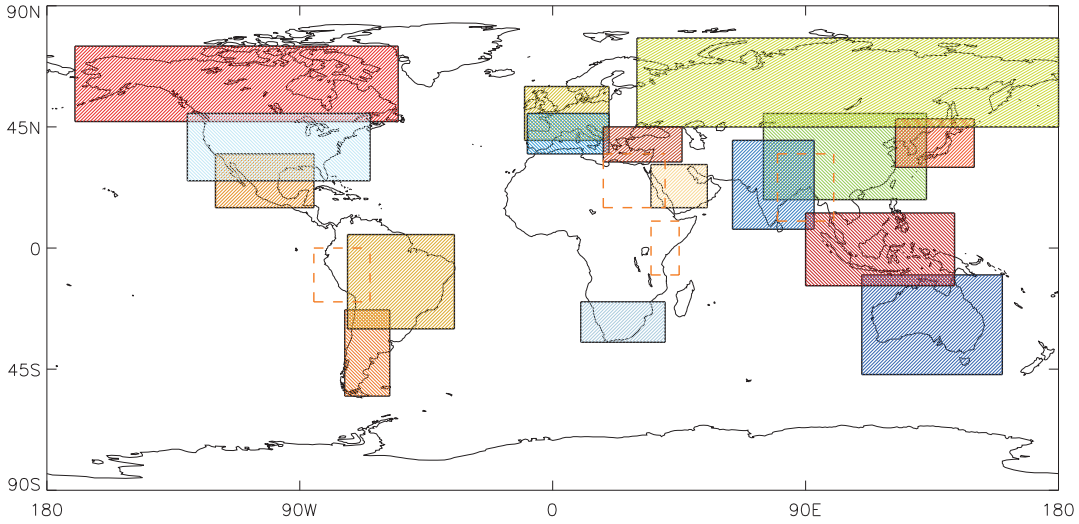

Figure 8. *The regions used in the attribution analysis. Regions marked with dashed orange boundaries correspond to non-G20 countries that were also included in the analysis.*

Region	Region Coordinates
Argentina	74-58W, 55-23S
Australia	110-160E, 47-10S
Bangladesh	80-100E, 10-35N
Brazil	73-35W, 30S-5N
Canada-Alaska	170-55W, 47-75N
China	75-133E, 18-50N
Egypt	18-40E, 15-35N
France-Germany-UK	10W-20E, 40-60N
India	64-93E, 7-40N
Indonesia	90-143E, 14S-13N
Italy-Spain	9W-20E, 35-50N
Japan-Korea	122-150E, 30-48N
Kenya	35-45E, 10S-10N
Mexico	120-85W, 15-35N
Peru	85-65W, 20-0S
Russia	30-185E, 45-78N
Saudi Arabia	35-55E, 15-31N
South Africa	10-40E, 35-20S
Turkey	18-46E, 32-45N

Table 6. *The coordinates of the regions used in the attribution analysis.*

References

ALEXANDER, L. V., ZHANG. X., PETERSON, T. C., CAESAR, J., GLEASON, B., KLEIN TANK, A. M. G., HAYLOCK, M., COLLINS, D., TREWIN, B., RAHIMZADEH, F., TAGIPOUR, A., RUPA KUMAR, K., REVADEKAR, J., GRIFFITHS, G., VINCENT, L., STEPHENSON, D. B., BURN, J., AGUILAR, E., BRUNET, M., TAYLOR, M., NEW, M., ZHAI, P., RUSTICUCCI, M. AND VAZQUEZ-AGUIRRE, J. L. 2006. Global observed changes in daily climate extremes of temperature and precipitation. *J. Geophys. Res.* 111, D05109. doi:10.1029/2005JD006290.

ALLEN M. R., TETT, S. F. B. (1999) Checking for model consistency in optimal fingerprinting. *Clim Dyn* 15: 419-434ALLEN, M. R, STOTT, P. A., (2003) Estimating signal amplitudes in optimal fingerprinting, part I: theory. *Clim Dyn* 21: 477-491

ATTAHER, S. M. AND MEDANY, M. A. 2008. Egypt in State of the Climate in 2007. LEVINSON, D. H. AND LAWRIMORE, J. H. eds. *Bulletin of the American Meteorological Society* 89, S109

ATTAHER, S. M. AND MEDANY, M. A. 2011. Adverse weather in Egypt in State of the Climate in 2010. *Bulletin of the American Meteorological Society* 92 (6), S193 BBC NEWS. 2010. Flash floods in Egypt and Israel kill seven, http://news.bbc.co.uk/1/hi/8466546.stm

BROHAN, P., KENNEDY, J.J., HARRIS, I., TETT, S.F.B. AND JONES, P.D. 2006. Uncertainty estimates in regional and global observed temperature changes: a new dataset from 1850. *J. Geophys. Res*. 111, D12106. doi:10.1029/2005JD006548.

CHRISTIDIS N., Stott, P. A., ZWIERS, F. W., SHIOGAMA, H., NOZAWA T. (2010) Probabilistic estimates of recent changes in temperature: a multi-scale attribution analysis. *Clim Dyn* 34: 1139-1156

CHRISTIDIS, N., STOTT, P. A., ZWIERS, F. W., SHIOGAMA, H., NOZAWA, T. 2011. The contribution of anthropogenic forcings to regional changes in temperature during the last decade. *Climate Dynamics* in press.

COMPO, G. P., J.S. WHITAKER, P.D. SARDESHMUKH, N. MATSUI, R.J. ALLAN, X. YIN, B.E. GLEASON, R.S. VOSE, G. RUTLEDGE, P. BESSEMOULIN, S. BRÖNNIMANN, M. BRUNET, R.I. CROUTHAMEL, A.N. GRANT, P.Y. GROISMAN, P.D. JONES, M.C. KRUK, A.C. KRUGER, G.J. MARSHALL, M. MAUGERI, H.Y. MOK, Ø. NORDLI, T.F. ROSS, R.M.

TRIGO, X.L. WANG, S.D. WOODRUFF AND S.J. WORLEY. 2011. The Twentieth Century Reanalysis Project, *Q. J. R.Met.S.* 137, 1-28, doi: 10.1002/qj.776

CORNES, R. C., AND P. D. JONES. 2011. An examination of storm activity in the northeast Atlantic region over the 1851–2003 period using the EMULATE gridded MSLP data series, *J. Geophys. Res*. 116, D16110, doi:10.1029/2011JD016007.

EEAA-MSEA - EGYPTIAN ENVIRONMENTAL AFFAIRS AGENCY. Ministry of State for Environmental Affairs. 2010. Egypt second national communication under the United Nations Framework Convention on Climate Change, http://unfccc.int/essential_background/library/items/3599.php?such=j&symbol=%20EGY/COM/2%20E#beg

EGYPT NEWS. 2007. Saturday the peak of a heat wave in Egypt, http://news.egypt.com/en/20070730323/news/-egypt-news/saturday-the-peak-of-a-heat-wave-in-egypt.html

K-1 Model Developers (2004) K-1 coupled GCM (MIROC) description, K-1 Tech Rep, H Hasumi and S Emori (eds), *Centre for Clim Sys Res*, Univ of Tokyo

LANZANTE, J. R. 1996. Resistant, robust and non-parametric techniques for the analysis of climate data: theory and examples, including applications to historical radiosonde station data. *Int. J. Clim*. 16, 1197–226.

MARTIN, G. M. , RINGER, M. A., POPE, V. D., JONES, A ., DEARDEN, C., HINTON, T. (2006) The physical properties of the atmosphere in the new Hadley Centre Global Environmental Model (HadGEM1). Part I: Model description and global climatology. *J Clim* 19: 1274-1301

PETERSON, T.C., VAUTARD, R., MCVICAR, T.R., THÉPAUT, J-N. AND BERRISFORD, P. 2011. [Global Climate] Surface Winds over Land in State of the Climate 2010. *Bulletin of the American Meteorological Society*, 92 (6), S57.

SANCHEZ-LUGO, A., KENNEDY, J.J. AND BERRISFORD, P. 2011. [Global Climate] Surface Temperatures in State of the Climate 2010. *Bulletin of the American Meteorological Society*, 92 (6), S36-S37.

SEN, P. K. 1968. Estimates of the regression coefficient based on Kendall's tau. *J. Am. Stat. Assoc*. 63, 1379–89.

WMO WORLD METEOROLOGICAL ORGANIZATION. 2008. Statement on Status of the Global Climate in 2007, WMO-NO. 1031.
http://www.wmo.int/pages/prog/wcp/wcdmp/statement/wmostatement_en.html

WMO WORLD METEOROLOGICAL ORGANIZATION. 2011. Statement on Status of the Global Climate in 2010, WMO-NO. 1074.
http://www.wmo.int/pages/prog/wcp/wcdmp/statement/wmostatement_en.html

Acknowledgements

We thank Lisa Alexander and Markus Donat (University of New South Wales) for their help and advice. We also thank reviewers from Egypt for their valuable input and advice.

Chapter 2 – Climate Change Projections

Introduction

Climate models are used to understand how the climate will evolve over time and typically represent the atmosphere, ocean, land surface, cryosphere, and biogeochemical processes, and solve the equations governing their evolution on a geographical grid covering the globe. Some processes are represented explicitly within climate models, large-scale circulations for instance, while others are represented by simplified parameterisations. The use of these parameterisations is sometimes due to processes taking place on scales smaller than the typical grid size of a climate model (a Global Climate Model (GCM) has a typical horizontal resolution of between 250 and 600km) or sometimes to the current limited understanding of these processes. Different climate modelling institutions use different plausible representations of the climate system, which is why climate projections for a single greenhouse gas emissions scenario differ between modelling institutes. This gives rise to "climate model structural uncertainty".

In response to a proposed activity of the World Climate Research Programme's (WCRP's; http://www.wcrp-climate.org/) Working Group on Coupled Modelling (WGCM), the Program for Climate Model Diagnosis and Intercomparison (PCMDI; http://www-pcmdi.llnl.gov/) volunteered to collect model output contributed by leading climate modelling centres around the world. Climate model output from simulations of the past, present and future climate was collected by PCMDI mostly during the years 2005 and 2006, and this archived data constitutes phase 3 of the Coupled Model Intercomparison Project (CMIP3). In part, the WGCM organised this activity to enable those outside the major modelling centres to perform research of relevance to climate scientists preparing the IPCC Fourth Assessment Report (AR4). This unprecedented collection of recent model output is commonly known as the "CMIP3 multi-model dataset". The GCMs included in this dataset are referred to regularly throughout this review, although not exclusively.

The CMIP3 multi-model ensemble has been widely used in studies of regional climate change and associated impacts. Each of the constituent models was subject to extensive testing by the contributing institute, and the ensemble has the advantage of having been constructed from a large pool of alternative model components, therefore sampling alternative structural assumptions in how best to represent the physical climate system. Being assembled on an opportunity basis, however, the CMIP3 ensemble was not designed to represent model uncertainties in a systematic manner, so it does not, in isolation, support robust estimates of the risk of different levels of future climate change, especially at a regional level.

Since CMIP3, a new (CMIP5) generation of coupled ocean-atmosphere models has been developed, which is only just beginning to be available and is being used for new projections for the IPCC Fifth Assessment Report (AR5).

These newer models typically feature higher spatial resolution than their CMIP3 counterparts, including in some models a more realistic representation of stratosphere-troposphere interactions. The CMIP5 models also benefit from several years of development in their parameterisations of small scale processes, which, together with resolution increases, are expected to result in a general improvement in the accuracy of their simulations of historical climate, and in the credibility of their projections of future changes. The CMIP5 programme also includes a number of comprehensive Earth System Models (ESMs) which explicitly simulate the earth's carbon cycle and key aspects of atmospheric chemistry, and also contain more sophisticated representations of aerosols compared to CMIP3 models.

The CMIP3 results should be interpreted as a useful interim set of plausible outcomes. However, their neglect of uncertainties, for instance in carbon cycle feedbacks, implies that higher levels of warming outside the CMIP3 envelope cannot be ruled out. In future, CMIP5 coupled model and ESM projections can be expected to produce improved advice on future regional changes. In particular, ensembles of ESM projections will be needed to provide a more comprehensive survey of possible future changes and their relative likelihoods of occurrence. This is likely to require analysis of the CMIP5 multi-model ESM projections, augmented by larger ensembles of ESM simulations in which uncertainties in physical and biogeochemical feedback processes can be explored more systematically, for example via ensembles of model runs in which key aspects of the climate model are slightly adjusted. Note that such an exercise might lead to the specification of wider rather than narrower uncertainties compared to CMIP3 results, if the effects of representing a wider range of earth system processes outweigh the effects of refinements in the simulation of physical atmosphere-ocean processes already included in the CMIP3 models.

Climate projections

The Met Office Hadley Centre is currently producing perturbed parameter ensembles of a single model configuration known as HadCM3C, to explore uncertainties in physical and biogeochemical feedback processes. The results of this analysis will become available in the next year and will supplement the CMIP5 multi-model ESM projections, providing a more comprehensive set of data to help progress understanding of future climate change. However, many of the studies covered in the chapter on climate impacts have used CMIP3 model output. For this reason, and because it is still the most widely used set of projections available, the CMIP3 ensemble output for temperature and precipitation, for the A1B emission scenario, for Egypt and the surrounding region is shown below.

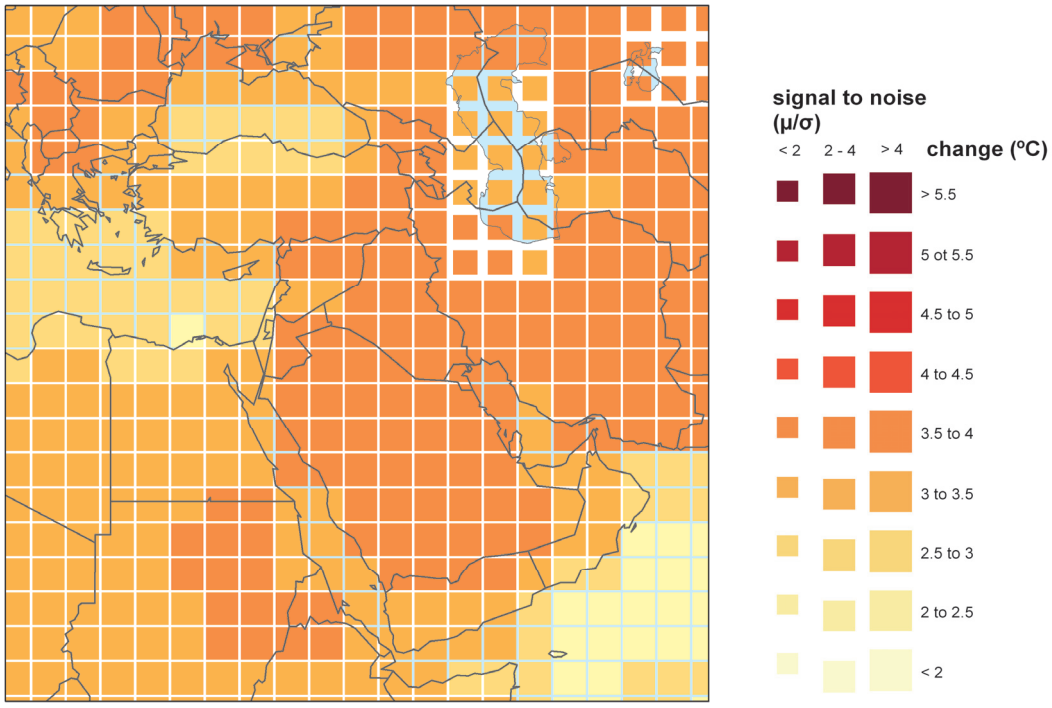

Figure 1. *Percentage change in average annual temperature by 2100 from 1960-1990 baseline climate, averaged over 21 CMIP3 models. The size of each pixel represents the level of agreement between models on the magnitude of the change.*

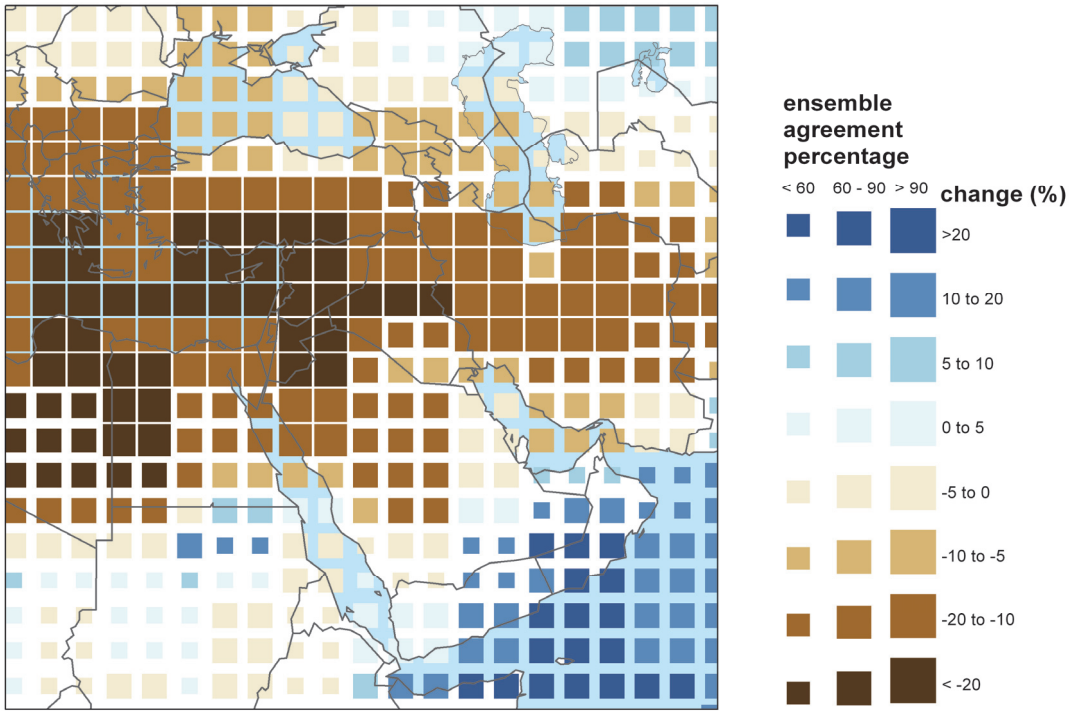

Figure 2. *Percentage change in average annual precipitation by 2100 from 1960-1990 baseline climate, averaged over 21 CMIP3 models. The size of each pixel represents the level of agreement between models on the sign of the change.*

Summary of temperature change in Egypt

Figure 1 shows the percentage change in average annual temperature by 2100 from 1960-1990 baseline climate, averaged over 21 CMIP3 models. All of the models in the CMIP3 ensemble project increased temperatures in the future, but the size of each pixel indicates how well the models agree over the magnitude of the increase.

Projected temperature increases over Egypt are around 3-3.5°C with a consistently good agreement between the models over the Middle East region in general.

Summary of precipitation change in Egypt

Figure 2 shows the percentage change in average annual precipitation by 2100 from 1960-1990 baseline climate, averaged over 21 CMIP3 models. Unlike for temperature, the models sometimes disagree over whether precipitation is increasing or decreasing over a region, so in this case the size of each pixel indicates the percentage of the models in the ensemble that agree on the sign of the change in precipitation.

Egypt is projected to experience mainly decreases in precipitation, in common with the wider Mediterranean and majority of the Middle East. Decreases of over 20% are projected in the

west of the country, with strong ensemble agreement. Smaller changes are projected towards the southeast.

Chapter 3 – Climate Change Impact Projections

Introduction

Aims and approach

This chapter looks at research on a range of projected climate change impacts, with focus on results for Egypt. It includes projections taken from the AVOID programme, for some of the impact sectors.

The aim of this work is to take a 'top down' approach to assessing global impacts studies, both from the literature and from new research undertaken by the AVOID programme. This project covers 23 countries, with summaries from global studies provided for each of these. This global approach allows some level of comparison between countries, whilst presenting information on a scale most meaningful to inform international policy.

The literature covered in this chapter focuses on research published since the Fourth Assessment Report (AR4) of the Intergovernmental Panel on Climate Change (IPCC) and should be read in conjunction with IPCC AR4 WG1 and WG2 reports. For some sectors considered, an absence of research developments since the IPCC AR4, means earlier work is cited as this helps describe the current level of scientific understanding. This report focuses on assessing scientific research about climate change impacts within sectors; it does not present an integrated analysis of climate change adaptation policies.

Some national and sub-national scale literature is reported to a limited extent to provide some regional context.

Impact sectors considered and methods

This report reviews the evidence for the impact of climate change on a number of sectors, for Egypt. The following sectors are considered in turn in this report:

- Crop yields
- Food security
- Water stress and drought
- Pluvial flooding and rainfall
- Fluvial flooding

- Tropical cyclones (where applicable)
- Coastal regions

Supporting literature

Literature searches were conducted for each sector with the Thomson Reuters Web of Science (WoS., 2011) and Google Scholar academic search engines respectively. Furthermore, climate change impact experts from each of the 23 countries reviewed were contacted. These experts were selected through a combination of government nomination and from experts known to the Met Office. They were asked to provide literature that they felt would be of relevance to this review. Where appropriate, such evidence has been included. A wide range of evidence was considered, including; research from international peer-reviewed journal papers; reports from governments, non-governmental organisations, and private businesses (e.g. reinsurance companies), and research papers published in national journals.

For each impact sector, results from assessments that include a global- or regional-scale perspective are considered separately from research that has been conducted at the national- or sub-national-scale. The consideration of global- and regional-scale studies facilitates a comparison of impacts across different countries, because such studies apply a consistent methodology for each country. While results from national- and sub-national-scale studies are not easily comparable between countries, they can provide a level of detail that is not always possible with larger-scale studies. However, the national- and sub-national scale literature included in this project does not represent a comprehensive coverage of regional-based research and cannot, and should not, replace individual, detailed impacts studies in countries. The review aims to present an up-to-date assessment of the impact of climate change on each of the sectors considered.

AVOID programme results

Much of the work in this report is drawn from modelling results and analyses coming out of the AVOID programme. The AVOID programme is a research consortium funded by DECC and Defra and led by the UK Met Office and also comprises the Walker Institute at the University of Reading, the Tyndall Centre represented through the University of East Anglia, and the Grantham Institute for Climate Change at Imperial College. The expertise in the AVOID programme includes climate change research and modelling, climate change

impacts in natural and human systems, socio-economic sciences, mitigation and technology. The unique expertise of the programme is in bringing these research areas together to produce integrated and policy-relevant results. The experts who work within the programme were also well suited to review the literature assessment part of this report. In this report the modelling of sea level rise impacts was carried out for the AVOID programme by the University of Southampton.

The AVOID programme uses the same emissions scenarios across the different impact sectors studied. These are a business as usual (IPCC SRES A1B) and an aggressive mitigation (the AVOID A1B-2016-5-L) scenario. Model output for both scenarios was taken from more than 20 GCMs and averaged for use in the impact models. The impact models are sector specific, and frequently employ further analytical techniques such as pattern scaling and downscaling in the crop yield models.

Data and analysis from AVOID programme research is provided for the following impact sectors:

- Crop yields
- Water stress and drought
- Fluvial flooding
- Coastal regions

Uncertainty in climate change impact assessment

There are many uncertainties in future projections of climate change and its impacts. Several of these are well-recognised, but some are not. One category of uncertainty arises because we don't yet know how mankind will alter the climate in the future. For instance, uncertainties in future greenhouse gas emissions depends on the future socio-economic pathway, which, in turn, depends on factors such as population, economic growth, technology development, energy demand and methods of supply, and land use. The usual approach to dealing with this is to consider a range of possible future scenarios.

Another category of uncertainties relate to our incomplete understanding of the climate system, or an inability to adequately model some aspects of the system. This includes:

- Uncertainties in translating emissions of greenhouse gases into atmospheric concentrations and radiative forcing. Atmospheric CO_2 concentrations are currently

rising at approximately 50% of the rate of anthropogenic emissions, with the remaining 50% being offset by a net uptake of CO_2 into the oceans and land biosphere. However, this rate of uptake itself probably depends on climate, and evidence suggests it may weaken under a warming climate, causing more CO_2 to remain in the atmosphere, warming climate further. The extent of this feedback is highly uncertain, but it not considered in most studies. The phase 3 of the Coupled Model Intercomparison Project (CMIP3), which provided the future climate projections for the IPCC Fourth Assessment Report (AR4), used a single estimate of CO_2 concentration rise for each emissions scenario, so the CMIP3 projections (which were used in most studies presented here, including AVOID) do not account for this uncertainty.

- Uncertainty in climate response to the forcing by greenhouse gases and aerosols. One aspect of this is the response of global mean temperature ("climate sensitivity"), but a more relevant aspect for impacts studies is the response of regional climates, including temperature, precipitation and other meteorological variables. Different climate models can give very different results in some regions, while giving similar results in other regions. Confidence in regional projections requires more than just agreement between models: physical understanding of the relevant atmospheric, ocean and land surface processes is also important, to establish whether the models are likely to be realistic.

- Additional forcings of regional climate. Greenhouse gas changes are not the only anthropogenic driver of climate change; atmospheric aerosols and land cover change are also important, and unlike greenhouse gases, the strength of their influence varies significantly from place to place. The CMIP3 models used in most impacts studies generally account for aerosols but not land cover change.

- Uncertainty in impacts processes. The consequences of a given changes in weather or climatic conditions for biophysical impacts such as river flows, drought, flooding, crop yield or ecosystem distribution and functioning depend on many other processes which are often poorly-understood, especially at large scales. In particular, the extent to which different biophysical impacts interact with each other has been hardly studied, but may be crucial; for example, impacts of climate change on crop yield may depend not only on local climate changes affecting rain-fed crops, but also remote climate changes affecting river flows providing water for irrigation.

- Uncertainties in non-climate effects of some greenhouse gases. As well as being a greenhouse gas, CO_2 exerts physiological influences on plants, affecting photosynthesis and transpiration. Under higher CO_2 concentrations, and with no other limiting factors, photosynthesis can increase, while the requirements of water for transpiration can decrease. However, while this has been extensively studied under experimental conditions, including in some cases in the free atmosphere, the extent to which the ongoing rise in ambient CO_2 affects crop yields and natural vegetation functioning remains uncertain and controversial. Many impacts projections assume CO_2 physiological effects to be significant, while others assume it to be non-existent. Studies of climate change impacts on crops and ecosystems should therefore be examined with care to establish which assumptions have been made.

In addition to these uncertainties, the climate varies significantly through natural processes from year-to-year and also decade-to-decade, and this variability can be significant in comparison to anthropogenic forcings on shorter timescales (the next few decades) particularly at regional scales. Whilst we can characterise the natural variability it will not be possible to give a precise forecast for a particular year decades into the future.

A further category of uncertainty in projections arises as a result of using different methods to correct for uncertainties and limitations in climate models. Despite being painstakingly developed in order to represent current climate as closely as possible, current climate models are nevertheless subject to systematic errors such as simulating too little or too much rainfall in some regions. In order to reduce the impact of these, '*bias correction*' techniques are often employed, in which the climate model is a source of information on the *change* in climate which is then applied to the observed present-day climate state (rather than using the model's own simulation of the present-day state). However, these bias-corrections typically introduce their own uncertainties and errors, and can lead to inconsistencies between the projected impacts and the driving climate change (such as river flows changing by an amount which is not matched by the original change in precipitation). Currently, this source of uncertainty is rarely considered

When climate change projections from climate models are applied to climate change impact models (e.g. a global hydrological model), the climate model structural uncertainty carries through to the impact estimates. Additional uncertainties include changes in future emissions and population, as well as parameterisations within the impact models (this is rarely considered). Figure 1 highlights the importance of considering climate model structural

uncertainty in climate change impacts assessment. Figure 1 shows that for 2°C prescribed global-mean warming, the magnitude of, and sign of change in average annual runoff from present, simulated by an impacts model, can differ depending upon the GCM that provides the climate change projections that drive the impact model. This example also shows that the choice of impact model, in this case a global hydrological model (GHM) or catchment-scale hydrological model (CHM), can affect the magnitude of impact and sign of change from present (e.g. see IPSL CM4 and MPI ECHAM5 simulations for the Xiangxi). To this end, throughout this review, the number of climate models applied in each study reviewed, and the other sources of uncertainty (e.g. emissions scenarios) are noted. Very few studies consider the application of multiple impacts models and it is recommended that future studies address this.

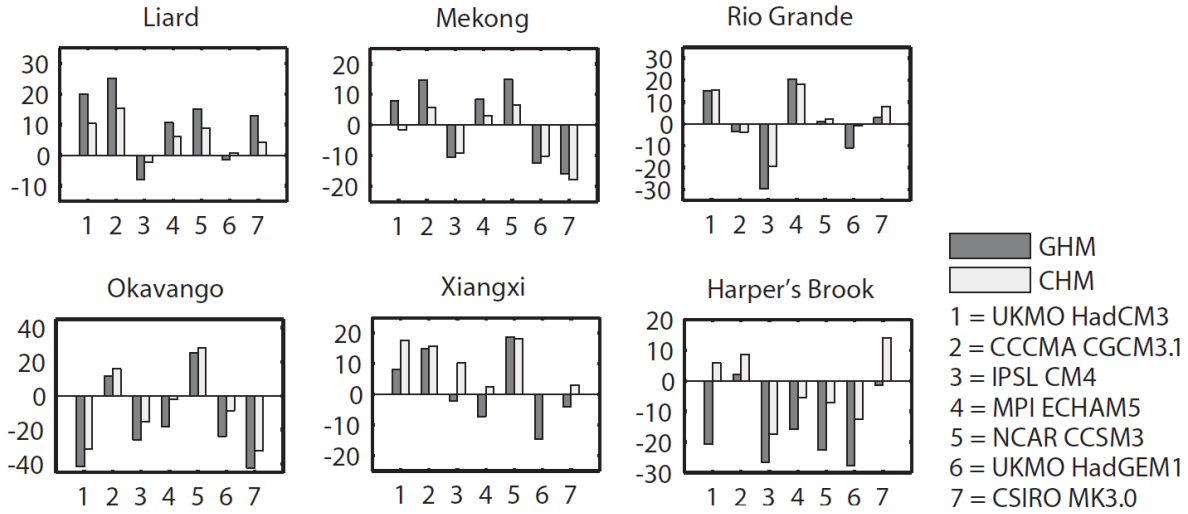

Figure 1. *Change in average annual runoff relative to present (vertical axis; %), when a global hydrological model (GHM) and a catchment-scale hydrological model (CHM) are driven with climate change projections from 7 GCMs (horizontal axis), under a 2°C prescribed global-mean warming scenario, for six river catchments. The figure is from Gosling et al. (2011).*

Summary of findings for each sector

Crop yields

- Quantitative crop yield projections under climate change scenarios for Egypt vary greatly across studies due to the application of different models, assumptions, and emissions scenarios.

- Over 90% of crop production in Egypt is fed by irrigation. An important uncertainty in projections of crop yield is therefore the evolution of future water availability with climate change in Egypt.

- Global- and regional-scale studies included here generally project yield deficits for wheat, rice and maize, three of Egypt's major crops, with climate change. Whether crops are rain-fed or irrigated has an important bearing on the results, and the balance between detrimental ozone effects and CO_2 fertilisation may determine whether losses or gains are realised under climate change.

- National-scale studies included here agree with each other that crop yields in Egypt could decline with climate change, and that adaptation and management methods could potentially reduce the magnitude of any losses.

- Important knowledge gaps and key uncertainties include the quantification of yield increases due to CO_2 fertilisation, quantification of yield reductions due to ozone damage and the extent to which crop diseases could affect crop yields with climate change.

Food security

- Egypt is currently a country with extremely low levels of undernourishment. Global-scale studies included here generally project that Egypt could experience increasing pressures on food security as a result of climate change.

- However, recent work by the AVOID programme demonstrates that adaptive measures could be crucial towards maintaining food security in Egypt under climate change.

- One study suggests that the national economy of Egypt presents a moderate vulnerability to climate change impacts on fisheries, although further studies are needed to understand the vulnerability of the fishing sector and it is possible adaptation options to climate change.

Water stress and drought

- The majority of national-scale and global-scale studies that have considered the effects of climate change on river discharge suggest that water stress could increase with climate change in Egypt.

- Recent simulations by the AVOID programme demonstrate high uncertainty in estimating the magnitude of increased water stress under climate change for Egypt, largely due to climate modelling uncertainty. However most of the models do not show much of the population experiencing a decrease in water stress with climate change.

- National-scale studies indicate that the discharge of the Nile could decline substantially in the future and that the population presents a high vulnerability to water stress with climate change, however the projections are strongly dependent on the choice of climate scenario and underlying GCM.

Pluvial flooding and rainfall

- The IPCC AR4 found consistency across GCMs that mean precipitation could decrease with climate change for Egypt, but that wet extremes could increase.

- Little has been published since AR4 on the impact of climate change on pluvial flooding for Egypt.

Fluvial flooding

- There is uncertainty regarding the magnitude to which flood season discharge in the Nile River could be affected with climate change and GCMs are not consistent in simulating the same sign of change.

- Simulations by the AVOID programme found that a large majority of models included show a tendency towards decreasing flood risk with climate change in the early 21st

century. Later in the century a majority of the models still agree on a decrease compared to the present-day average annual flood risk, but especially in the A1B scenario a small number of models do start to show larger increases in flood risk by this time.

Tropical cyclones

- Egypt is not impacted by tropical cyclones.

Coastal regions

- Several studies conclude that Egypt is highly vulnerable to sea level rise (SLR).
- In one study that considered the impact of a 1m SLR for 84 developing countries, Egypt was ranked the 2nd highest with respect to the coastal population affected, 3rd highest for coastal GDP affected and 5th highest for proportion of urban areas affected.
- Around 15% (2.7 million people) of Egypt's coastal population could be affected by a 10% intensification of the current 1-in-100-year storm surge combined with a 1m SLR.
- Simulations by the Coastal Research Institute suggest that the total area of the Nile Delta affected in 2025, 2050, 2075 and 2100, could be 153, 256, 450, and 761 km^2, respectively, under an SRES A1FI scenario.

Crop yields

Headline

Crop yield projections from global-scale studies under climate change scenarios for Egypt vary greatly across studies, due to the application of different climate and crops models, assumptions, and emissions scenarios. One study reviewed here highlights the large uncertainty in crop yield projections that arises from the application of different GCMs; the sign of change in yields with climate change can vary across GCMs. National-scale assessments agree with each other that crop yields in Egypt could decline with climate change.

Over 90% of crop production in Egypt is fed by irrigation. To this end, an important uncertainty is whether water availability will remain secure with climate change for Egypt. Other important knowledge gaps and uncertainties, which are applicable to Egypt, as well as at the global-scale, include; the quantification of yield increases due to CO_2 fertilisation and yield reductions due to ozone damage (Ainsworth and McGrath, 2010, Iglesias et al., 2009, Averney et al., 2011), and the extent crop diseases could affect crop yields with climate change (Luck et al., 2011).

Results from the AVOID programme for Egypt indicate that the projected changes in local climate lead to conditions which are less suitable for cultivation over most of current cropland areas. Changes in the availability of Nile river water for irrigation have not been considered in this analysis.

Supporting literature

Introduction

The impacts of climate change on crop productivity are highly uncertain due to the complexity of the processes involved. Most current studies are limited in their ability to capture the uncertainty in regional climate projections, and often omit potentially important aspects such as extreme events and changes in pests and diseases. Importantly, there is a lack of clarity on how climate change impacts on drought are best quantified from an agricultural perspective, with different metrics giving very different impressions of future risk. The dependence of some regional agriculture on remote rainfall, snowmelt and glaciers adds to the complexity - these factors are rarely taken into account, and most studies focus solely

on the impacts of local climate change on rain-fed agriculture. However, irrigated agricultural land produces approximately 40-45 % of the world's food (Doll and Siebert 2002), and the water for irrigation is often extracted from rivers which can depend on climatic conditions far from the point of extraction. Hence, impacts of climate change on crop productivity often need to take account of remote as well as local climate changes. Indirect impacts via sea-level rise, storms and diseases have also not been quantified. Perhaps most seriously, there is high uncertainty in the extent to which the direct effects of CO_2 rise on plant physiology will interact with climate change in affecting productivity. Therefore, at present, the aggregate impacts of climate change on large-scale agricultural productivity cannot be reliably quantified (Gornall et al, 2010). This section summarises findings from a range of post IPCC AR4 assessments to inform and contextualise the analysis performed by AVOID programme for this project. The results from the AVOID work are discussed in the next section.

Due to scarce precipitation, Egypt's agricultural land, comprising just 3% of total area, is confined to the narrow Nile Valley from Aswan to Cairo and the flat Nile Delta north of Cairo (Mougou et al., 2008). Even then, Egypt is characterised by a very high percentage (95%) of crop production using some form of irrigation (Attaher et al., 2010), with land being cultivated more than once per year. Wheat, maize, rice, potatoes and tomatoes are some of the important crops grown in Egypt (see Table 1) (FAO, 2008).

Harvested area (ha)		Quantity (Metric ton)		Value ($1000)	
Wheat	1220000	Sugar cane	16400000	Tomatoes	2180000
Maize	819000	Tomatoes	9200000	Rice, paddy	1470000
Rice, paddy	745000	Wheat	7970000	Wheat	1010000
Tomatoes	240000	Rice, paddy	7250000	Grapes	710000
Oranges	222000	Maize	6540000	Potatoes	488000
Sorghum	154000	Sugar beet	5130000	Dates	415000
Potatoes	137000	Potatoes	3560000	Oranges	375000

Table 1. *The top 7 crops by harvested area, quantity and value according to the FAO (2008) in Egypt. Crops that feature in all lists are shaded green; crops that feature in two top 7 lists are shaded amber. Data is from FAO (2008) and has been rounded down to three significant figures.*

A number of impact model studies looking at crop yield which include results for some of the main crops in Egypt have been conducted. They apply a variety of methodological approaches, including using different climate model inputs and treatment of other factors that might affect yield, such as impact of increased CO_2 in the atmosphere on plant growth and adaption of agricultural practises to changing climate conditions. These different models, assumptions and emissions scenarios mean that there are a range of crop yield projections for Egypt.

Important knowledge gaps and key uncertainties which are applicable to the Egypt as well as at the global-scale, include; the quantification of yield increases due to CO_2 fertilisation and yield reductions due to ozone damage (Ainsworth and McGrath, 2010, Iglesias et al., 2009, Averney et al., 2011), and the extent crop diseases could affect crop yields with climate change (Luck et al., 2011).

Most crop simulation models do not include the direct effect of extreme temperatures on crop development and growth, thus only changes in mean climate conditions are considered to affect crop yields for the studies included here.

Assessments that include a global or regional perspective

Recent past

Crop yield changes could be due to a variety of factors, which might include, but not be confined to, a changing climate. In order to assess the impact of recent climate change (1980-2008) on wheat, maize, rice and soybean, Lobell et al. (2011) looked at how the overall yield trend in these crops changed in response to changes in climate over the period studied. The study was conducted at the global-scale but national estimates for Egypt were also calculated. Lobell et all. (2011) divided the climate-induced yield trend by the overall yield trend for 1980–2008, to produce a simple metric of the importance of climate relative to all other factors. The ratio produced indicates the influence of climate on the productivity trend overall. So for example a value of –0.1 represents a 10% reduction in yield gain due to climate change, compared to the increase that could have been achieved without climate change, but with technology and other gains. This can also be expressed as 10 years of climate trend being equivalent to the loss of roughly 1 year of technology gains. For Egypt, small negative effects on maize and soybean yields were estimated, relative to what could have been achieved without the climate trends, but the trends were too small for the impact to a matter for concern. (see Table 2).

Crop	Trend
Maize	-0.2 to -0.1
Rice	0.0 to 0.1
Wheat	-0.1 to 0.0
Soybean	-0.2 to -0.1

Table 2. *The estimated net impact of climate trends for 1980-2008 on crop yields. Climate-induced yield trend divided by overall yield trend. Data is from Lobell et al. (2011).*

Climate change studiesGlobal studies on changes in crop yield due to climate change covered in this report are derived mainly from applying Global Climate Model (GCM) output to crop models. The results for the Egypt are presented.

Included in this report are recent studies have applied climate projections from GCMs to crop yield models to assess the global-scale impact of climate change on crop yields, include impact estimates at the national-scale for Egypt (Iglesias and Rosenzweig, 2009, Giannakopoulos et al., 2005). The process of CO_2 fertilisation of some crops is usually included in most climate impact studies of yields. However, other gases can influence crop yield and are not always included in impacts models. An example of this is ozone (O_3) and so a study which attempts to quantify the potential impact on crop yield of changes in ozone in the atmosphere is also included (Avnery et al. 2011). In addition to these studies, the AVOID programme analysed the patterns of climate change for 21 GCMs, to establish an index of 'climate suitability' of agricultural land. Climate suitability is not directly equivalent to crop yields, but is a means of looking at a standard metric across all the countries included in this project, and of assessing the level of agreement on variables that affect crop production, between all 21 GCMs.

Iglesias and Rosenzweig (2009) repeated an earlier study presented by Parry et al. (2004) by applying climate projections from the HadCM3 GCM (instead of HadCM2, which was applied by Parry et al. (2004)), under seven SRES emissions scenarios and for three future time periods. This study used consistent crop simulation methodology and climate change scenarios globally, and weighted the model site results by their contribution to regional and national, and rain-fed and irrigated production. The study also applied a quantitative estimation of physiological CO_2 effects on crop yields and considered the affect of adaptation by assessing the country or regional potential for reaching optimal crop yield. The results from the study are presented in Table 3 and Table 4. Wheat yield was projected to be above baseline (1970-2000) levels in 2020 and 2050 by six and five emission scenarios respectively. In 2080 wheat yield was below the baseline level under all emission scenarios. Rice yield deficits were simulated from 2020 up to 2080. All emission scenarios projected increasing maize yield deficits with climate change for Egypt.

Scenario	Year	Wheat	Rice	Maize
	2020	1.35	-0.65	-4.30
	2050	-1.59	-2.59	-10.76
A1F1	2080	-20.10	-21.10	-22.56
	2020	0.91	-1.09	-5.49
	2050	0.71	-1.29	-9.48
A2a	2080	-9.00	-10.00	-17.64
	2020	1.56	-0.44	-4.37
	2050	1.66	-0.34	-8.23
A2b	2080	-6.05	-7.05	-14.73
	2020	1.87	-0.13	-3.87
	2050	2.76	0.76	-8.00
A2c	2080	-7.10	-8.10	-16.86
	2020	0.35	-1.65	-5.06
	2050	0.71	-0.29	-7.61
B1a	2080	-0.65	-3.65	-10.12
	2020	-0.86	-2.86	-7.59
	2050	-2.62	-3.62	-10.80
B2a	2080	-4.79	-5.79	-13.62
	2020	0.25	-1.75	-5.74
	2050	0.14	-0.86	-8.12
B2b	2080	-10.27	-11.27	-19.91

Table 3. *Wheat, rice and maize yield changes (%) relative to baseline scenario (1970-2000) for different emission scenarios and future time periods for Egypt. Some emissions scenarios were run in an ensemble simulation (e.g. A2a, A2b, A2c). Data is from Iglesias and Rosenzweig (2009).*

	Wheat		Rice		Maize	
	Up	Down	Up	Down	Up	Down
Baseline to 2020	6	1	0	7	0	7
Baseline to 2050	5	2	1	6	0	7
Baseline to 2080	0	7	0	7	0	7
2020 to 2050	3	4	4	3	0	7
2050 to 2080	0	7	0	7	0	7

Table 4. *The number of emission scenarios that predict yield gains ("Up") or yield losses ("Down") for wheat, rice and maize between two points in time for Egypt. Data is from Iglesias and Rosenzweig (2009).*

Giannakopoulos et al. (2005, 2009) applied climate projections with the HadCM3 GCM under the SRES A2 and B2 emissions scenarios to assess climate change impacts for the Mediterranean basin for the period 2031-2060 under the A2 and B2 emissions scenarios. Climate data were used as input to the CROPSYST (Cropping Systems Simulation Model) (Stockle et al. 2003) crop model to project crop productivity changes (compared to 1961-1990) for a range of different crop types. The crop types were divided into 'C4' summer crop, 'C3' summer crop, legumes, tuber crops and cereals, where 'C4' and 'C3' refer to two plant physiology types that affect the way plants take up CO_2 from the atmosphere. 'C3' crops are

able to benefit from CO_2 enrichment of the atmosphere, whereas 'C4' crops are not. This process is simulated by CROPSYST. The process is important because the benefit from CO_2 enrichment can potentially off-set some of the negative impacts of climate change for that crop. For Egypt the 'C4' summer crop studied was irrigated maize, the 'C3' summer crop was rain-fed sunflowers, the legume was rain-fed beans, the tuber crop was irrigated potato and the cereal-rain was fed wheat. The studied indicated that bean and potato crops in particular could be negatively affected by climate change, in the absence of adaptation in Egypt (see Figure 2).

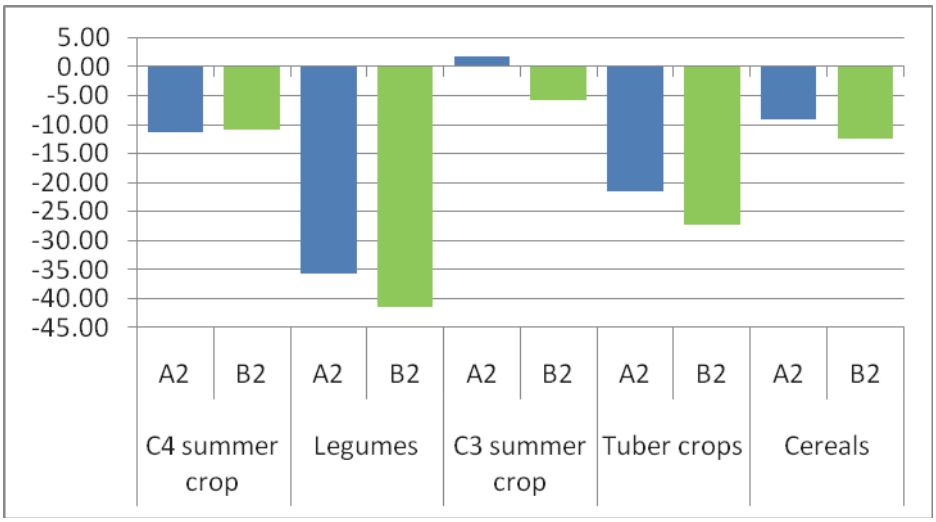

Figure 2. *Impact of climate change on crop productivity in Egypt for different types of crops. The Y-axis is expressed as percentage difference between future (A2 and B2 scenarios respectively) and present yields. After Giannakopoulos et al. (2005, 2009).*

Elsewhere, several recent studies have assessed the impact of climate change on a global-scale and include impact estimates for North Africa as a whole (Fischer, 2009, Nelson et al., 2009, Tatsumi et al., 2011). Whilst these studies provide a useful indicator of crop yields under climate change for the *region*, it should be noted that the crop yields presented in such cases are not definitive *national* estimates. This is because the yields are averaged over the entire region, which includes other countries as well as Egypt.

Nelson et al. (2009) applied two GCMs in combination with the DSSAT crop model under the SRES A2 emissions scenario to project future yields of rice, maize, soybean, wheat and groundnut with and without CO_2 enrichment, and for rain-fed and irrigated lands, for several regions across the globe. Table 5 represents the results for Middle East and North Africa, the World Bank regional grouping in which Egypt is included. It can be seen that increased CO_2 levels were of benefit to all crops simulated, whether rain-fed or irrigated. However the effects of CO_2 fertilisation in the case of wheat and maize in particular are not projected to

be large enough to fully compensate for factors which could lead to yield reductions, such as increasing temperatures, out to 2050.

GCM and CO_2 fertilisation	Rice		Maize		Soybean		Wheat		Groundnut	
	Rf.	Irr.	Rf.	Irr.	Rf.	Irr.	Rf.	Irr.	Rf.	Irr.
CSIRO NoCF	0	-13.3	58.6	0.1	17.5	-4.2	-2.6	-12.8	-20.5	-11.6
NCAR NoCF	0	-29.5	-46.7	-1.0	-84.2	-14.0	-8.1	-19.7	23.6	-28.5
CSIRO CF	0	1.7	61.8	-0.4	26.0	5.6	8.8	-5.8	-11.8	4.3
NCAR CF	0	-14.4	-46.3	-1.1	-76.4	-5.0	2.0	-13.4	23.6	-15.6

Table 5. *Projected yield changes (%) by 2050 compared to baseline (yields with 2000 climate) using two GCMs with (CF) and without CO_2 fertilisation effect (NoCF). Rain-fed (Rf.) and Irrigated (Irr.) crop lands were assessed separately. Data is from Nelson et al. (2009).*

The impact of future climate on crop yields of rain-fed cereals was investigated by Fischer (2009) projected global 'production potential' changes for 2050 using the GAEZ (Global Agro-Ecological Zones) crops model with climate change scenarios from the HadCM3 and CSIRO GCMs respectively, under SRES A2 emissions. The impact of future climate on crop yields of rain-fed cereals are presented in Table 6 (relative to yield realised under current climate) for North Africa. It should, however, be noted that a lot of crop land is fed by irrigation in North Africa. As with the study by Nelson et al. (2009) CO_2 fertilization was found to offset, but by no means fully compensate for the projected impacts of climate change. Both studies also projected that wheat would be the most negatively affected crop.

	CO_2 fert.	2020s		2050s		2080s	
		CSIRO	HADCM3	CSIRO	HADCM3	CSIRO	HADCM3
Rain-fed wheat	Yes	1	2	4	-9	-18	-28
	No	-2	n/a [1]	-2	n/a	-25	n/a
Rain-fed maize	Yes	66	38	160	56	183	60
	No	64	n/a	153	n/a	171	n/a
Rain-fed cereals	Yes	n/a	2	n/a	-8	n/a	23
	No	n/a	n/a	n/a	n/a	n/a	n/a
Rain-fed sorghum	Yes	12	n/a	31	n/a	20	n/a
	No	10	n/a	27	n/a	15	n/a

Table 6. *Impacts of climate change on the production potential of rain-fed cereals in current cultivated land (% change with respect to yield realised under current climate), with two GCMs and with and without CO_2 fertilisation ("CO_2 fert.") under SRES A2 emissions for North Africa. Data is from Fischer (2009).*

Tatsumi et al. (2011) applied an improved version of the GAEZ crop model (iGAEZ) to simulate crop yields on a global scale for wheat, potato, cassava, soybean, rice, sweet potato, maize, green beans. The impact of global warming on crop yields from the 1990s to

2090s was assessed by projecting five GCM outputs under the SRES A1B scenario and comparing the results for crop yields as calculated using the iGAEZ model for the period of 1990-1999. The results for North Africa are displayed in Table 7.

Wheat	Potato	Cassava	Soybean	Rice	Sweet potato	Maize	Green beans
-0.97	-3.2	-3.94	12.11	-	-4.05	-	16.49

Table 7. *Average change in yield (%), during 1990s-2090s in North Africa. Data is from Tatsumi et al. (2011).*

In addition to the studies looking at the effect of changes in climate and CO_2 concentrations on crop yield, Avnery et al. (2011) investigated the effects of ozone surface exposure on crop yield losses for soybeans, maize and wheat under the SRES A2 and B1 scenarios respectively. Two metrics of ozone exposure were investigated; seasonal daytime (08:00-19:59) mean O_3 (M12) and accumulated O_3 above a threshold of 40 ppbv (AOT40). The results for Egypt are presented in Table 8.

	A2		B1	
	M12	AOT40	M12	AOT40
Soybeans	-	-	-	-
Maize	-	-	-	-
Wheat	10-15	30-45	6-8	20-25

Table 8. *National relative crop yield losses (%) for 2030 under A2 and B1 emission scenarios according to the M12 (seasonal daytime (08:00–19:59) mean) and AOT40 (accumulated O_3 above a threshold of 40 ppbv) metrics of O_3 exposure. Data is from Avnery et al. (2011).*

National-scale or sub-national scale assessments

Climate change studies

Included in this section are results from recent studies that have applied crop models, alongside meteorological models and information for global climate models, to produce national or sub-national scale projections of future crop yields in Egypt.

Attaher and Medany (2008) concluded that the crop-water requirements of the important strategic crops in Egypt could increase under all SRES scenarios of climate change, by a range of 5-13% by 2100, although it is not clear from their study, what the baseline current day value represents. In addition, the vulnerability of on-farm irrigation in the Egyptian agricultural regions and the acceptable adaptation measures vary according to the local conditions of each region (EEAA, 2010). Moreover, the high vulnerability of on farm irrigation systems in Egypt has been attributed to low irrigation system efficacy and irrigation

management patterns (EEAA, 2010). This suggests possible implications for management in the future. To this end, Attaher et al. (2010) applied climate change projections from the HadCM3 GCM under two emissions scenarios to assess the impact of climate change on crop water demand, water use efficiency, crop yield and other parameters in the near, medium and far future for a range of crops (wheat, maize, tomato, potato). When representing cultivation under traditional surface irrigation systems with 50% efficiency, yield averaged over a range of crops declined in three future time slices (2025s, 2050s and 2100s) under all emissions scenarios; see Table 9. Improving surface irrigation efficiency to 75% or changing from surface to drip irrigation, however, offset yield losses due to climatic change.

Note that it is not clear from this study whether this comparison is between two individual years, or between two time averaged periods, which somewhat undermines the value of the data.

	Current	A1			B1		
		2025s	2050s	2100s	2025s	2050s	2100s
Total crop yield (kg/fed)	7322	6948	6117	5322	6991	6455	6291
Yield change (%) relative to baseline (Current)	-	-5.1	-16.5	-27.3	-4.5	-11.8	-14.1

Table 9. *Total crop yield (averaged over crops) and yield change for current and future climate scenarios under A1 and B1 emissions. Data is from Attaher et al. (2010).*

Mougou et al. (2008) applied climate projections from the HadCM3 GCM under A1 and B2 SRES emissions scenarios to simulate rain-fed and irrigated wheat yield under various adaptation measures. The regional temperature increases corresponding to the A1 and B2 scenarios were 3.6°C and 1.5°C respectively, although the study does not report the time horizon for which this is for, or referenced from. Projected yield changes for three irrigated wheat cultivars under A1 and B2 were all negative (see Table 10). Under the SRES B2 scenario, rain-fed wheat yield declined by more than 50% if rainfall was reduced by 20%. However, an increase in rainfall by 20% increased yield by less than 5%.

Irrigated wheat	**Cultivars**	**A1**	**B2**
	Giza-168	-37	-30
	Sakha-8	-26	-4
	Sakha-69	n/a	-28
Rain-fed wheat	**Rainfall scenarios**	**Current**	**B2**
	-20%	-49	-55
	-10%	-26	-34
	Baseline	0	0
	+10%	+9	+0.5
	+20%	+11	+3

Table 10. *Projected wheat yield change (%) under future climate scenarios for Egypt. Data is from Mougou et al. (2008).*

Several local case studies, reported in Egypt's second national communication under the United Nations Framework Convention on Climate Change (UNFCC) (EEAA, 2010), found that crop yields could decline in Egypt with climate change, which generally supports the results from other national-scale studies (Attaher et al., 2010, Mougou et al., 2008). AVOID programme results

To further quantify the impact of climate change on crops, the AVOID programme simulated the effect of climate change on the suitability of land for crop cultivation for all countries reviewed in this literature assessment based upon the patterns of climate change from 21 GCMs (Warren et al., 2010). This ensures a consistent methodological approach across all countries and takes consideration of climate modelling uncertainties.

Methodology

The effect of climate change on the suitability of land for crop cultivation is characterised here by an index which defines the percentage of cropland in a region with 1) a decrease in suitability or 2) an increase in suitability. A threshold change of 5% is applied here to characterise decrease or increase in suitability. The crop suitability index is calculated at a spatial resolution of 0.5°x0.5°, and is based on climate and soil properties (Ramankutty et al., 2002). The baseline crop suitability index, against which the future changes are measured, is representative of conditions circa 2000. The key features of the climate for the crop suitability index are temperature and the availability of water for plants. Changes in these were derived from climate model projections of future changes in temperature and precipitation, with some further calculations then being used to estimate actual and potential evapotranspiration as an indicator of water availability. It should be noted that changes in

atmospheric CO_2 concentrations can decrease evapotranspiration by increasing the efficiency of water use by plants (Ramankutty et al., 2002), but that aspect of the index was not included in the analysis here. Increased CO_2 can also increase photosynthesis and improve yield to a small extent, but again these effects are not included. Exclusion of these effects may lead to an overestimate of decreases in suitability.

The index here is calculated only for grid cells which contain cropland circa 2000, as defined in the global crop extent data set described by Ramankutty et al. (2008) which was derived from satellite measurements. It is assumed that crop extent does not change over time. The crop suitability index varies significantly for current croplands across the world (Ramankutty et al., 2002), with the suitability being low in some current cropland areas according to this index. Therefore, while climate change clearly has the potential to decrease suitability for cultivation if temperature and precipitation regimes become less favourable, there is also scope for climate change to increase suitability in some existing cropland areas if conditions become more favourable in areas where the suitability index is not at its maximum value of 1. It should be noted that some areas which are not currently croplands may already be suitable for cultivation or may become suitable as a result of future climate change, and may become used a croplands in the future either as part of climate change adaptation or changes in land use arising for other reasons. Such areas are not included in this analysis.

Results

Crop suitability was estimated under the pattern of climate change from 21 GCMs with two emissions scenarios; 1) SRES A1B and 2) an aggressive mitigation scenario where emissions follow A1B up to 2016 but then decline at a rate of 5% per year thereafter to a low emissions floor (denoted A1B-2016-5-L). The application of 21 GCMs is an attempt to quantify the uncertainty due to climate modelling, although it is acknowledged that only one crop suitability impacts model is applied. Simulations were performed for the years 2030, 2050, 2080 and 2100. The results for Egypt are presented in Figure 3.

In Egypt, most croplands depend on irrigation water from the Nile rather than on local climatic conditions. However, for consistency with other countries in this analysis, the changes in local climate over current Egyptian croplands has been assessed in the context of suitability for cultivation. This may be of some relevance to the issue of irrigation needs.

Under the climate projections, only one model projects an increase in suitability for cultivation in current Egyptian croplands. In the A1B scenario this increase is first seen in 2050, for 3% of current cropland area increasing to 8% by 2100. Under the mitigation

scenario, this single model projects 2% of current Egyptian croplands to have become more suitable by 2100. All other models project no increase in suitability. By 2030, under both emissions scenarios, between 40% and 67% of current Egyptian croplands are projected to become less suitable for cultivation as defined by local climatic conditions. By 2100 this rises to 67%-87% for the A1B scenario and 58%-77% for the mitigation scenario.

It should be noted that the effects of rising CO_2 on evapotranspiration, which were not included in the analysis here, may be particularly important in arid areas such as Egypt. This effect may lessen the decline in suitability to some extent.

So, for Egypt, projected changes in local climate lead to conditions which are less suitable for cultivation over most of current cropland areas. Changes in the availability of Nile river water for irrigation have not been considered in this analysis.

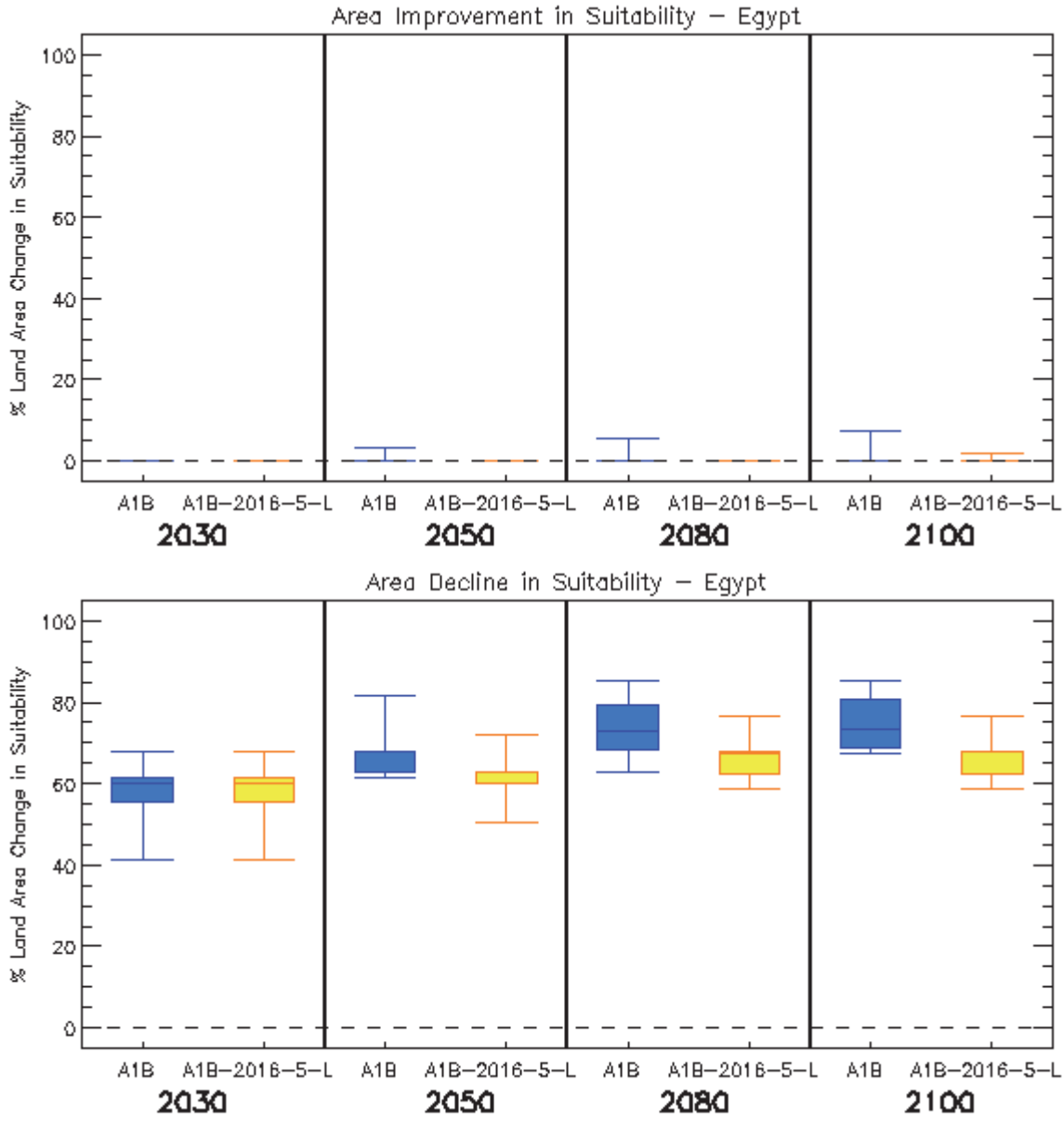

Figure 3. *Box and whisker plots for the impact of climate change on increased crop suitability (top panel) and decreased crop suitability (bottom panel) for Egypt, from 21 GCMs under two emissions scenarios (A1B and A1B-2016-5-L), for four time horizons. The plots show the 25th, 50th, and 75th percentiles (represented by the boxes), and the maximum and minimum values (shown by the extent of the whiskers).*

Food security

Headline

A number of simulation studies imply that Egypt may experience increasing pressures on food security as a result of climate change. However, socio-economic factors may play an important role in alleviating this somewhat. One study suggests that the national economy of Egypt presents a moderate vulnerability to climate change impacts on fisheries, although further studies are needed to understand the vulnerability of the fishing sector and possible adaptation options to climate change.

Introduction

Food security is a concept that encompasses more than just crop production, but is a complex interaction between food availability and socio-economic, policy and health factors that influence access to food, utilisation and stability of food supplies. In 1996 the World Food Summit defined food security as existing 'when all people, at all times, have physical and economic access to sufficient, safe and nutritious food to meet their dietary needs, and their food preferences are met for an active and healthy life'.

As such this section cannot be a comprehensive analysis of all the factors that are important in determining food security, but does attempt to assess a selection of the available literature on how climate change, combined with projections of global and regional population and policy responses, may influence food security.

Assessments that include a global or regional perspective

Egypt is not a country of high concern in terms of food security, particularly in a global context. According to FAO statistics Egypt has extremely low levels of undernourishment, (less than 5% of the population). However, a number of simulation studies imply that Egypt may experience increasing pressures on food security as a result of climate change.

A study by Falkenmark et al. (2009) looked at projections of available water for crops and suggested that Egypt would be a food importing country in 2050. This was based on a global analysis of food security under climate change scenarios for the 2050s that considers the importance of water availability for ensuring global food security. The study presents an analysis of water constraints and opportunities for global food production on current croplands and assesses five main factors:

1) how far improved land and water management might go towards achieving global food security,

2) the water deficits that would remain in regions currently experiencing water scarcity and which are aiming at food self-sufficiency,

3) how the water deficits above may be met by importing food,

4) the cropland expansion required in low income countries without the needed purchasing power for such imports, and

5) the proportion of that expansion pressure which will remain unresolved due to potential lack of accessible land.

Simulations were generated by only the LPJml dynamic global vegetation and water balance model (Gerten et al. 2004) with population growth and climate change under the SRES A2 emission scenario. Falkenmark et al. (2009) summarise the impacts of future improvements (or lack thereof) in water productivity for each country across the globe and show that this generates either a deficit or a surplus of water in relation to food water requirements in each country. These can be met either by trade or by horizontal expansion (by converting other terrestrial ecosystems to crop land). The study estimated that in 2050 around one third of the world's population will live in each of three regions: those that export food, those that import food, and those that have to expand their croplands at the expense of other ecosystems because they do not have enough purchasing power to import their food. The simulations demonstrated that Egypt could be a food importing country in 2050.

The International Food Policy Research Institute (IFPRI) have produced a report and online tool that describes the possible impact of climate change on two major indicators of food security; 1) the number of children aged 0-5 malnourished, and 2) the average daily kilocalorie availability (Nelson et al., 2010, IFPRI, 2010)**.** The study considered three broad socio-economic scenarios; 1) a 'pessimistic' scenario, which is representative of the lowest of the four GDP growth rate scenarios from the Millennium Ecosystem Assessment GDP scenarios and equivalent to the UN high variant of future population change, 2) a 'baseline' scenario, which is based on future GDP rates estimated by the World Bank and a population change scenario equivalent to the UN medium variant, and 3) an 'optimistic' scenario that is representative of the highest of the four GDP growth rate scenarios from the Millennium Ecosystem Assessment GDP scenarios and equivalent to the UN low variant of future population change. Nelson et al. (2010) also considered climate modelling and emission

uncertainty and included a factor to account for CO_2 fertilisation in their work. The study applied two GCMs, the CSIRO GCM (denoted CSI) and the MIROC GCM (denoted MIR), and forced each GCM with two SRES emissions scenarios (A1B and B1). They also considered a no climate change emissions scenario, which they called 'perfect mitigation' (note that in most other climate change impact studies that this is referred to as the baseline). The perfect mitigation scenario is useful to compare the effect of climate change against what might have happened without, but is not a realistic scenario itself. Estimates for both indicators of food security from 2010 to 2050, for Egypt, are presented in Table 11 and Table 12. Figure 4 displays the effect of climate change, calculated by comparing the 'perfect mitigation' scenario with each baseline, optimistic and pessimistic scenario. The results show that by 2050, even though average daily kilocalorie availability is higher than it is in 2010, it is higher in the absence of climate change (perfect mitigation) by around 300 kilocalories, than under climate change. Whilst by 2050 climate change is attributable for an average 9% decline in kilocalorie availability, the absolute value of available kilocalories in Egypt remains high (above 3,000) under all scenarios. However, the number of malnourished children does go up over time, both with and without the effect of climate change, although the increase is higher under the climate change scenarios. By 2050, there are generally less than 50,000 malnourished children in the absence of climate change (relative to around 450,000 in 2010) but under climate change there are around 200,000-500,000 (depending upon scenario). Indeed, Figure 4 shows that under the baseline socio-economic scenario, child malnourishment attributable to climate change is over 500% under both emissions scenarios. Moreover, malnourishment is largely more sensitive to socio-economic development pathway than to future emissions. This implies that Egypt is highly vulnerable to food security issues due to climate change but that socioeconomic factors play an important role in alleviating this. Figure 5 and Figure 6 show how the changes projected for Egypt compare with the projections for the rest of the globe (IFPRI, 2010).

Scenario	2010	2050
Baseline CSI A1B	3147	3229
Baseline CSI B1	3153	3266
Baseline MIR A1B	3122	3119
Baseline MIR B1	3138	3199
Baseline Perfect Mitigation	3209	3536
Pessimistic CSI A1B	3134	3001
Pessimistic CSI B1	3141	3035
Pessimistic MIR A1B	3109	2893
Pessimistic MIR B1	3120	2946
Pessimistic Perfect Mitigation	3196	3287
Optimistic CSI A1B	3084	3568
Optimistic CSI B1	3089	3595
Optimistic MIR A1B	3058	3433
Optimistic MIR B1	3068	3489
Optimistic Perfect Mitigation	3143	3894

Table 11. *Average daily kilocalorie availability simulated under different climate and socioeconomic scenarios, for Egypt (IFPRI, 2010).*

Scenario	2010	2050
Baseline CSI A1B	0.43	0.22
Baseline CSI B1	0.43	0.19
Baseline MIR A1B	0.45	0.29
Baseline MIR B1	0.44	0.24
Baseline Perfect Mitigation	0.39	0.03
Pessimistic CSI A1B	0.44	0.43
Pessimistic CSI B1	0.44	0.4
Pessimistic MIR A1B	0.46	0.52
Pessimistic MIR B1	0.45	0.47
Pessimistic Perfect Mitigation	0.4	0.21
Optimistic CSI A1B	0.48	0.01
Optimistic CSI B1	0.48	No data
Optimistic MIR A1B	0.5	0.08
Optimistic MIR B1	0.49	0.05
Optimistic Perfect Mitigation	0.44	No data

Table 12. *Number of malnourished children (aged 0-5; millions) simulated under different climate and socioeconomic scenarios, for Egypt (IFPRI, 2010).*

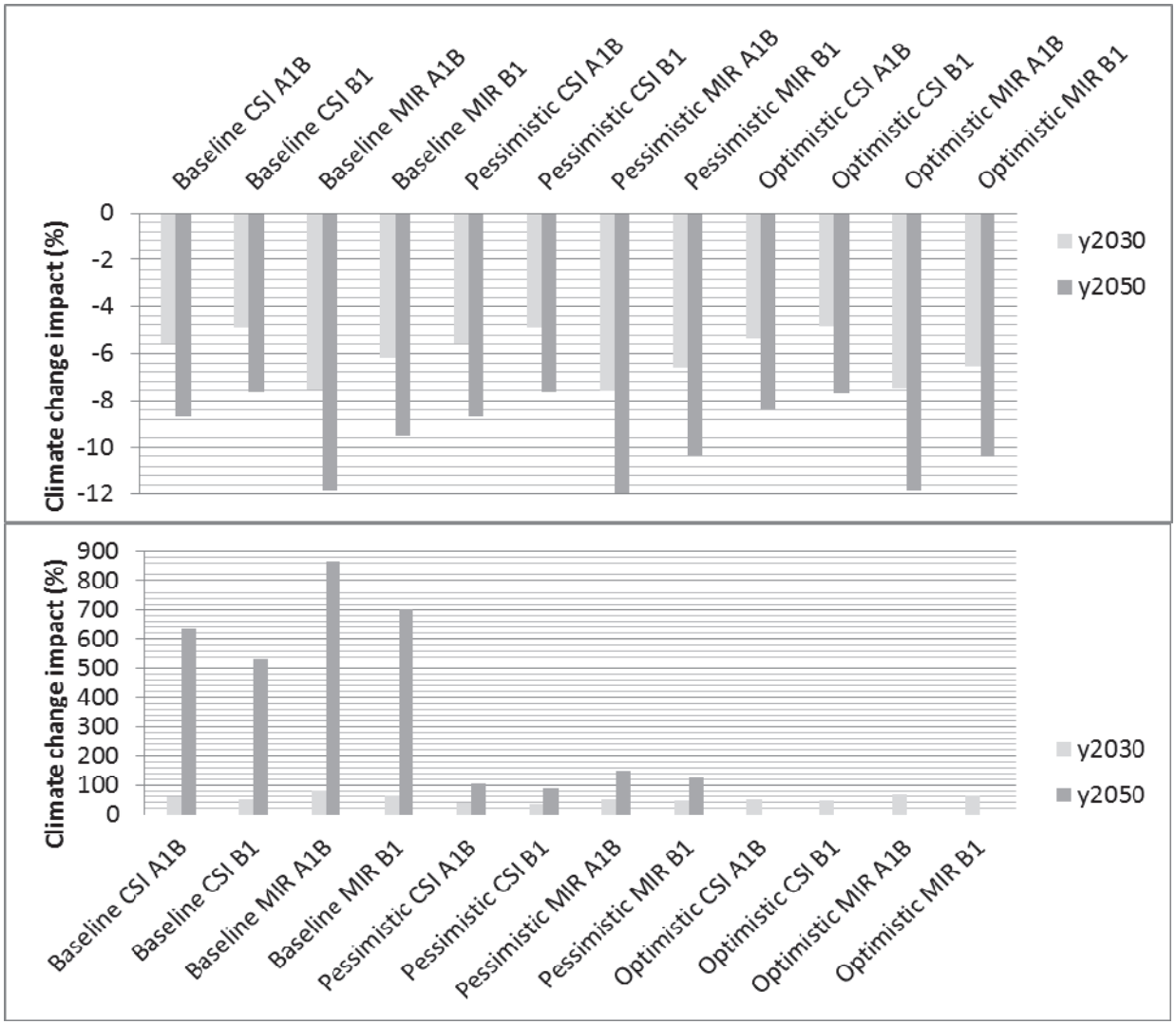

Figure 4. *The impact of climate change on average daily kilocalorie availability (top panel) and number of malnourished children (bottom) for Egypt (IFPRI, 2010).*

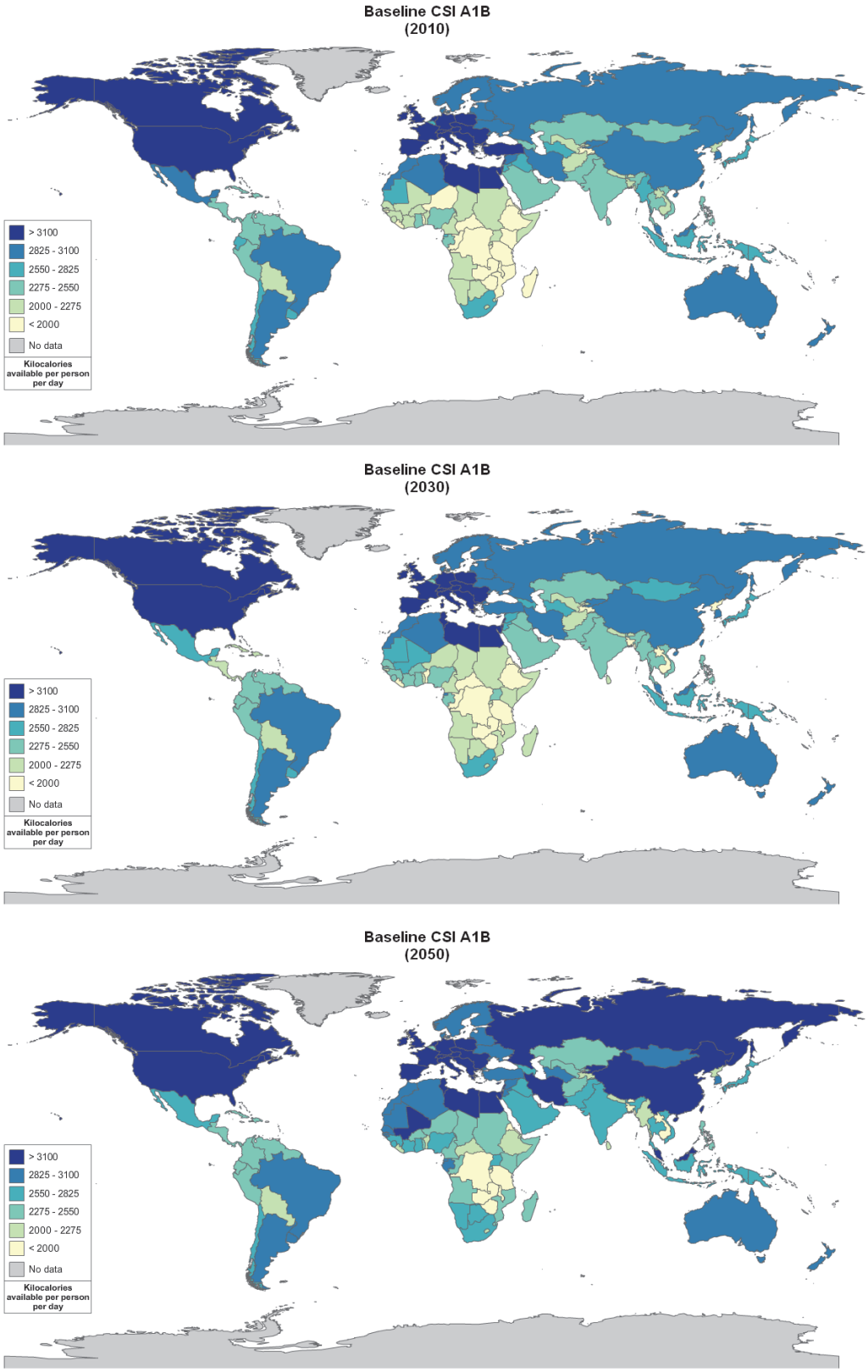

Figure 5. *Average daily kilocalorie availability simulated by the CSIRO GCM (CSI) under an A1B emissions scenario and the baseline socioeconomic scenario, for 2010 (top panel), 2030 (middle panel) and 2050 (bottom panel). The figure is from IFPRI (IFPRI, 2010). The changes shown are the combination of both climate change and socio-economic changes. Note that no simulations were undertaken for child malnourishment in 2050 under the optimistic scenario*

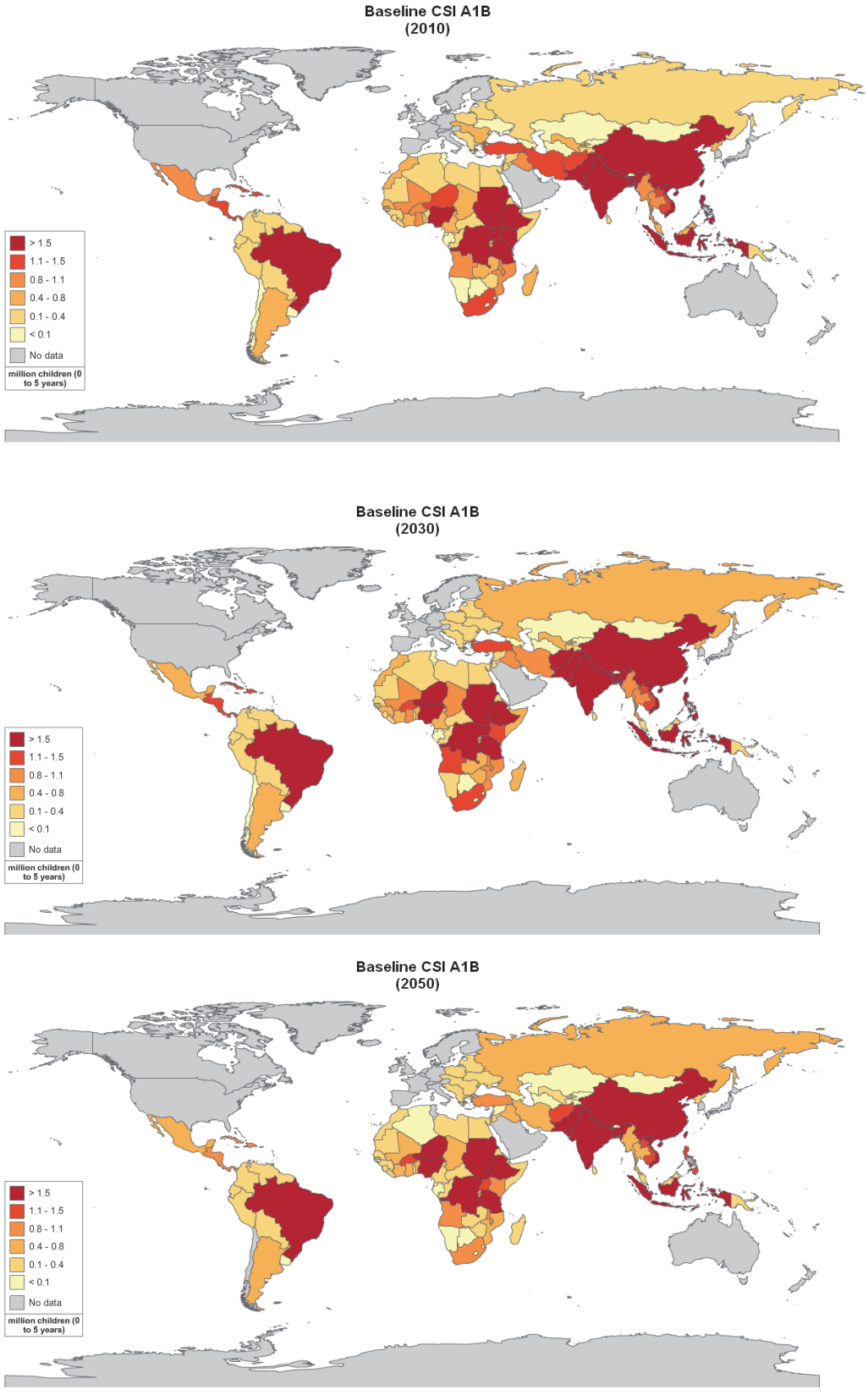

Figure 6. *Number of malnourished children (aged 0-5; millions) simulated by the CSIRO GCM (CSI) under an A1B emissions scenario and the baseline socioeconomic scenario, for 2010 (top panel), 2030 (middle panel) and 2050 (bottom panel). The figure is from IFPRI (IFPRI, 2010). The changes shown are the combination of both climate change and socio-economic changes.*

It is important to note that up until recently, projections of climate change impacts on global food supply have tended to focus solely on production from terrestrial biomes, with the large contribution of animal protein from marine capture fisheries often ignored. However, recent studies have addressed this knowledge gap (Allison et al. 2009, Cheung et al., 2010). In addition to the direct affects of climate change, changes in the acidity of the oceans, due to increases in CO_2 levels, could also have an impact of marine ecosystems, which could also affect fish stocks. However, this relationship is complex and not well understood, and studies today have not been able to begin to quantify the impact of ocean acidification on fish stocks.

Allison et al. (2009) present a global analysis that compares the vulnerability of 132 national economies to potential climate change impacts on their capture fisheries. The study considered a country's vulnerability to be a function of the combined effect of projected climate change, the relative importance of fisheries to national economies and diets, and the national societal capacity to adapt to potential impacts and opportunities. Climate change projections from a single GCM under two emissions scenarios (SRES A1FI and B2) were used in the analysis. Allison et al. (2009) concluded that the national economy of Egypt presented a moderate vulnerability to climate change impacts on fisheries. In contrast, countries in Central and Western Africa (e.g. Malawi, Guinea, Senegal, and Uganda), Peru and Colombia in north-western South America, and four tropical Asian countries (Bangladesh, Cambodia, Pakistan, and Yemen) were identified as most vulnerable (see Figure 7). It should be noted, however, that results from studies that have applied only a single climate model or climate change scenario should be interpreted with caution. This is because they do not consider other possible climate change scenarios which could result in a different impact outcome, in terms of magnitude and in some cases sign of change.

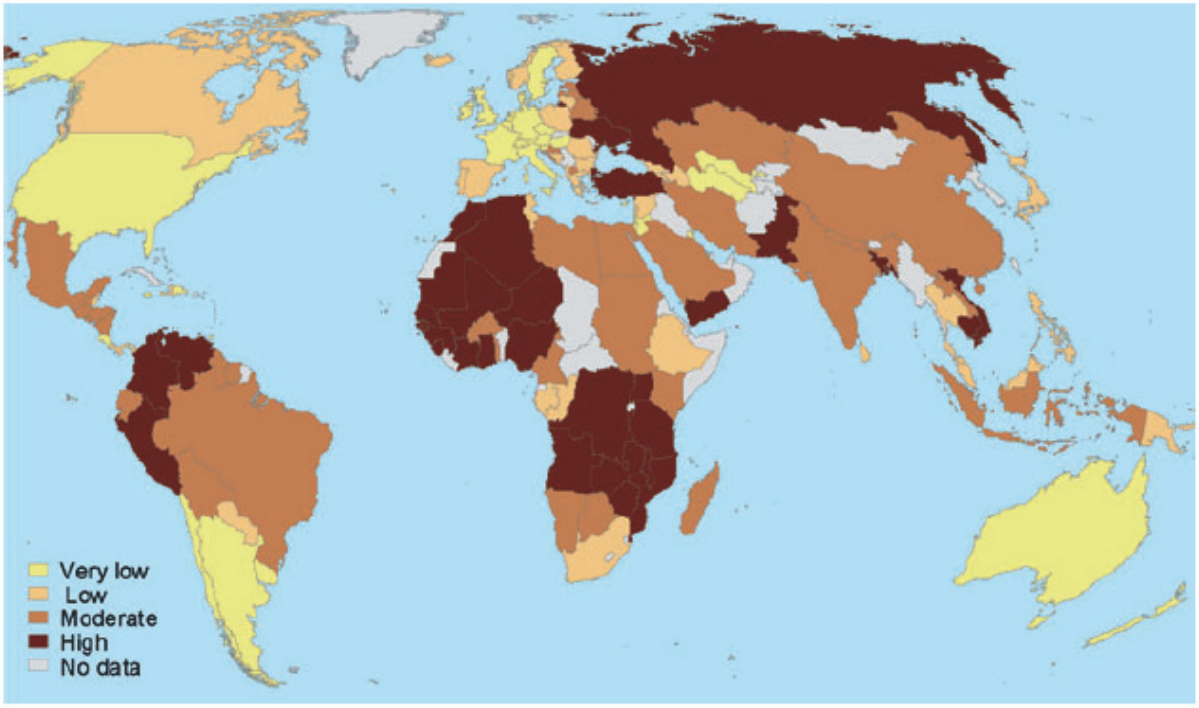

Figure 7. *Vulnerability of national economies to potential climate change impacts on fisheries under SRES B2 (Allison et al., 2009). Colours represent quartiles with dark brown for the upper quartile (highest index value), yellow for the lowest quartile, and grey where no data were available.*

National-scale or sub-national scale assessments

Allison et al. (2009) concluded that the national economy of Egypt presents a moderate vulnerability to climate change impacts on fisheries. Egypt's second national communication under the United Nations Framework Convention on Climate Change (UNFCC) also highlights the vulnerability of Egyptian fisheries to climate change (EEAA, 2010). The report notes that more than 80% of fish production in Egypt comes from aquaculture projects in the northern part of the Nile Delta and that the country currently produces about 93% of its consumption of fish. Climate change could increase sea temperature causing wild fish distribution to shift northwards and to move to deeper water (EEAA, 2010). Furthermore, aquaculture projects may suffer from water shortages due to the scarcity in fresh water supply that might affect the country due to climate change (Beyene et al., 2010) and increased temperatures might also affect the production of some fish species. However, further studies are needed to understand the vulnerability of the fishing sector and it is possible adaptation options to climate change.

Water stress and drought

Headline

The majority of national-scale and global-scale studies that have considered the effects of climate change on river discharge suggest that water stress could increase with climate change in Egypt. Recent simulations by the AVOID programme demonstrate high uncertainty in estimating the magnitude of increased water stress under climate change for Egypt, largely due to climate modelling uncertainty; similar uncertainties have been highlighted in national-scale studies. National-scale studies indicate that the discharge of the Nile could decline substantially with climate change.

Supporting literature

Introduction

For the purposes of this report droughts are considered to be extreme events at the lower bound of climate variability; episodes of prolonged absence or marked deficiency of precipitation. Water stress is considered as the situation where water stores and fluxes (e.g. groundwater and river discharge) are not replenished at a sufficient rate to adequately meet water demand and consumption.

A number of impact model studies looking at water stress and drought for the present (recent past) and future (climate change scenario) have been conducted. These studies are conducted at global or national scale and include the application of global water 'availability' or 'stress' models driven by one or more climate change scenario from one or more GCM. The approaches variously include other factors and assumptions that might affect water availability, such as the impact of changing demographics and infrastructure investment, etc. These different models (hydrological and climate), assumptions and emissions scenarios mean that there are a range of water stress projections for Egypt. This section summarises findings from these studies to inform and contextualise the analysis performed by the AVOID programme for this project. The results from the AVOID work and discussed in the next section.

Important knowledge gaps and key uncertainties which are applicable to Egypt as well as at the global-scale, include; the appropriate coupling of surface water and groundwater in hydrological models, including the recharge process, improved soil moisture and evaporation dynamics, inclusion of water quality, inclusion of water management (Wood et al. 2011) and

further refinement of the down-scaling methodologies used for the climate driving variables (Harding et al. 2011). Further research should also explore (1) the impacts on Nile Delta groundwater aquifer recharge due to projected decreases of Nile River discharges, and (2) the impacts on groundwater abstraction as the main source for supplementary irrigation at the coastal zones of the Nile Delta.

Assessments that include a global or regional perspective

Recent past

Recent research presented by Vörösmarty et al. (2010) describes the calculation of an '*Adjusted Human Water Security Threat'* (HWS) indicator. The indicator is a function of the cumulative impacts of 23 biophysical and chemical drivers simulated globally across 46,517 grid cells representing 99.2 million km^2. With a digital terrain model at its base, the calculations in each of the grid boxes of this model take account of the multiple pressures on the environment, and the way these combine with each other, as water flows in river basins. The level of investment in water infrastructure is also considered. This infrastructure measure (the *investment benefits factor*) is based on actual existing built infrastructure, rather than on the financial value of investments made in the water sector, which is a very unreliable and incomplete dataset. The analysis described by Vörösmarty et al. (2010) represents the current state-of-the-art in applied policy-focussed water resource assessment. In this measure of water security, the method reveals those areas where this is lacking, which is a representation of human water stress. One drawback of this method is that no analysis is provided in places where there is 'no appreciable flow', where rivers do not flow, or only do so for such short periods that they cannot be reliably measured. This method also does not address places where water supplies depend wholly on groundwater or desalination, being piped in, or based on wastewater reuse. It is based on what is known from all verified peer reviewed sources about surface water resources as generated by natural ecosystem processes and modified by river and other hydraulic infrastructure (Vörösmarty et al., 2010).

Here, the present day HWS is mapped for Egypt. The model applied operates at 50km resolution, so, larger countries appear to have smoother coverage than smaller countries, but all are mapped and calculated on the same scale, with the same data and model, and thus comparisons between places are legitimate. It is important to note that this analysis is a comparative one, where each place is assessed *relative* to the rest of the globe. In this way, this presents a realistic comparison of conditions across the globe. As a result of this, however, some places may seem to be less stressed than may be originally considered.

One example is Australia, which is noted for its droughts and long dry spells, and while there are some densely populated cities in that country where water stress is a real issue, for most of the country, *relative to the rest of the world*, the measure suggests water stress (as measured by HWS defined by Vörösmarty et al. (2010)), is not a serious problem.

Figure 8 presents the results of this analysis for Egypt. The Nile and its tributaries are the only surface water bodies included in this analysis. To this end, the remainder of Egypt is characterised as “no appreciable flow”. Most of the population and economic activity takes place close to the river. In other parts of the country, water resources are provided from groundwater fed springs and oases. Egypt also benefits from favourable water sharing arrangements which results in it receiving the biggest share of rainfall resources of all ten countries in the Nile Basin. Hence, on the basis of this analysis, the level of threat to human water security is moderate to low. Figure 8 generally reflects the dominance of surface water usage via the Nile in Egypt; indeed, 97.6% of Egypt’s total renewable water resource is from surface water, whereas 2.4% is from groundwater recharge (UN, 2007).

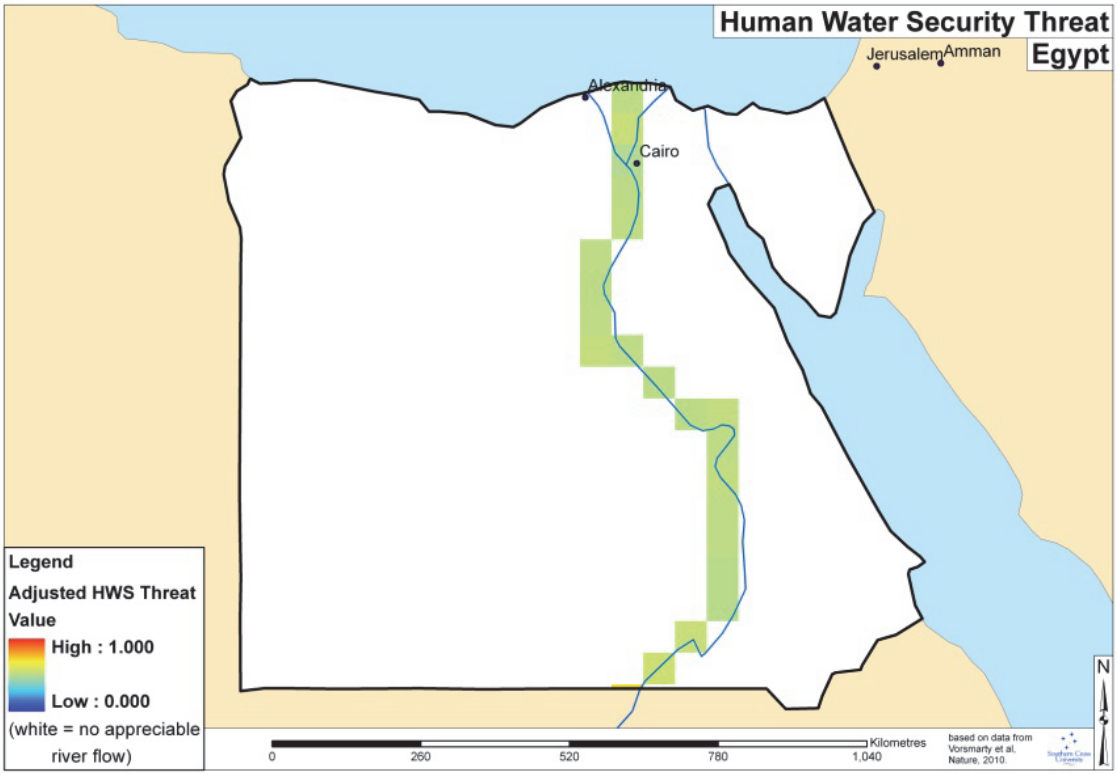

Figure 8. *Present Adjusted Human Water Security Threat (HWS) for Egypt, calculated following the method described by Vörösmarty et al. (2010).*

Smakhtin et al. (2004) present a first attempt to estimate the volume of water required for the maintenance of freshwater-dependent ecosystems at the global scale. This total environmental water requirement (EWR) consists of ecologically relevant low-flow and high-flow components. The authors argue that the relationship between water availability, total use and the EWR may be described by the water stress indicator (WSI). If WSI exceeds 1.0, the basin is classified as “environmentally water scarce”. In such a basin, the discharge has already been reduced by total withdrawals to such levels that the amount of water left in the basin is less than EWR. Smaller index values indicate progressively lower water resources exploitation and lower risk of “environmental water scarcity.” Basins where WSI is greater than 0.6 but less than 1.0 are arbitrarily defined as heavily exploited or “environmentally water stressed” and basins where WSI is greater than 0.3 but less than 0.6 are defined as moderately exploited. In these basins, 0-40% and 40-70% of the utilizable water respectively is still available before water withdrawals come in conflict with the EWR. Environmentally “safe” basins are defined as those where WSI is less than 0.3. The global distribution of WSI for the 1961-1990 time horizon is shown in Figure 9.

Similar results are presented by Schuol et al. (2008); the authors applied the Soil Water Assessment Tool (SWAT) to determine the freshwater components of blue water (water yield), green water flow (evapotranspiration), and green water storage (soil water) across Africa in the present climate. Results showed that Egypt exhibits very high water stress, although the assessment did not realistically take into account the immense water management infrastructure that is in place.

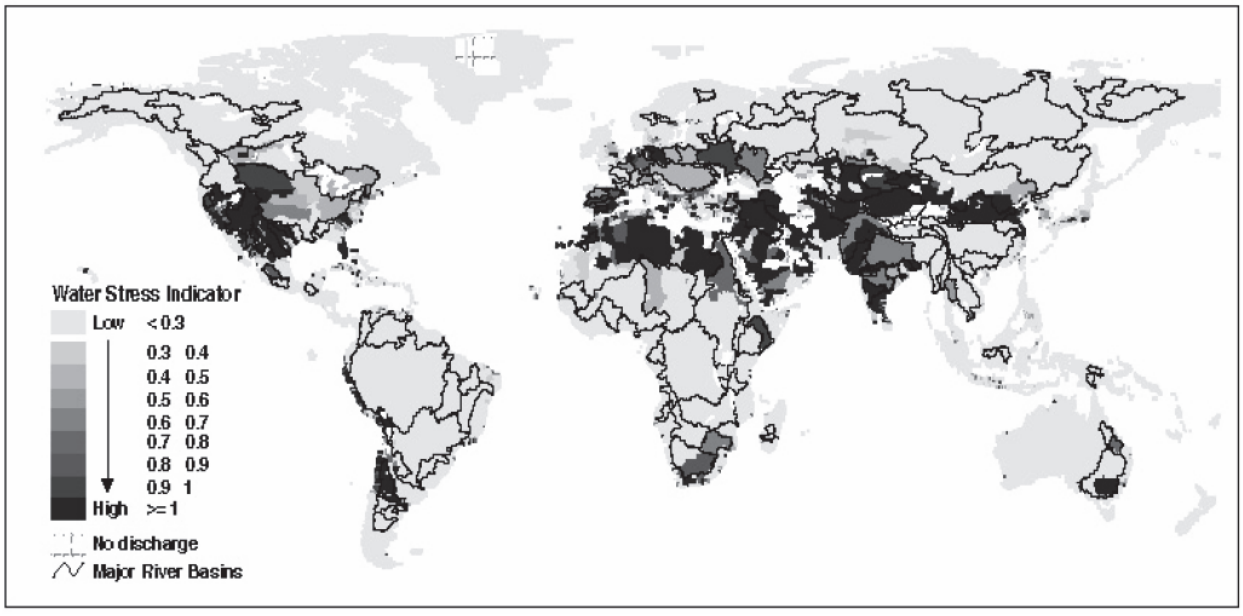

Figure 9. *A map of the major river basins across the globe and the water stress indicator (WSI) for the 1961-1990 time horizon. The figure is from Smakhtin et al. (2004).*

Climate change studies

Rockstrom et al. (2009) applied the LPJml vegetation and water balance model (Gerten et al. 2004) to assess green-blue water (irrigation and infiltrated water) availability and requirements. The authors applied observed climate data from the CRU TS2.1 gridded dataset for a present-day simulation, and climate change projections from the HadCM2 GCM under the SRES A2 scenario to represent the climate change scenario for the year 2050. The study assumed that if water availability was less than 1,300m^3/capita/year, then the country was considered to present insufficient water for food self-sufficiency. The simulations presented by Rockstrom et al. (2009) should not be considered as definitive, however, because the study only applied one climate model, which means climate modelling uncertainty was overlooked. The results from the two simulations are presented in Figure 10. Rockstrom et al. (2009) found that globally in 2050 and under the SRES A2 scenario, around 59% of the world's population could be exposed to "blue water shortage" (i.e. irrigation water shortage), and 36% exposed to "green water shortages" (i.e. infiltrated rain shortage). Egypt was found to be exposed to high green-blue water stress by 2050.

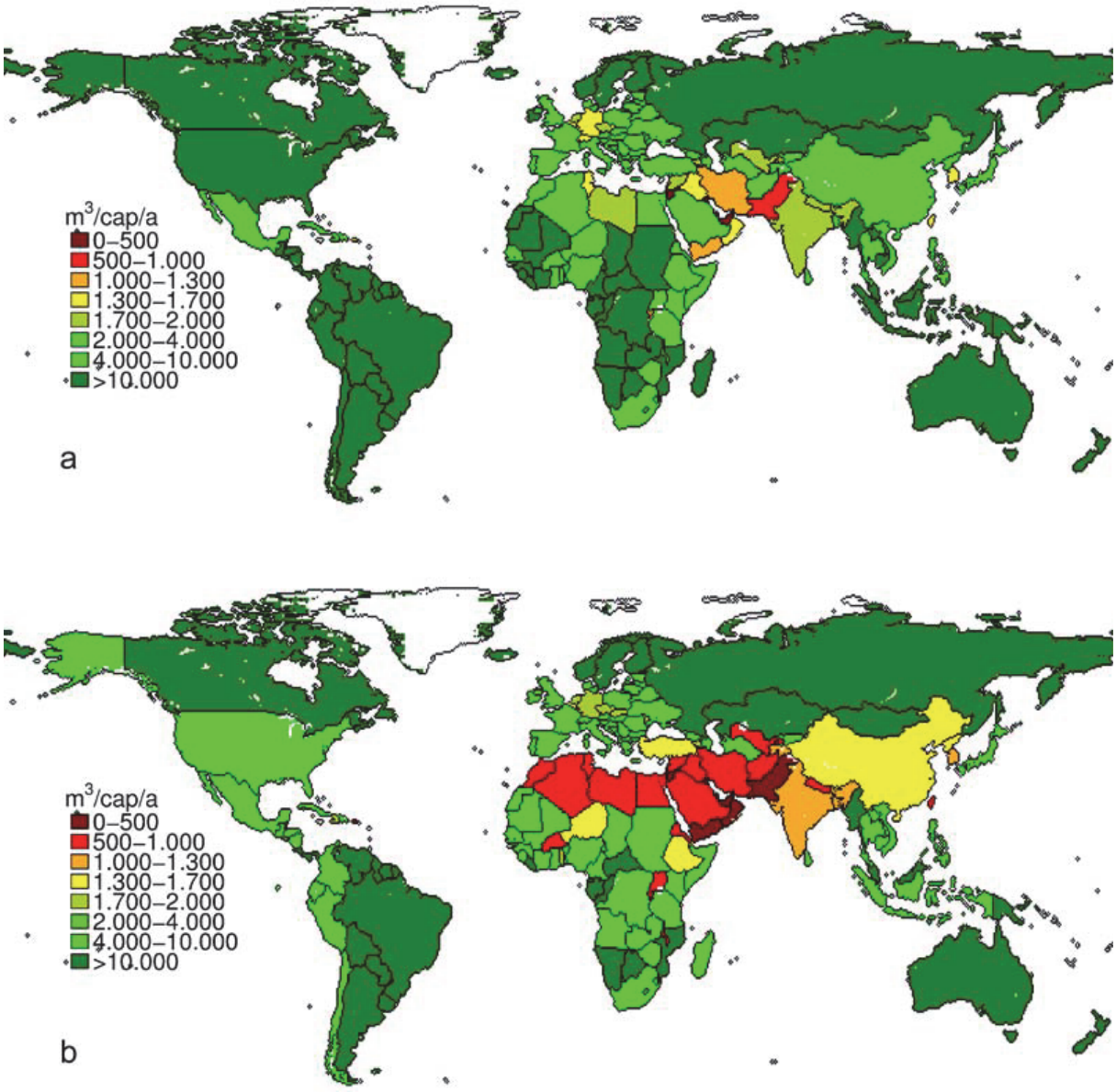

Figure 10. *Simulated blue-green water availability (m^3/capita/year) for present climate (top panel) and including both demographic and climate change under the SRES A2 scenario in 2050 (bottom panel). The study assumed that if water availability was less than 1,300m^3/capita/year, then the country was considered to present insufficient water for food self-sufficiency. The figure is from Rockstrom et al. (2009).*

Similarly, a global-scale assessment presented by Menzel and Matovelle (2010) showed that five out of six simulations with climate and socio-economic changes suggested that Egypt could experience severe water stress by 2050. Menzel and Matovelle (2010) applied the WaterGAP global hydrological model in their study, which specifically includes groundwater recharge. Moreover, the authors estimated water stress, based upon simulations of river discharge and groundwater recharge (blue water availability).

Doll (2009) presents updated estimates of the impact of climate change on groundwater resources by applying a new version of the WaterGAP hydrological model. The study accounted for the number of people affected by changes in groundwater resources under climate change relative to present (1961-1990). To this end, the study provides an assessment of the vulnerability of humans to decreases in available groundwater resources (GWR). This indicator was termed the “Vulnerability Index” (VI), defined as; VI = -% change GWR * Sensitivity Index (SI). The SI component was a function of three more specific sensitivity indicators that include an indicator of water scarcity (calculated from the ratio between consumptive water use to low flows), an indicator for the dependence upon groundwater supplies, and an indicator for the adaptive capacity of the human system. Doll (2009) applied climate projections from two GCMs (ECHAM4 and HadCM3) to WaterGAP, for two scenarios (SRES A2 and B2), for the 2050s. Figure 11 presents each of these four simulations respectively. There is variation across scenarios and GCMs. But there is consensus that vulnerability is high in the North African Mediterranean. However, no decrease in GWR with climate change was simulated for Egypt, which implies that Egypt is not vulnerable to water stress in this assessment. However, it should be noted that 97.6% of Egypt’s total renewable water resource is from surface water, whereas only 2.4% is from groundwater recharge (UN, 2007), which is the focus of the study presented by Doll (2009). Therefore the results are unlikely to be representative of the total (surface water and groundwater recharge) water security situation for Egypt.

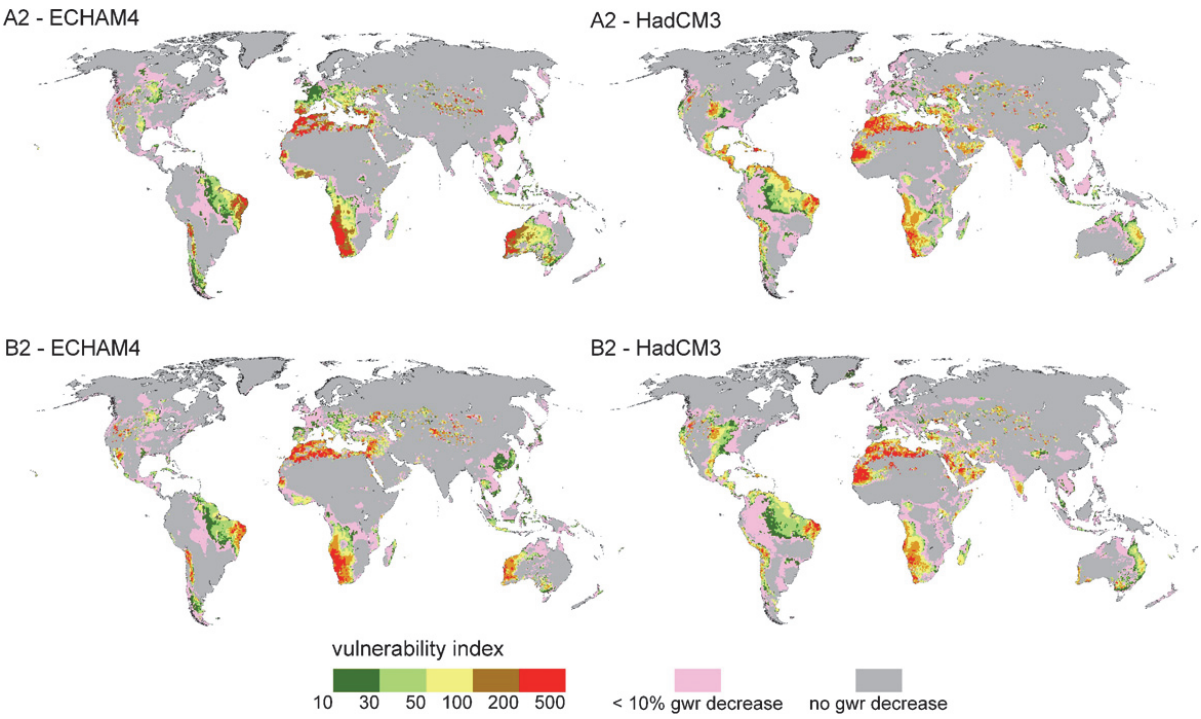

Figure 11. *Vulnerability index (VI) showing human vulnerability to climate change induced decreases of renewable groundwater resources (GWR) by the 2050s under two emissions scenarios for two GCMs. VI is only defined for areas with a GWR decrease of at least 10% relative to present (1961-1990). The figure is from Doll (2009).*

National-scale or sub-national scale assessments

A number of national-scale studies point towards decreased discharge of the Nile and high vulnerability to water stress in Egypt with climate change. However, Egypt's second national communication under the United Nations Framework Convention on Climate Change (UNFCC) notes that these projections are strongly dependent on the choice of the climate scenario and the underlying GCM (EEAA, 2010). This broadly supports the conclusions from Figure 12.

Agrawala et al. (2004) concluded that population, land use and agriculture and economic activity in Egypt are all being constrained along the Nile Valley and Delta, which makes Egypt extremely vulnerable to any adverse impacts on Nile water availability. The authors note that Nile water availability could be increasingly stressed due to higher demand and higher evaporative losses with climate change. This potential vulnerability could be seriously exacerbated should climatic impacts be accompanied by any concomitant reduction in the country's allocation of Nile water, or even unaccounted for excessive abstraction from upstream countries.

Egypt's second national communication under the UNFCC (EEAA, 2010) reported that the impacts of potential future hydropower dam operation in the upstream part of the Nile Basin

under climate scenarios could be associated with wetter and warmer climate in most of the Upper Blue Nile River Basin but higher and more severe low flows by 2050. Mid to long term droughts were reported to become less frequent. Moreover, potential future dam operations were considered unlikely to significantly affect water availability to Sudan and Egypt based on simulated outflows from six GCMs and several operation scenarios (EEAA, 2010). The report notes, however, that the results are uncertain due to climate modelling uncertainty.

Beyene et al. (2010) assessed the potential impacts of climate change on the hydrology and water resources of the Nile River basin using a macro scale hydrology model. The authors applied climate change projections from 11 GCMs under two global emissions scenarios (A2 and B1). Beyene et al. (2010) found that while all GCMs agreed with respect to the direction of 21st Century temperature changes, there was considerable variability in the magnitude, direction, and seasonality of projected precipitation changes. Streamflow was simulated to decline during mid- (2040–2069) and late (2070–2099) century as a result of both precipitation declines and increased evaporative demand. The predicted multi-model average streamflow at High Aswan Dam (HAD) as a percentage of historical (1950–1999) annual average was 111 (114), 92 (93) and 84 (87) for A2 (B1) emissions scenarios. Implications of these streamflow changes on the water resources of the Nile River basin were analyzed by quantifying the annual hydropower production and irrigation water release at HAD. The long-term HAD release for irrigation decreases to 87 (89) and 86 (84)% of historical in 2040–2069 and 2070–2099 century, respectively, for the A2 (B1) global emissions scenarios. Beyene et al. (2010) conclude that Egyptian agricultural water supplies could be negatively impacted, especially in the second half of the century.

AVOID programme results

To further quantify the impact of climate change on water stress and the inherent uncertainties, the AVOID programme calculated water stress indices for all countries reviewed in this literature assessment based upon the patterns of climate change from 21 GCMs (Warren et al., 2010), following the method described by Gosling et al. (2010) and Arnell (2004). This ensures a consistent methodological approach across all countries and takes consideration of climate modelling uncertainties.

Methodology

The indicator of the effect of climate change on exposure to water resources stress has two components. The first is the number of people within a region with an *increase in exposure to stress*, calculated as the sum of 1) people living in water-stressed watersheds with a

significant reduction in runoff due to climate change and 2) people living in watersheds which become water-stressed due to a reduction in runoff. The second is the number of people within a region with a *decrease in exposure to stress*, calculated as the sum of 1) people living in water-stressed watersheds with a significant increase in runoff due to climate change and 2) people living in watersheds which cease to be water-stressed due to an increase in runoff. It is not appropriate to calculate the net effect of "increase in exposure" and "decrease in exposure", because the consequences of the two are not equivalent. A water-stressed watershed has an average annual runoff less than $1000m^3$/capita/year, a widely used indicator of water scarcity. This indicator may underestimate water stress in watersheds where per capita withdrawals are high, such as in watersheds with large withdrawals for irrigation.

Average annual runoff (30-year mean) is simulated at a spatial resolution of 0.5x0.5° using a global hydrological model, MacPDM (Gosling and Arnell, 2011), and summed to the watershed scale. Climate change has a "significant" effect on average annual runoff when the change from the baseline is greater than the estimated standard deviation of 30-year mean annual runoff: this varies between 5 and 10%, with higher values in drier areas.

The pattern of climate change from 21 GCMs was applied to MacPDM, under two emissions scenarios; 1) SRES A1B and 2) an aggressive mitigation scenario where emissions follow A1B up to 2016 but then decline at a rate of 5% per year thereafter to a low emissions floor (denoted A1B-2016-5-L). Both scenarios assume that population changes through the 21st century following the SRES A1 scenario as implemented in IMAGE 2.3 (van Vuuren et al., 2007). The application of 21 GCMs is an attempt to quantify the uncertainty due to climate modelling, although it is acknowledged that only one impacts model is applied (MacPDM). Simulations were performed for the years 2030, 2050, 2080 and 2100. Following Warren et al. (2010), changes in the population affected by increasing or decreasing water stress represent the additional percentage of population affected due to climate change, not the absolute change in the percentage of the affected population relative to present day.

Results

The results for Egypt are presented in Figure 12. They show that most models indicate that the percentage of Egypt's population exposed to water stress could increase substantially with climate change but there is high uncertainty. The results also indicate that most of the models do not show much of the population experiencing a decrease in water stress with climate change.

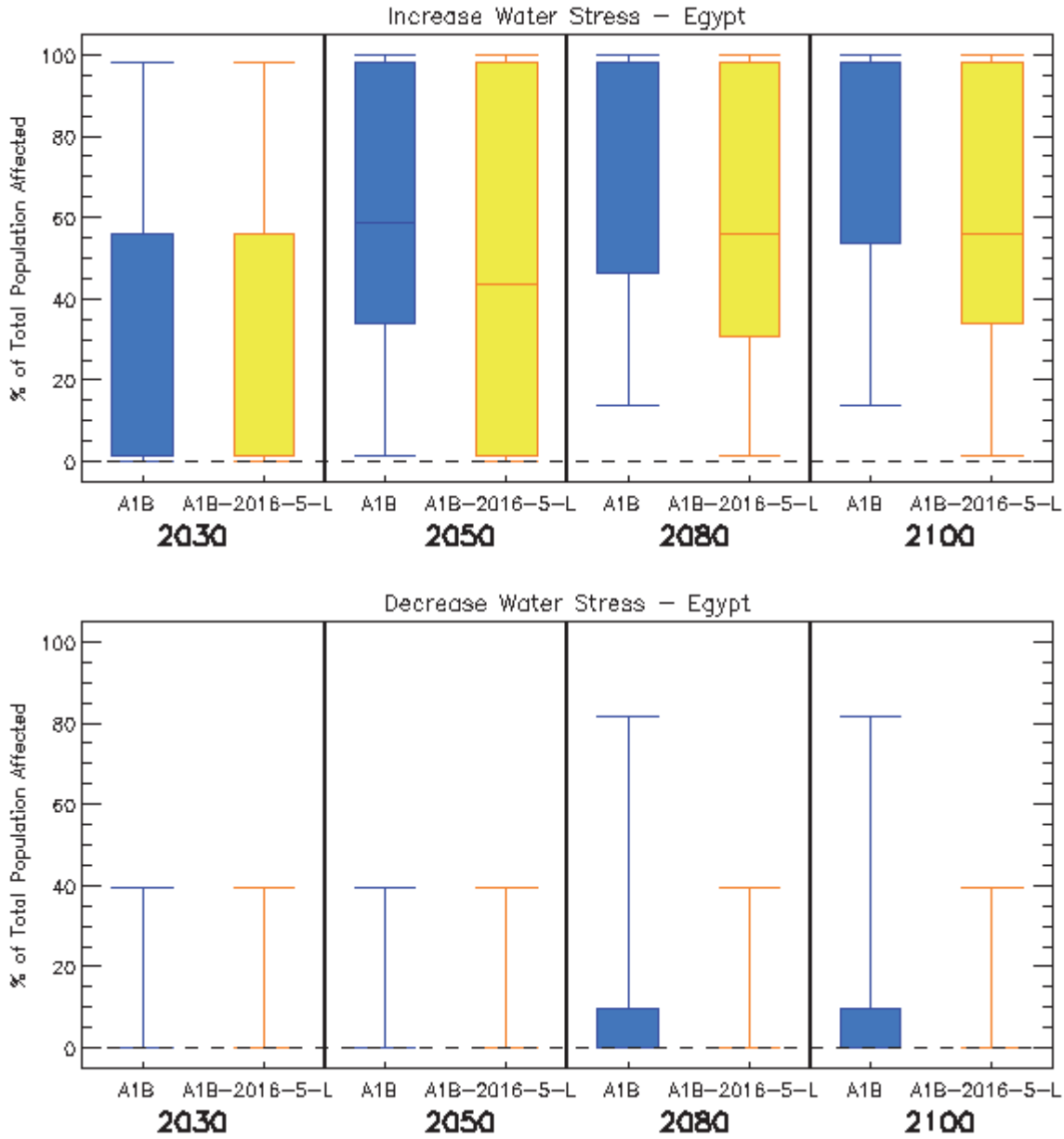

Figure 12. *Box and whisker plots for the impact of climate change on increased water stress (top panel) and decreased water stress (bottom panel) in Egypt, from 21 GCMs under two emissions scenarios (A1B and A1B-2016-5-L), for four time horizons. The plots show the 25th, 50th, and 75th percentiles (represented by the boxes), and the maximum and minimum values (shown by the extent of the whiskers).*

Pluvial flooding and rainfall

Headline

The IPCC AR4 found consistency across GCMs that mean precipitation could decrease with climate change for Egypt, but with potential increases in rainfall extremes. Little has been published since on the impact of climate change on pluvial flooding for Egypt, although one study conducted for the Nile Basin confirms the conclusions of the IPCC.

Introduction

Pluvial flooding can be defined as flooding derived directly from heavy rainfall, which results in overland flow if it is either not able to soak into the ground or exceeds the capacity of artificial drainage systems. This is in contrast to fluvial flooding, which involves flow in rivers either exceeding the capacity of the river channel or breaking through the river banks, and so inundating the floodplain. Pluvial flooding can occur far from river channels, and is usually caused by high intensity, short-duration rainfall events, although it can be caused by lower intensity, longer-duration events, or sometimes by snowmelt. Changes in mean annual or seasonal rainfall are unlikely to be good indicators of change in pluvial flooding; changes in extreme rainfall are of much greater significance. However, even increases in daily rainfall extremes will not necessarily result in increases in pluvial flooding, as this is likely to be dependent on the sub-daily distribution of the rainfall as well as local factors such as soil type, antecedent soil moisture, land cover (especially urbanisation), capacity and maintenance of artificial drainage systems etc. It should be noted that both pluvial and fluvial flooding can potentially result from the same rainfall event.

Assessments that include a global or regional perspective

The IPCC AR4 (2007a) stated that annual rainfall is likely to decrease in much of Mediterranean Africa. A 20% reduction in the annual mean could be typical along the coast by 2100 under the A1B scenario, with drying seen throughout much of the year (IPCC, 2007a, p. 868). However, increases in maximum annual rainfall could be above 50% on an annual basis, with higher increases in summer and autumn. Increases are also projected at the 75% quartile for rainfall during these seasons.

National-scale or sub-national scale assessments

Literature searches yielded no results for national-scale or sub-national scale studies for this impact sector.

Fluvial flooding

Headline

There is uncertainty regarding the magnitude to which flood season discharge in the Nile River could be affected with climate change and GCMs are not consistent in simulating the same sign of change. Simulations by the AVOID programme, based upon simulations with 21 climate models, found that a large majority of the models show a tendency towards decreasing flood risk with climate change in the early 21st century. Later in the century a majority of the models still agree on a decrease compared to the present-day average annual flood risk, but especially in the A1B scenario a small number of models starts to show larger increases. Future studies should seek to further quantify the uncertainty in climate projections.

Introduction

This section summarises findings from a number of post IPCC AR4 assessments on river flooding in Egypt to inform and contextualise the analysis performed by the AVOID programme for this project. The results from the AVOID work are discussed in the next section.

Fluvial flooding involves flow in rivers either exceeding the capacity of the river channel or breaking through the river banks, and so inundating the floodplain. A complex set of processes is involved in the translation of precipitation into runoff and subsequently river flow (routing of runoff along river channels). Some of the factors involved are; the partitioning of precipitation into rainfall and snowfall, soil type, antecedent soil moisture, infiltration, land cover, evaporation and plant transpiration, topography, groundwater storage. Determining whether a given river flow exceeds the channel capacity, and where any excess flow will go, is also not straightforward, and is complicated by the presence of artificial river embankments and other man-made structures for example. Hydrological models attempt to simplify and conceptualise these factors and processes, to allow the simulation of runoff and/or river flow under different conditions. However, the results from global-scale hydrological modelling need to be interpreted with caution, especially for smaller regions, due to the necessarily coarse resolution of such modelling and the assumptions and simplifications this entails (e.g. a 0.5^{o} grid corresponds to landscape features spatially averaged to around 50-55km for mid- to low-latitudes). Such results provide a consistent,

high-level picture, but will not show any finer resolution detail or variability. Smaller-scale or catchment-scale hydrological modelling can allow for more local factors affecting the hydrology, but will also involve further sources of uncertainty, such as in the downscaling of global climate model data to the necessary scale for the hydrological models. Furthermore, the application of different hydrological models and analysis techniques often makes it difficult to compare results for different catchments.

Assessments that include a global or regional perspective

Since the publication of the IPCC AR4 several studies have been published looking at the projected impacts of climate change on water resources of the Nile Basin. However few of these have investigated specifically peak river flows and flood hazards. A global modelling study presented by Hirabayashi et al. (2008), which applied climate change projections from a single GCM, suggests that by the end of the 21st century under the A1B emissions scenario, the return period of what was a 100-year flood event in the Nile Basin in the 20th century decreases to about 16 years. This could mean that extreme peak discharges may occur more than 6 times more frequently in the future. It should be noted, however, that results from studies that have applied only a single climate model or climate change scenario should be interpreted with caution. This is because they do not consider other possible climate change scenarios which could result in a different impact outcome, in terms of magnitude and in some cases sign of change.

National-scale or sub-national scale assessments

Beyene et al. (2010) simulated monthly changes Nile River discharge under two emission scenarios (A2 and B1) with 11 GCMs. Their results project mostly an increase (up to +30%) in discharge during the flood season (July-September) early in the century (2010-2039). By the end of the century, however, this trend changed and most models simulated a decrease in discharge during the high-flow season, due to higher temperatures and hence more evaporation upstream in the Nile Basin. There was, however, a considerable spread amongst the GCMs and at least 3 GCMs still projected an increase up to +20% in flood season discharge in this period.

Two recent studies have used the Nile Forecast System (NFS) to project changes in the Blue Nile, which is the main contributor of discharge during high-flow season (Elshamy et al., 2009, Soliman et al., 2009). The studies applied different approaches to downscale climate simulations from GCMs. Soliman et al. (2009) applied dynamical downscaling with a RCM and found that by the middle of the century (2034-2055) under the A1B emissions scenario,

the seasonality of the Blue Nile river flow increased, with an increase in early flood season (June-August) discharge by 10%, and a decrease in river flows later during the flood season and during the dry season. Elshamy et al. (2009) applied statistical downscaling of three GCMs and found a slight increasing trend in flood season discharge of the Blue Nile under the A2 emissions scenario, and less change under B2. In their study, one GCM showed an increase in flood season river flow early in the century (up to the 2030s) followed by a reduction later on. For all these studies it is important to note the role of transboundary water management decisions in determining water resource availability and flood management across the Nile Basin (for example see Conway (2005)).

AVOID programme results

To quantify the impact of climate change on fluvial flooding and the inherent uncertainties, the AVOID programme calculated an indicator of flood risk for all countries reviewed in this literature assessment based upon the patterns of climate change from 21 GCMs (Warren et al., 2010). This ensures a consistent methodological approach across all countries and takes consideration of climate modelling uncertainties.

Methodology

The effect of climate change on fluvial flooding is shown here using an indicator representing the percentage change in average annual flood risk within a country, calculated by assuming a standardised relationship between flood magnitude and loss. The indicator is based on the estimated present-day (1961-1990) and future flood frequency curve, derived from the time series of runoff simulated at a spatial resolution of 0.5°x0.5° using a global hydrological model, MacPDM (Gosling and Arnell, 2011). The flood frequency curve was combined with a generic flood magnitude–damage curve to estimate the average annual flood damage in each grid cell. This was then multiplied by grid cell population and summed across a region, producing in effect a population-weighted average annual damage. Flood damage is thus assumed to be proportional to population in each grid cell, not the value of exposed assets, and the proportion of people exposed to flood is assumed to be constant across each grid cell (Warren et al., 2010).

The national values are calculated across major floodplains, based on the UN PREVIEW Global Risk Data Platform (preview.grid.unep.ch). This database contains gridded estimates, at a spatial resolution of 30 arc-seconds (0.00833°x0.00833°), of the estimated frequency of flooding. From this database the proportion of each 0.5°x0.5° grid cell defined as floodplain was determined, along with the numbers of people living in each 0.5°x0.5° grid cell in flood-

prone areas. The floodplain data set does not include “small” floodplains, so underestimates actual exposure to flooding. The pattern of climate change from 21 GCMs was applied to MacPDM, under two emissions scenarios; 1) SRES A1B and 2) an aggressive mitigation scenario where emissions follow A1B up to 2016 but then decline at a rate of 5% per year thereafter to a low emissions floor (denoted A1B-2016-5-L). Both scenarios assume that population changes through the 21st century following the SRES A1 scenario as implemented in IMAGE 2.3 (van Vuuren et al., 2007). The application of 21 GCMs is an attempt to quantify the uncertainty due to climate modelling, although it is acknowledged that only one impacts model is applied (MacPDM). Simulations were performed for the years 2030, 2050, 2080 and 2100. The result represents the change in flood risk due to climate change, not the change in flood risk relative to present day (Warren et al., 2010).

Results

The results for Egypt are presented in Figure 13. By the 2030s, the models project a range of changes in mean fluvial flooding risk over Egypt in both scenarios, with some models projecting decreases and others increases but with a balance towards a decrease in flood risk. The largest decrease projected for the 2030s is a 70% decline in the average annual flood risk, while the largest increase is 50%.

By 2100 the model projections from the different models becomes greater. This is more pronounced for the A1B scenario than the mitigation scenario. Under the mitigation scenario, most models still project a lower flood risk (down to −90%), but some project an increase. The mean across all projections is a 40% decrease, and the largest increase is approximately +80%. Under the A1B scenario, three quarters of models project a decreased flood. The largest projected increase is approximately +210%, but the mean projection across all models is a decrease in the annual average flood risk of around 50%.

So for Egypt, the models show a greater tendency towards decreasing flood risk at first in both scenarios. Later in the century a majority of the models still agree on a decrease compared to the present-day average annual flood risk, but especially in the A1B scenario a small number of models starts to show larger increases. The differences between the model projections are greater later in the century and particularly for A1B.

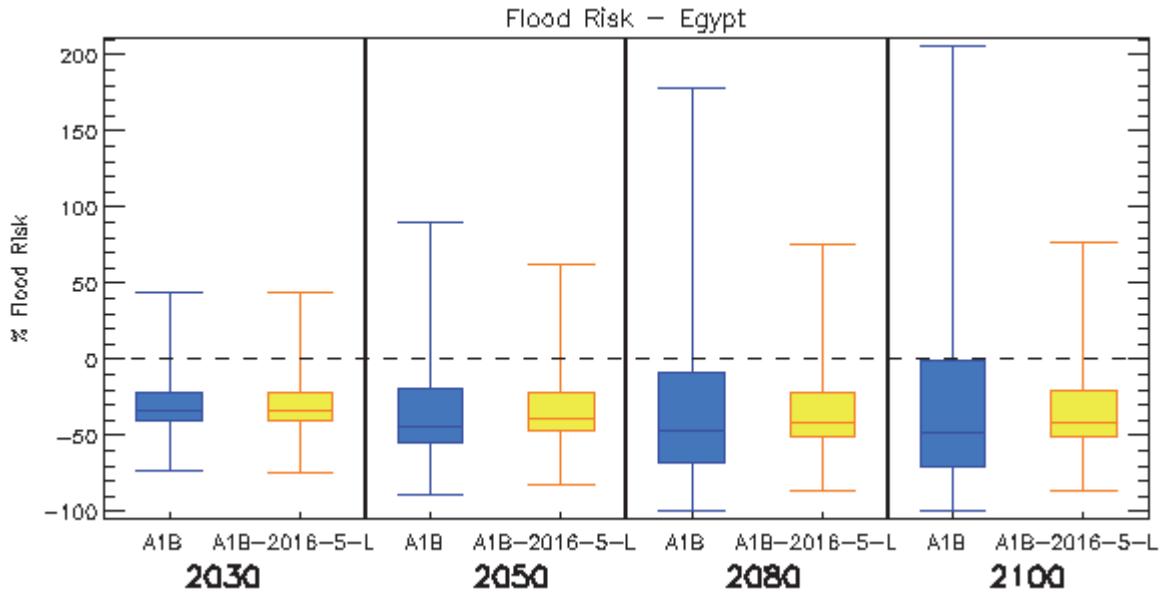

***Figure 13**. Box and whisker plots for the percentage change in average annual flood risk within Egypt, from 21 GCMs under two emissions scenarios (A1B and A1B-2016-5-L), for four time horizons. The plots show the 25th, 50th, and 75th percentiles (represented by the boxes), and the maximum and minimum values (shown by the extent of the whiskers).*

Tropical cyclones

This country is not impacted by tropical cyclones.

Coastal regions

Headline

Several studies conclude that Egypt is highly vulnerable to sea level rise (SLR). In one study that considered the impact of a 1m SLR for 84 developing countries, Egypt was ranked the 2nd highest with respect to the coastal population affected, 3rd highest for coastal GDP affected and 5th highest for proportion of urban areas affected. Around 15% (2.7 million people) of Egypt's coastal population could be affected by a 10% intensification of the current 1-in-100-year storm surge combined with a 1m SLR. Simulations by the Coastal Research Institute suggest that the total area of the Nile Delta affected in 2025, 2050, 2075 and 2100, could be 153, 256, 450, and 761 km^2, respectively, under an SRES A1FI scenario.

Assessments that include a global or regional perspective

The IPCC AR4 concluded that at the time, understanding was too limited to provide a best estimate or an upper bound for global SLR in the twenty-first century (IPCC, 2007b). However, a range of SLR, excluding accelerated ice loss effects was published, ranging from 0.19m to 0.59m by the 2090s (relative to 1980-2000), for a range of scenarios (SRES A1FI to B1). The IPCC AR4 also provided an illustrative estimate of an additional SLR term of up to 17cm from acceleration of ice sheet outlet glaciers and ice streams, but did not suggest this is the upper value that could occur. Although there are published projections of SLR in excess of IPCC AR4 values (Nicholls et al., 2011), many of these typically use semi-empirical methods that suffer from limited physical validity and further research is required to produce a more robust estimate. Linking sea level rise projections to temperature must also be done with caution because of the different response times of these two climate variables to a given radiative forcing change.

Nicholls and Lowe (2004) previously showed that mitigation alone would not avoid all of the impacts due to rising sea levels, adaptation would likely be needed too. Recent work by van Vuuren et al. (2011) estimated that, for a world where global mean near surface temperatures reach around 2°C by 2100, global mean SLR could be 0.49m above present levels by the end of the century. Their sea level rise estimate for a world with global mean temperatures reaching 4°C by 2100 was 0.71m, suggesting around 40% of the future increase in sea level to the end of the 21st century could be avoided by mitigation. A qualitatively similar conclusion was reached in a study by Pardaens et al. (2011), which

examined climate change projections from two GCMs. They found that around a third of global-mean SLR over the 21st century could potentially be avoided by a mitigation scenario under which global-mean surface air temperature is near-stabilised at around 2°C relative to pre-industrial times. Under their baseline business-as-usual scenario the projected increase in temperature over the 21st century is around 4°C, and the sea level rise range is 0.29-0.51m (by 2090-2099 relative to 1980-1999; 5% to 95% uncertainties arising from treatment of land-based ice melt and following the methodology used by the IPCC AR4). Under the mitigation scenario, global mean SLR in this study is projected to be 0.17-0.34m.

The IPCC 4th assessment (IPCCa) followed Nicholls and Lowe (2004) for estimates of the numbers of people affected by coastal flooding due to sea level rise. Nicholls and Lowe (2004) projected for the South Mediterranean region that an additional 1.6 million people per year could be flooded due to sea level rise by the 2080s relative to the 1990s for the SRES A2 Scenario (note this region also includes other countries, such as Libya and Algeria). However, it is important to note that this calculation assumed that protection standards increased as GDP increased, although there is no additional adaptation for sea level rise. More recently, Nicholls et al. (2011) also examined the potential impacts of sea level rise in a scenario that gave around 4°C of warming by 2100. Readings from Figure 3 from Nicholls et al. (2011) for the southern Mediterranean region suggest that less than an approximate 5 million additional people could be flooded for a 0.5 m SLR (assuming no additional protection). Nicholls et al. (2011) also looked at the consequence of a 2m SLR by 2100, however as we consider this rate of SLR to have a low probability we don't report these figures here.

Useful global-scale analyses of the impacts of SLR on coastal regions for several developing countries are presented by Dasgupta et al. (2009a, 2009b, 2010). Dasgupta et al. (2009a) investigated the consequences of prescribed SLR (1-5m in 1m increments) by GIS land inundation mapping but they did not consider any effects of climate change (e.g. variability in storm surges). Indeed, the authors note that their impacts estimates are conservative because of this and they note that even a small SLR can significantly magnify the impact of storm surges, which occur regularly and with devastating consequences in some coastal areas. The analysis was limited to 84 developing countries, and it was assumed that the level of coastal protection remained at present-day levels for all SLR scenarios. Out of the 84 countries that Dasgupta et al. (2009a) considered, Egypt was ranked the 2nd highest with respect to the coastal population impacted, 3rd highest for coastal GDP affected and 5th highest for proportion of urban areas affected, due to a 1m SLR (see Table 14). Dasgupta et al. (2009a) note that these impacts are disproportionately high in the Nile delta; e.g. a

comparison of satellite images of the Nile delta for 2000 and the projected image for a prescribed 1m SLR reveals that 25% of the delta could be inundated (Figure 14).

Rank	Land area	Population	GDP	Urban areas	Agricultural land	Wetlands
1	The Bahamas (11.57)	Vietnam (10.79)	Vietnam (10.21)	Vietnam (10.74)	Egypt (13.09)	Vietnam (28.67)
2	Vietnam (5.17)	Egypt (9.28)	Mauritania (9.35)	Guyana (10.02)	Vietnam (7.14)	Jamaica (28.16)
3	Qatar (2.70)	Mauritania (7.95)	Egypt (6.44)	French Guiana (7.76)	Suriname (5.60)	Belize (27.76)
4	Belize (1.90)	Suriname (7.00)	Suriname (6.35)	Mauritania (7.50)	The Bahamas (4.49)	Qatar (21.75)
5	Puerto Rico (1.64)	Guyana (6.30)	Benin (5.64)	Egypt (5.52)	Argentina (3.19)	The Bahamas (17.75)
6	Cuba (1.59)	French Guiana (5.42)	The Bahamas (4.74)	Libya (5.39)	Jamaica (2.82)	Libya (15.83)
7	Taiwan & China (1.59)	Tunisia (4.898)	Guyana (4.64)	UAE (4.80)	Mexico (1.60)	Uruguay (15.14)
8	The Gambia (1.33)	UAE (4.59)	French Guiana (3.02)	Tunisia (4.50)	Myanmar (1.48)	Mexico (14.85)
9	Jamaica (1.27)	The Bahamas (4.56)	Tunisia (2.93)	Suriname (4.20)	Guyana (1.16)	Benin (13.78)
10	Bangladesh (1.12)	Benin (4.93)	Ecuador (2.66)	The Bahamas (3.99)	Taiwan & China (1.05)	Taiwan & China (11.70)

Table 14. *The top 10 most impacted countries with a 1m SLR according to a study across 84 developing countries. Figures in parenthesis are the percentage impact for each country; e.g. 13.09% of all agricultural land in Egypt was simulated to be affected by a 1m SLR. Countries considered in this review are highlighted. Adapted from Dasgupta et al. (2009a).*

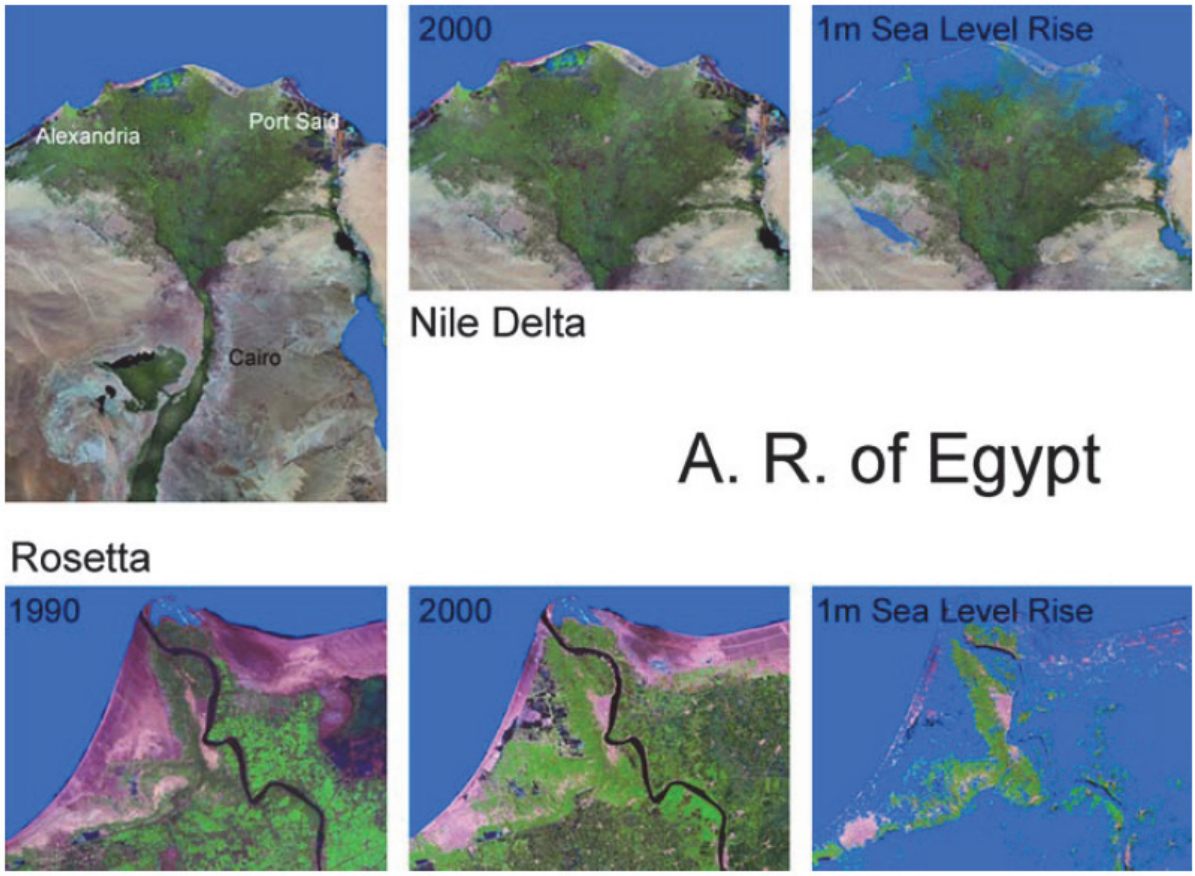

Figure 14. *Inundation zones for a 1m SLR in the Nile Delta and at Rosetta. The figure is from Dasgupta et al. (2009a).*

In a different study, Dasgupta et al. (2009b) considered the same 84 developing countries as Dasgupta et al. (2009a), but rather than investigating impacts under several magnitudes of prescribed SLR, Dasgupta et al. (2009b) considered a 10% intensification of the current 1-in-100-year storm surge combined with a 1m SLR. GIS inundation models were applied in the analysis and the method means that uncertainty associated with the climate system is inherently overlooked. Nevertheless, the projections give a useful indicator of the possible impact of SLR in Egypt and they serve to confirm the high vulnerability of Egypt identified by Dasgupta et al. (2009a). Table 15 shows that around 15% (2.7 million people) of Egypt's coastal population could be affected.

Country	**Incremental Impact: Land Area (sq. km)**	Projected Impact as a % of Coastal Total	**Incremental Impact: Population**	Projected Impact as a % of Coastal Total	**Incremental Impact: GDP (mil. USD)**	Projected Impact as a % of Coastal Total	**Incremental Impact: Agricultural Area (sq. km)**	Projected Impact as a % of Coastal Total	**Incremental Impact: Urban Extent (sq. km)**	Projected Impact as a % of Coastal Total	**Incremental Impact: Wetlands (sq. km)**	Projected Impact as a % of Coastal Total
Africa												
South Africa	607	43.09	48,140	32.91	174	30.98	70	34.48	93	48.10	132	46.23
Egypt	2,290	13.61	2,600,000	14.68	4,600	16.67	692	5.23	627	15.30	640	28.36
Kenya	274	41.93	27,400	40.23	10	32.05	40	22.13	9	38.89	177	52.51
Americas												
Argentina	2,400	18.03	278,000	19.52	2,240	16.42	157	9.93	313	27.47	459	11.30
Brazil	6,280	15.08	1,100,000	30.37	4,880	28.48	275	16.47	960	33.67	2,590	11.48
Mexico	9,130	29.04	463,000	20.56	2,570	21.22	310	10.89	701	18.35	1,760	52.25
Peru	727	36.69	61,000	46.90	177	46.18	5	26.92	54	42.72	20	37.91
Asia												
China	11,800	17.52	10,800,000	16.67	31,200	17.15	6,640	11.66	2,900	15.70	4,360	39.77
Rep. of Korea	902	61.73	863,000	50.48	10,600	47.86	237	66.75	335	48.15	77	78.81
India	8,690	29.33	7,640,000	28.68	5,170	27.72	3,740	23.64	1,290	30.04	2,510	32.31
Indonesia	14,400	26.64	5,830,000	32.75	7,990	38.71	4,110	26.12	1,280	33.25	2,680	26.97
Saudi Arabia	1,360	41.58	243,000	42.92	2,420	40.60	0	0.00	390	45.85	715	51.04
Bangladesh	4,450	23.45	4,840,000	16.01	2,220	19.00	2,710	17.52	433	18.30	3,890	24.29

Table 15. *The impact of a 1m SLR combined with a 10% intensification of the current 1-in-100-year storm surge. Impacts are presented as incremental impacts, relative to the impacts of existing storm surges. Each impact is presented in absolute terms, then as a percentage of the coastal total; e.g. 9.93% of Argentina's coastal agricultural land is impacted. The table is adapted from a study presented by Dasgupta et al. (2009b), which considered impacts in 84 developing countries. Only those countries relevant to this review are presented here and all incremental impacts have been rounded down to three significant figures.*

Dasgupta et al. (2010) repeated this analysis to show that out of the 84 countries considered, Egypt presented the 6th highest percentage increase from present in the exposed population to a 1m SLR and a 10% intensification of storm surges; the increase was 190.3% (see Table 16). For coastal GDP, this country was also 6th highest with an increase of 213.7%. Also, Egypt was 4th highest for urban area affected, with an increase of 247.6%, relative to present. Egypt was the highest ranked country for coastal agricultural impacts, with an increase of nearly 400%. In conclusion, the results demonstrate that Egypt is highly vulnerable to SLR.

Rank	Land area	Population	GDP	Urban	Agriculture	Wetlands
1	Ivory Coast (285.2)	Ivory Coast (590.7)	Ivory Coast (1025.5)	Ivory Coast (500.0)	Egypt (398.3)	Algeria (400.5)
2	D.Rep.Congo (266.6)	D.Rep.Congo (285.8)	Gabon (282.5)	Gabon (300.0)	Mozambique (237.8)	Chile (400.0)
3	Sri Lanka (243.0)	Mauritania (270.2)	D.Rep.Congo (252.7)	Honduras (300.0)	Sri Lanka (218.2)	Angola (398.8)
4	Honduras (226.4)	Gabon (260.6)	Gambia (232.7)	Egypt (247.6)	Pakistan (216.7)	Nigeria (274.4)
5	Nigeria (226.3)	Gambia (204.3)	Mauritania (221/3)	Bangladesh (211.9)	Mexico (210.5)	D.Rep.Congo (220.0)
6	Nicaragua (218.6)	Egypt (190.3)	Egypt (213.7)	Cameroon (200.0)	Bangladesh (209.5)	Haiti (211.1)
7	Benin (193.3)	Sri Lanka (185.1)	Bangladesh (193.6)	Gambia (198.7)	Cuba (200.0)	Guinea (200.0)
8	Gambia (159.0)	Honduras (164.4)	Belize (192.1)	Congo (197.8)	Colombia (200.0)	Dom.Republic (198.4)
9	Guatemala (158.0)	Nicaragua (160.6)	Nicaragua (189.0)	Belize (195.2)	Cambodia (191.7)	Guatemala (197.3)
10	Haiti (147.8)	Bangladesh (154.8)	Cameroon (179.2)	Cuba (194.3)	Uruguay (175.0)	Gambia (192.3)

***Table 16**. The top 10 countries out of 84 developing countries, with largest increases in values of exposed indicators (relative to no SLR; values shown in parenthesis), under a prescribed 1m SLR and 10% intensification of storm surges. Countries considered in this review are highlighted. Data sourced from Dasgupta et al. (2010).*

Hanson et al. (2011) present estimates of the exposure of the world's large port cities (population exceeding one million inhabitants in 2005) to coastal flooding due to SLR and storm surge now and in the 2070s. The results generally support the projections presented by Dasgupta et al. (2009a, 2009b, 2010), that Egypt could be highly impacted by SLR. Population exposure was calculated as a function of elevation against water levels related to the 1 in 100 year storm surge. The analysis assumed a homogenous SLR of 0.5m by 2070. For tropical storms a 10% increase in extreme water levels was assumed, with no expansion in affected area; while for extratropical storms, a 10% increase in extreme water levels was assumed. A uniform 0.5 m decline in land levels was assumed from 2005 to the 2070s in those cities which are historically susceptible (usually port cities located in deltas). This

approach provided a variable change in extreme water level from around 0.5m in cities only affected by global SLR, to as much as 1.5m for cities affected by global SLR, increased storminess and human-induced subsidence. Population projections were based upon the UN medium variant, where global population stabilises at around 9 billion by 2050. Figure 15 shows that Egyptian port cities were in the top 10 countries for population exposure to SLR projections in the 2070s. Considering climate change, subsidence, and socio-economic factors; the exposed port city population increases from around 2 million in present to 5 million in the 2070s. Generally, exposure change in developing country cities is more strongly driven by socioeconomic changes, while developed country cities see a more significant effect from climate change (Hanson et al., 2011).

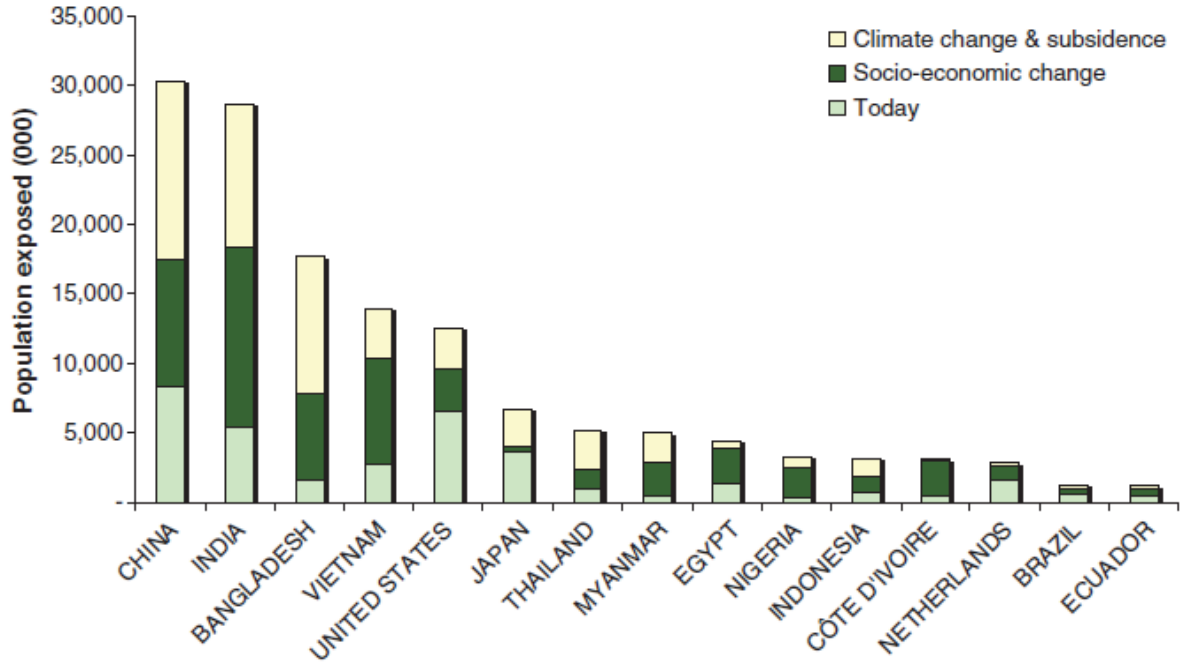

Figure 15. *The top 15 countries in the 2070s for port city exposure to SLR, based upon a global analysis of 136 port cities (Hanson et al., 2011). The proportions associated with current exposure, climate change and subsidence, and socio-economic changes are displayed.*

To further quantify the impact of SLR and some of the inherent uncertainties, the DIVA model was used to calculate the number of people flooded per year for global mean sea level increases (Brown et al., 2011). The DIVA model (DINAS-COAST, 2006) is an integrated model of coastal systems that combines scenarios of water level changes with socio-economic information, such as increases in population. The study uses two climate scenarios; 1) the SRES A1B scenario and 2) a mitigation scenario, RCP2.6. In both cases an SRES A1B population scenario was used. The results are shown in Table 17.

	A1B		RCP	
	Low	**High**	**Low**	**High**
Additional people flooded (1000s)	205.90	2251.67	110.63	938.11
Loss of wetlands area (% of country's total wetland)	36.28%	50.85%	36.14%	42.68%

Table 17. *Number of additional people flooded (1000s), and percentage of total wetlands lost by the 2080s under the high and low SRES A1B and mitigation (RCP 2.6) scenarios (Brown et al., 2011).*

National-scale or sub-national scale assessments

The severity of the global-scale impact assessments for the impact of SLR on Egypt (Dasgupta et al., 2009a, Dasgupta et al., 2009b, Dasgupta et al., 2010, Hanson et al., 2011) are confirmed by national-scale studies. For example, UNEP (2008) showed that under prescribed SLR of 0.5m, 4 million people could be affected and 1,800km^2 of land could be submerged in Egypt. With a 1.5m SLR, this rises to 8 million people affected and 5,700km^2 of land submerged. El-Nahry and Doluschitz (2010) assessed the impact of a 1m SLR for the Nile delta. They showed that 6,900km^2 of cropland, wetland and fish ponds representing 28.93% of the total area of the Nile Delta could be submerged with a 1m SLR and that for a 1.5m SLR, this could be 8,425km^2 representing 35.33% of the total area of the Nile Delta. At 2m SLR, 12,110km^2 representing 50.78% of the total area of the Nile Delta could be submerged. These estimates are higher than those presented by Dasgupta et al. (2009b) for Egypt (see Table 13). Indeed, comparison of other national-scale estimates with the global-scale assessment of Dasgupta et al. (2009b) suggest that the latter study may be underestimating SLR impacts. These differences may be explained in part because the national-scale studies apply higher resolution digital elevation models than are applied by Dasgupta et al. (2009b), thus affording them a more appropriate estimate of potential submergence.

Egypt's second national communication under the United Nations Framework Convention on Climate Change (UNFCC) (EEAA, 2010), reports on the latest results from the Coastal Research Institute (CoRI). CoRI present results of simulations of the total area of the Nile Delta affected by SLR for four future time horizons under an A1FI SLR scenario. CoRI considered the present situation of coastal defence, namely that the boundaries of the lakes are above zero level and the low lands at Abu-Qir Bay are protected by the Mohamed Ali Sea Wall, which was constructed in 1830. The total area of the Nile Delta affected in 2025, 2050, 2075 and 2100, could be 153, 256, 450, and 761 km^2 respectively. Without the

Mohamed Ali Sea Wall and zero level for lake's boarders, the total area affected was 701, 1729, 3010 and 3600 km^2 respectively. The report concludes that under the "worst case conditions" (i.e. A1FI scenario), the Mohamed Ali Sea Wall could have a noticeable role in the protection of the low land area after the year 2025. It is noted that estimates reported by CoRI (EEAA, 2010) (761 km^2 affected in 2100) are different from the estimates reported by Dasgupta et al. (2009b) (2,290 km^2 affected by a prescribed 1m SLR combined with a 10% intensification of the current 1-in-100-year storm surge). This is because the studies applied different SLR scenarios and the former study present estimates for the Nile Delta only (as opposed to the whole of the Egyptian coastline).

References

ABOU-HADID, A. F. 2006. Assessment of Impacts, Adaptation and Vulnerability to Climate Change in North Africa: Food Production and Water Resources, Final Report, Assessments of Impacts and Adaptations to Climate Change (AIACC).

AGRAWALA, S., MOEHNER, A., EL RAEY, M., CONWAY, D., VAN AALST, M., HAGENSTAD, M. & SMITH, J. 2004. Development and Climate Change in Egypt, Focus on Coastal Resources and the Nile. Working Party on Global and Structural Policies.

AINSWORTH, E. A. & MCGRATH, J. M. 2010. Direct Effects of Rising Atmospheric Carbon Dioxide and Ozone on Crop Yields. In: LOBELL, D. & BURKE, M. (eds.) Climate Change and Food Security. Springer Netherlands.

ALLISON, E. H., PERRY, A. L., BADJECK, M.-C., NEIL ADGER, W., BROWN, K., CONWAY, D., HALLS, A. S., PILLING, G. M., REYNOLDS, J. D., ANDREW, N. L. & DULVY, N. K. 2009. Vulnerability of national economies to the impacts of climate change on fisheries. Fish and Fisheries, 10, 173-196.

ARAB REPUBLIC OF EGYPT, CABINET OF MINISTRIES, MINISTRY OF STATE FOR ENVIRONMENTAL AFFAIRS, EGYPTIAN ENVIRONMENTAL AFFAIRS AGENCY & CLIMATE CHANGE CENTRAL DEPARTMENT 2010. Egypt National Environmental, Economic and Development Study (NEEDS) for Climate Change. United Nations Framework Convention on Climate Change. Cairo, Egypt.

ARNELL, N. W. 2004. Climate change and global water resources: SRES emissions and socio-economic scenarios. Global Environmental Change, 14, 31-52.

ATTAHER, S. M., MEDANY, M. A. & EL-GINDY, A. 2010. Feasibility of some adaptation measures of on-farm irrigation in Egypt under water scarcity conditions. Options Mediterraneennes, 2010. 95, 307-312.

AVNERY, S., MAUZERALL, D. L., LIU, J. F. & HOROWITZ, L. W. 2011. Global crop yield reductions due to surface ozone exposure: 2. Year 2030 potential crop production losses and economic damage under two scenarios of O3 pollution. Atmospheric Environment, 45, 2297-2309.

BETTS, R. A., BOUCHER, O., COLLINS, M., COX, P. M., FALLOON, P. D., GEDNEY, N., HEMMING, D. L., HUNTINGFORD, C., JONES, C. D., SEXTON, D. M. H. & WEBB, M. J.

2007. Projected increase in continental runoff due to plant responses to increasing carbon dioxide. Nature, 448, 1037-1041.

BEYENE, T., LETTENMAIER, D. P. & KABAT, P. 2010. Hydrologic impacts of climate change on the Nile River Basin: implications of the 2007 IPCC scenarios. Climatic Change, 100, 433-461.

BROWN, S., NICHOLLS, R., LOWE, J.A. and PARDAENS, A. (2011), Sea level rise impacts in 24 countries. Faculty of Engineering and the Environment and Tyndall Centre for Climate Change Research, University of Southampton.

BUSINESS MONITOR INTERNATIONAL 2011. Egypt Insurance Report Q2 2011. Business Monitor International.

CHAKRABORTY, S. & NEWTON, A. C. 2011. Climate change, plant diseases and food security: an overview. Plant Pathology, 60, 2-14.

CIA 2011. World Factbook. US Central Intelligence Agency.

CTF 2011. CTF Investment Plan for Egypt - Climate Investment Funds. Clean Technology Funds.

DASGUPTA, S., LAPLANTE, B., MEISNER, C., WHEELER, D. & YAN, J. 2009a. The impact of sea level rise on developing countries: a comparative analysis. Climatic Change, 93, 379-388.

DASGUPTA, S., LAPLANTE, B., MURRAY, S. & WHEELER, D. 2009b. Sea-level rise and storm surges: a comparative analysis of impacts in developing countries. Washington DC, USA: World Bank.

DASGUPTA, S., LAPLANTE, B., MURRAY, S. & WHEELER, D. 2010. Exposure of developing countries to sea-level rise and storm surges. Climatic Change, 1-13.

DINAS-COAST Consortium. 2006 DIVA 1.5.5. Potsdam, Germany: Potsdam Institute for Climate Impact Research (on CD-ROM)

DOLL, P. 2009. Vulnerability to the impact of climate change on renewable groundwater resources: a global-scale assessment. Environmental Research Letters, 4.

BETTS, R. A., BOUCHER, O., COLLINS, M., COX, P. M., FALLOON, P. D., GEDNEY, N., HEMMING, D. L., HUNTINGFORD, C., JONES, C. D., SEXTON, D. M. H. & WEBB, M. J.

2007. Projected increase in continental runoff due to plant responses to increasing carbon dioxide. Nature, 448, 1037-1041.

CONWAY, D. From headwater tributaries to international river: Observing and adapting to climate variability and change in the Nile basin. 2005. Global Environmental Change - Human and Policy Dimensions, 15, 2, 99-114 Doi: 10.1016/j.gloenvcha.2005.01.003

EEAA 2010. Egypt. Egypt second national communication under the United Nations Framework Convention on Climate Change. Cairo, Egypt: Egyptian Environmental Affairs Agency. Ministry of State for Environmental Affairs.

EID, H., ANTON, N. & TARRAD, A. 1994. Comparative study on Egyptian wheat varieties and their response to high temperatures. Agricultural Science Moshtohor (Egypt) 32, 143-154.

EL-AFANDI, G., KHALIL, F. A. & OUDA, S. A. 2010. Using irrigation scheduling to increase water productivity of wheat-maize rotation under climate change conditions. Chilean Journal of Agricultural Research, 70, 474-484.

EL-NAHRY, A. & DOLUSCHITZ, R. 2010. Climate change and its impacts on the coastal zone of the Nile Delta, Egypt. Environmental Earth Sciences, 59, 1497-1506.

ELSHAMY, M. E., SAYED, M. A.-A. & BADAWY, B. 2009. Impacts of climate change on Nile flows at Dongola using statistically downscaled GCM scenarios. Nile Water Science & Engineering Magazine, 2, 1-14.

FALKENMARK, M., ROCKSTRÖM, J. & KARLBERG, L. 2009. Present and future water requirements for feeding humanity. Food Security, 1, 59-69.

FAO. 2008. Food and Agricultural commodities production [Online]. Available: http://faostat.fao.org/site/339/default.aspx [Accessed 1 June 2011].

FISCHER, G. 2009. World Food and Agriculture to 2030/50: How do climate change and bioenergy alter the long-term outlook for food, agriculture and resource availability? Expert Meeting on How to Feed the World in 2050. Food and Agriculture Organization of the United Nations, Economic and Social Development Department.

FSF 2009. Financial Standards Report Egypt: Insurance Core Principles. Financial Standards Foundation.

FUNG, F., LOPEZ, A. & NEW, M. 2011. Water availability in +2°C and +4°C worlds. Philosophical Transactions of the Royal Society A: Mathematical, Physical and Engineering Sciences, 369, 99-116.

GERTEN D., SCHAPHOFF S., HABERLANDT U., LUCHT W., SITCH S. 2004 . Terrestrial vegetation and water balance: hydrological evaluation of a dynamic global vegetation model International Journal Water Resource Development 286:249–270

GIANNAKOPOULOS, C., BINDI, M., MORIONDO, M., LESAGER, P. & TIN, T. 2005. Climate change impacts in the Mediterranean resulting from a 2 °C global temperature rise. WWF Report. Gland, Switzerland: WWF.

GIANNAKOPOULOS, C., LE SAGER, P., BINDI, M., MORIONDO, M., KOSTOPOULOU, E. & GOODESS, C. M. 2009. Climatic changes and associated impacts in the Mediterranean resulting from a 2 °C global warming. Global and Planetary Change, 68, 209-224.

Gornall, J., Betts, R., Burke, E., Clark, R., Camp, J., Willett, K., Wiltshire, A. 2010. Implications of climate change for agricultural productivity in the early twenty-first century. Phil. Trans. R. Soc. B, DOI: 10.1098/rstb.2010.0158

GOSLING, S., TAYLOR, R., ARNELL, N. & TODD, M. 2011. A comparative analysis of projected impacts of climate change on river runoff from global and catchment-scale hydrological models. Hydrology and Earth System Sciences, 15, 279–294.

GOSLING, S. N. & ARNELL, N. W. 2011. Simulating current global river runoff with a global hydrological model: model revisions, validation, and sensitivity analysis. Hydrological Processes, 25, 1129-1145.

GOSLING, S. N., BRETHERTON, D., HAINES, K. & ARNELL, N. W. 2010. Global hydrology modelling and uncertainty: running multiple ensembles with a campus grid. Philosophical Transactions of the Royal Society A: Mathematical, Physical and Engineering Sciences, 368, 4005-4021.

HANSON, S., NICHOLLS, R., RANGER, N., HALLEGATTE, S., CORFEE-MORLOT, J., HERWEIJER, C. & CHATEAU, J. 2011. A global ranking of port cities with high exposure to climate extremes. Climatic Change, 104, 89-111.

HARDING, R., BEST, M., BLYTH, E., HAGEMANN, D., KABAT, P., TALLAKSEN, L.M., WARNAARS, T., WIBERG, D., WEEDON, G.P., van LANEN, H., LUDWIG, F., HADDELAND, I. 2011. Preface to the “Water and Global Change (WATCH)” special

collection: Current knowledge of the terrestrial global water cycle. Journal of Hydrometeorology, DOI: 10.1175/JHM-D-11-024.1

HIRABAYASHI, Y., KANAE, S., EMORI, S., OKI, T. & KIMOTO, M. 2008. Global projections of changing risks of floods and droughts in a changing climate. Hydrological Sciences Journal-Journal Des Sciences Hydrologiques, 53, 754-772.

IFPRI. 2010. International Food Policy Research Institute (IFPRI) Food Security CASE maps. Generated by IFPRI in collaboration with StatPlanet. [Online]. Available: www.ifpri.org/climatechange/casemaps.html [Accessed 21 June 2010].

IGLESIAS, A., GARROTE, L., QUIROGA, S. & MONEO, M. 2009. Impacts of climate change in agriculture in Europe. PESETA-Agriculture study. JRC Scientific and Technical Reports.

IGLESIAS, A. & ROSENZWEIG, C. 2009. Effects of Climate Change on Global Food Production under Special Report on Emissions Scenarios (SRES) Emissions and Socioeconomic Scenarios: Data from a Crop Modeling Study. . Palisades, NY: Socioeconomic Data and Applications Center (SEDAC), Columbia University.

IPCC 2007a. Climate Change 2007: The Physical Science Basis. Contribution of Working Group I to the Fourth Assessment Report of the Intergovernmental Panel on Climate Change In: SOLOMON, S., QIN, D., MANNING, M., CHEN, Z., MARQUIS, M., AVERYT, K. B., TIGNOR, M. & MILLER, H. L. (eds.). Cambridge, United Kingdom and New York, NY, USA.

IPCC 2007b. Summary for Policymakers. In: PARRY, M. L., CANZIANI, O. F., PALUTIKOF, J. P., VAN DER LINDEN, P. J. & HANSON, C. E. (eds.) Climate Change 2007: Impacts, Adaptation and Vulnerability. Contribution of Working Group II to the Fourth Assessment Report of the Intergovernmental Panel on Climate Change. Cambridge: Cambridge University Press.

LOBELL, D. B., SCHLENKER, W. & COSTA-ROBERTS, J. 2011. Climate Trends and Global Crop Production Since 1980. Science.

LUCK, J., SPACKMAN, M., FREEMAN, A., TRE¸BICKI, P., GRIFFITHS, W., FINLAY, K. & CHAKRABORTY, S. 2011. Climate change and diseases of food crops. Plant Pathology, 60, 113-121.

MENZEL, L. & MATOVELLE, A. 2010. Current state and future development of blue water availability and blue water demand: A view at seven case studies. Journal of Hydrology, 384, 245-263.

MOUGOU, R., ABOU-HADID, A., IGLESIAS, A., MEDANY, M., NAFTI, A., CHETALI, R., MANSOUR, M. & EID, H. 2008. Adapting Dryland and Irrigated Cereal Farming to Climate Change in Tunisia and Egypt. In: LEARY, N., ADEJUWON, J., BARROS, V., BURTON, I., KULKARNI, J. & LASCO, R. (eds.) Climate change and adaptation. London: Earthscan.

NICHOLLS, R. J. and LOWE, J. A. (2004). "Benefits of mitigation of climate change for coastal areas." Global Environmental Change 14(3): 229-244.

NICHOLLS, R. J., MARINOVA, N., LOWE, J. A., BROWN, S., VELLINGA, P., DE GUSMÃO, G., HINKEL, J. and TOL, R. S. J. (2011). "Sea-level rise and its possible impacts given a 'beyond 4◦C world' in the twenty-first century." Philosophical Transactions of the Royal Society A 369: 1-21.

NELSON, G. C., ROSEGRANT, M. W., KOO, J., ROBERTSON, R., SULSER, T., ZHU, T., RINGLER, C., MSANGI, S., PALAZZO, A., BATKA, M., MAGALHAES, M., VALMONTE-SANTOS, R., EWING, M. & LEE, D. 2009. Climate change. Impact on Agriculture and Costs of Adaptation. Washington, D.C.: International Food Policy Research Institute.

NELSON, G. C., ROSEGRANT, M. W., PALAZZO, A., GRAY, I., INGERSOLL, C., ROBERTSON, R., TOKGOZ, S., ZHU, T., SULSER, T. & RINGLER, C. 2010. Food Security, Farming and Climate Change to 2050. Research Monograph, International Food Policy Research Institute. Washington, DC.

PARDAENS, A. K., LOWE, J., S, B., NICHOLLS, R. & DE GUSMÃO, D. 2011. Sea-level rise and impacts projections under a future scenario with large greenhouse gas emission reductions. Geophysical Research Letters, 38, L12604.

PARRY, M. L., ROSENZWEIG, C., IGLESIAS, A., LIVERMORE, M. & FISCHER, G. 2004. Effects of climate change on global food production under SRES emissions and socio-economic scenarios. Global Environmental Change-Human and Policy Dimensions, 14, 53-67.

RAMANKUTTY, N., EVAN, A. T., MONFREDA, C. & FOLEY, J. A. 2008. Farming the planet: 1. Geographic distribution of global agricultural lands in the year 2000. Global Biogeochemical Cycles, 22, GB1003.

RAMANKUTTY, N., FOLEY, J. A., NORMAN, J. & MCSWEENEY, K. 2002. The global distribution of cultivable lands: current patterns and sensitivity to possible climate change. Global Ecology and Biogeography, 11, 377-392.

ROCKSTRÖM, J., FALKENMARK, M., KARLBERG, L., HOFF, H., ROST, S. & GERTEN, D. 2009. Future water availability for global food production: The potential of green water for increasing resilience to global change. Water Resources Research, 45.

SCHUOL, J., ABBASPOUR, K. C., YANG, H., SRINIVASAN, R. & ZEHNDER, A. J. B. 2008. Modeling blue and green water availability in Africa. Water Resources Research, 44.

SMAKHTIN, V., REVENGA, C. & DOLL, P. 2004. A pilot global assessment of environmental water requirements and scarcity. Water International, 29, 307-317.

SOLIMAN, E. S. A., SAYED, M. A.-A. & JEULAND, M. 2009. Impact assessment of future climate change for the Blue Nile basin using a RCM nested in a GCM. Nile Water Science & Engineering Magazine, 2, 31-38.

STERMAN, D. 2009. Climate Change in Egypt: Rising Sea Level, Dwindling Water Supplies [Online]. [Accessed July 12 2011].

STOCKLE, C.O., DONATELLI, M., NELSON, R., 2003 CropSyst, a cropping systems simulation model. European Journal of Agronomy 18, 289-307.

STRZEPEK, K., YATES, D. & EL QUOSY, D. 1996. Vulnerability assessment of water resources in Egypt to climatic change in the Nile Basin. Climate Research, 06, 89-95.

STRZEPEK, K., YATES, D., YOHE, G., TOL, R. & MADER, N. 2001. Constructing “not Implausible” Climate and Economic Scenarios for Egypt. Integrated Assessment, 2, 139-157.

TATSUMI, K., YAMASHIKI, Y., VALMIR DA SILVA, R., TAKARA, K., MATSUOKA, Y., TAKAHASHI, K., MARUYAMA, K. & KAWAHARA, N. 2011. Estimation of potential changes in cereals production under climate change scenarios. Hydrological Processes,Special Issue: Japan Society of Hydrology and water resources, 25 (17), 2715-2725

UN 2007. State of Water Resources in the ESCWA Region. United Nations.

UNEP 2008. Vital water graphics: an overview of the state of the world's fresh and marine waters. 2nd Edition, Nairobi, Kenya, United Nations Environment Programme.

VAN VUUREN, D., DEN ELZEN, M., LUCAS, P., EICKHOUT, B., STRENGERS, B., VAN RUIJVEN, B., WONINK, S. & VAN HOUDT, R. 2007. Stabilizing greenhouse gas concentrations at low levels: an assessment of reduction strategies and costs. Climatic Change, 81, 119-159.

VAN VUUREN, D. P., ISAAC, M., KUNDZEWICZ, Z. W., ARNELL, N., BARKER, T., CRIQUI, P., BERKHOUT, F., HILDERINK, H., HINKEL, J., HOF, A., KITOUS, A., KRAM, T., MECHLER, R. & SCRIECIU, S. 2011. The use of scenarios as the basis for combined assessment of climate change mitigation and adaptation. Global Environmental Change, 21, 575-591.

VÖRÖSMARTY, C. J., MCINTYRE, P. B., GESSNER, M. O., DUDGEON, D., PRUSEVICH, A., GREEN, P., GLIDDEN, S., BUNN, S. E., SULLIVAN, C. A., LIERMANN, C. R. & DAVIES, P. M. 2010. Global threats to human water security and river biodiversity. Nature, 467, 555-561.

WARREN, R., ARNELL, N., BERRY, P., BROWN, S., DICKS, L., GOSLING, S., HANKIN, R., HOPE, C., LOWE, J., MATSUMOTO, K., MASUI, T., NICHOLLS, R., O'HANLEY, J., OSBORN, T., SCRIECRU, S. 2010 The Economics and Climate Change Impacts of Various Greenhouse Gas Emissions Pathways: A comparison between baseline and policy emissions scenarios, AVOID Report, AV/WS1/D3/R01. http://www.metoffice.gov.uk/avoid/files/resources-researchers/AVOID_WS1_D3_01_20100122.pdf

WHO 2005. The Way Forward: Annual Report 2004.

WOOD, E.F., ROUNDY, J.K., TROY, T.J., van BEEK, L.P.H., BIERKENS, M.F.P., BLYTH, E., de ROO, A., DOLL, P., EK, M., FAMIGLIETTI, J., GOCHIS, D., van de GIESEN, N., HOUSER, P., JAFFE, P.R., KOLLET, S., LEHNER, B., LETTENMAIER, D.P., PETERS-LIDARD, C., SIVAPALAN, M., SHEFFIELD, J., WADE, A. & WHITEHEAD, P. 2011. Hyperresolution global land surface modelling: Meeting a grand challenge for monitoring Earth's terrestrial water. Water Resources Research, 47, W05301.

WOS. 2011. Web of Science [Online]. Available: http://thomsonreuters.com/products_services/science/science_products/a-z/web_of_science [Accessed August 2011].

Acknowledgements

Funding for this work was provided by the UK Government Department of Energy and Climate Change, along with information on the policy relevance of the results.

The research was led by the UK Met Office in collaboration with experts from the University of Nottingham, Walker Institute at the University of Reading, Centre for Ecology and Hydrology, University of Leeds, Tyndall Centre — University of East Anglia, and Tyndall Centre — University of Southampton.

Some of the results described in this report are from work done in the AVOID programme by the UK Met Office, Walker Institute at the University of Reading, Tyndall Centre — University of East Anglia, and Tyndall Centre — University of Southampton.

The AVOID results are built on a wider body of research conducted by experts in climate and impact models at these institutions, and in supporting techniques such as statistical downscaling and pattern scaling.

The help provided by experts in each country is gratefully acknowledged — for the climate information they suggested and the reviews they provided, which enhanced the content and scientific integrity of the reports.

The work of the independent expert reviewers at the Centre for Ecology and Hydrology, University of Oxford, and Fiona's Red Kite Climate Consultancy is gratefully acknowledged.

Finally, thanks go to the designers, copy editors and project managers who worked on the reports.

Met Office
FitzRoy Road, Exeter
Devon, EX1 3PB
United Kingdom

Tel: 0870 900 0100
Fax: 0870 900 5050
enquiries@metoffice.gov.uk
www.metoffice.gov.uk

Produced by the Met Office.